NTNU

Norwegian University of
Science and Technology

Simulation of Combined Hydrate Control and H_2S Removal Using Aspen Plus

Mari Iselin Lilleng

Chemical Engineering and Biotechnology
Submission date: June 2016
Supervisor: Hanna Knuutila, IKP

Norwegian University of Science and Technology
Department of Chemical Engineering

Preface

This thesis was written in the spring of 2016 at the Department of Chemical Engineering at the Norwegian University of Science and Technology (NTNU). It was written as a part of my specialization in gas purification for the Environmental Engineering and Reactor Technology Group. With this thesis, my education at the master program Chemical Engineering and Biotechnology is completed.

I would like to give special thanks to my supervisor, Associate Professor Hanna Knuutila, for all of her support and guidance throughout the semester. My motivation has always been greater walking out of her office.

Additionally, I would like to thank my family and friends for motivational support during these five years of study.

"I declare that this is an independent work according to the exam regulations of the Norwegian University of Science and Technology (NTNU)"

Trondheim, 19th of June 2016

Mari Iselin Lilleng

Abstract

Removal of water (H_2O) and acid gas contaminants, like hydrogen sulfide (H_2S) and carbon dioxide (CO_2), are essential in natural gas purification. Due to gas quality specifications and protection of installed equipment including subsea pipelines, impurities need to be removed efficiently. Well designed gas treatment processes have been developed, where fine removal of water and acid gas typically are performed by absorption utilizing glycols and alkanolamines. Inhibition of gas hydrates in pipelines is crucial upstream a processing facility, because pipeline blockages have the possibility of causing complete process shutdown. Research towards complete subsea processing is now conducted, where the aim is to develop new process technology that can enhance and increase the production efficiency of reservoirs already in operation. Hydrate inhibition, acid gas removal and fine removal of water are traditionally performed in three different processing units. Designing a process where these systems can be combined, may give more efficient and compact processing equipment. In this thesis, the main goal was to conduct a simulation of combined H_2S and water removal from natural gas by absorption in methyldiethanolamine (MDEA) and monoethylene glycol (MEG). Simulations were performed in Aspen plus version 8.6 and the template 'ElecNRTL_Rate_Based_MDEA_model' was used. The aim was to examine the absorption performance predicted by Aspen Plus of the combined process.

A vapor liquid validation (VLE) was performed where H_2S, CO_2, methane (CH_4) and H_2O solubility in aqueous MDEA and pure MEG were compared to literature data. In total, 500 experimental data points were compared to the solubility curves predicted by Aspen Plus, which gave average absolute deviations ranging from 3.5% to 218.6% for temperatures from 25 ^oC to 130 ^oC. Validation of H_2S and CO_2 mixtures in a MDEA-MEG-H_2O solvent with low water content, revealed high partial pressures of the acid gas components compared to literature data. It was found that absorption of H_2S and CO_2 required use of aqueous MDEA, because of how the chemical reactions were defined in the template.

The absorption simulations were performed for three different natural gas compositions, which were defined to be CH_4 saturated with water, having H_2S and CO_2 contents ranging from 49.8 ppm and 5.6% to 4.5% and 8%, respectively. The absorption performance using a mixed MDEA-MEG solvent in one contactor, where various solvent concentrations were examined, was found to be insufficient with respect to water removal. Absorption of H_2S and CO_2 in MDEA, and H_2O in MEG, including regeneration of the solvents were simulated separately. No recommendations for optimal operating conditions were made, due to lack of operational data that could be used for comparison. However, some operational areas which were considered as energy efficient for the different composition cases, where chosen for further analysis. Molar liquid-gas ratios, for obtaining 4 ppm H_2S in the sweet gas utilizing a 45 wt% MDEA solvent at 100 bar, ranged from 0.75 to 1.7 at these operational areas. Specific reboiler duties ranged from 3.79 MJ/kg acid gas to 4.96 MJ/kg acid gas. H_2S and CO_2 recoveries were up to 99.3% and 99.5%. Because equilibrium based calculations were defined in the absorber, the amount of absorbed CO_2 were high for all simulations and results revealed less than 1% CO_2 in the sweet gas for the same cases.

For water removal, it was found that MEG concentrations above 99% should be used depending on the water content and temperature of the wet gas. Conventional regeneration of MEG in a distillation column to this level of purity, resulted in reboiler temperatures above 190 ^{o}C, and were found to exceed the recommended limits with respect to thermal degradation, which are around 165 ^{o}C.

Sammendrag

Når naturgass skal renses, er fjerning av vann (H_2O) og sure gasskomponenter, som hydrogensulfid (H_2S) og karbondioksid (CO_2), essensielle deler av prosessen. Disse komponentene må fjernes på en effektiv måte fordi det stilles strenge krav til gasskvalitet og for å beskytte installert utstyr og rørlinjer. Fjerning av vann og sur gass gjøres vanligvis ved absorpsjon i glykoler og alkanolaminer, og det finnes gode løsninger på prosessutstyr for dette. Inhibering av gasshydrater i rørlinjer er viktig oppstrøms et prosessanlegg, fordi det kan være fare for nedstengning av anlegget hvis rørlinjene blir fullstendig blokkert. Det forskes nå på subsea-prosessering, der målet er å utvikle ny teknologi som kan forbedre og øke produksjonseffektiviteten i reservoarer som allerede driftes. Hydratinhibering, fjerning av sur gass og fjerning av vann utføres tradisjonelt i tre ulike delprosesser. Utvikling av utstyr som kan kombinere disse delprosessene, kan potensielt øke effektiviteten og gi mer kompakt utstyr. Hovedmålet med denne masteroppgaven var å utføre simuleringer av kombinert fjerning av H_2S og H_2O fra naturgass ved å bruke metyldietanolamin (MDEA) og monoetyleneglykol (MEG) som absorbenter. Simuleringene ble utført i Aspen Plus versjon 8.6 og malen 'ElecNRTL_Rate_Based_MDEA_model' ble brukt. Målet var å undersøke hvor gode resultater Aspen Plus ga for den kombinerte prosessen.

En validering av gass-væske likevekter (VLE) ble utført, og løseligheten av H_2S, CO_2, metan (CH_4) og H_2O i vannholdige MDEA løsninger og ren MEG ble sammenlignet med litteraturdata. Totalt ble 500 eksperimentelle datapunkter sammenlignet med løselighetskurvene predikert av Aspen Plus, og ga gjennomsnittlige avvik fra 3.5% til 218.6% for temperaturer fra 25 ^oC til 130 ^oC. Validering av H_2S og CO_2 blandinger i MDEA-MEG-H_2O løsninger med lavt vanninnhold, resulterte i høye partialtrykk for de sure komponentene sammenlignet med litteraturdata. Det ble funnet ut av absorpsjon av H_2S og CO_2 krever bruk av vannholdig MDEA på grunn av hvordan de kjemiske reaksjonene er definert i modellmalen.

Simuleringene ble gjort for tre ulike gasskomposisjoner, som ble definert til å være CH_4 mettet med vann, med varierende innhold av sur gass. H_2S og CO_2 konsentrasjonene varierte henholdsvis fra 49.8 ppm og 5.6% til 4.5% og 8%. Absorpsjonsresultatene som ble funnet ved å bruke en blandet MDEA-MEG absorbent i én kolonne, ga utilstrekkelige resultater med tanke på fjerning av vann. Flere absorbentkonsentrasjoner ble undersøkt i denne analysen. Absorpsjon av H_2S og CO_2 i MDEA, og H_2O i MEG, der regenerering av absorbentene ble inkludert, ble derfor simulert som separate prosesser. Det ble ikke konkludert med anbefalinger til optimale driftsområder på grunn av mangel på driftsdata som kunne brukes som sammenligning. Det ble tatt ut noen driftsbetingelser for videre analyser basert på hva som ble ansett som optimalt energiforbruk i kokeren. Molare væske-gass rater inn på absorpsjonskolonnen og spesifikk varmeeffekt i kokeren, for å oppnå 4 ppm H_2S ved å bruke en 45 vekt% vannholdig MDEA løsning ved 100 bar, varierte henholdsvis fra 0.75 til 1.7 og 3.79 MJ/kg sur gass til 4.96 MJ/kg sur gass for disse driftspunktene. Gjenvunnet H_2S og CO_2 var opp til 99.3% og 99.5% for disse kjøringene. Likevektsbaserte kalkuleringer var definert i

absorpsjonskolonnen og resulterte i store mengder absorbert CO_2 i alle simuleringene. Mindre enn 1% CO_2 ble observert i den prosesserte gassen for de samme kjøringene forklart over.

Det ble funnet ut at MEG konsentrasjoner høyere enn 99 vekt% burde brukes for å fjerne vann, avhengig av vanninnholdet og temperaturen til den våte gassen som kommer inn på kolonnen. Regenerering av MEG i en enkel destillasjonskolonne ga høye temperaturer, over 190 ^oC, i kokeren for å oppnå denne renheten. Disse var over anbefalte temperaturer med tanke på termisk degradering som er rundt 165 ^oC.

Table of Contents

List of figures

List of tables

List of symbols

Symbol	Description	Unit
c_s	Concentration of solvent *s*	wt% or %
G	Molar gas flowrate	kmol/h
g	Gas	-
K_{eq}	Equilibrium constant	-
K_i	Equilibrium constant for reaction *i*	-
L	Molar liquid flowrate	kmol/h
Mm_i	Molecular weight of component *i*	kg/kmol
n	Number of data points or column stages	-
$\dot{n}_i$	Molar flow component *i*	kmol/h
P_{exp}	Experimental partial pressure	kPa
P_i	Partial pressure of component *i*	kPa
P_{sim}	Simulated partial pressure	kPa
P_{tot}	Total pressure	kPa
Q_s	Specific reboiler duty	MJ/kg acid gas
s	solvent	-
T	Temperature	^{o}C / K
w_{H_2O}	Weight percent water	%
x_i	Mole fraction component *i* in liquid phase	-
y_i	Mole fraction component *i* in vapor phase	-
α_i	Loading component *i*	mol *i*/mol solvent
α_{exp}	Experimental loading	mol *i*/mol solvent
$\%\Delta_i$	Percentage deviation	%
$\overline{\%\Delta}$	Average deviation	%

Abbreviations

Abbreviation	Description
AD	Average absolute deviation
AAD	Absolute average deviation
CH_4	Methane
CO_2	Carbon dioxide
H_2O	Water
H_2S	Hydrogen sulfide
MDEA	Methyldiethanolamine
MEA	Monoethanolamine
MEG	Monoethylene glycol
NTNU	Norwegian University of Science and Technology
OECD	Organization for Economic Cooperation and Development
PFD	Process Flow diagram
ppm	Parts per million
SFI	Centre for Research-based Innovation
SUBPRO	Subsea production and processing
TEG	Triethylene glycol
VLE	Vapor liquid equilibrium
wt	Weight

Chapter 1 Introduction

1.1 Background

In natural gas processing, removal of water and acid gas are important parts of the value chain. Removal of these contaminants are usually done in different system units at different points in the process. Hydrate inhibition and gas dehydration, are crucial parts of the process for flow assurance and to prevent pipeline blockages. Formation of gas hydrates in pipelines is a big concern for flow assurance engineers and can in the worst case scenario block pipelines completely, resulting in process shutdown. In offshore processing, hydrate inhibitors are widely used for flow assurance before the gas enters the topside facility. Fine removal of water (H_2O) is usually performed in a gas dehydration unit topside, to minimize the probability of water condensing during pipeline transportation.

In addition to water, natural gas is often contaminated with acid gas impurities as well. Acid gas, like hydrogen sulfide (H_2S) and carbon dioxide (CO_2), form weak acids in aqueous environments and can increase the rate of corrosion in pipelines. The main application area of natural gas is as fuel, and CO_2 removal is also important to reach an adequate fuel heating value. Specifications for gas to be transported are therefore typically 2-3% CO_2 (by volume) and maximum 4 ppm H_2S [1, 2]. A typical water dew point requirement for gas transportation in pipelines, on the Norwegian Continental shelf, is -18 ^oC at 70 bara [3].

1.2 Scope of thesis

Chemical and physical absorption are widely used methods for acid gas removal as well as dehydration of natural gas. The objective of this thesis was to investigate how well combining H_2S removal with hydrate control could be simulated in Aspen Plus version 8.6, using methyldiethanolamine (MDEA) and monoethylene glycol (MEG) as absorbents. The natural gas to be processed was assumed to be saturated with water containing both H_2S and CO_2. The first task was to do a validation of the vapor-liquid equilibrium (VLE) model available in Aspen Plus against literature data. Gas solubility, giving information about how much acid gas that is absorbed in the solvent and the partial pressure of the gas at equilibrium, is important information for how a gas treating plant should be designed [2]. A collection of experimental data available in literature was found and VLE validations of the gas-amine and gas-glycol systems were performed. The VLE validation is important to conduct, to find out how reliable the model in Aspen Plus is. A built in template model was used as a basis for all the simulations.

Designing new process equipment is challenging and expensive, and simulation tools like Aspen Plus can be used to get a preliminary understanding of how the process should be optimized and operated. It was desirable to investigate the absorption performance in a mixed MDEA-MEG solvent for different natural gas compositions. This was to see if Aspen Plus

gave reasonable results for a combined acid gas and water removal unit. Due to lack of plant data for this process for comparison, general gas specifications, as given above, were used as target values for examining the performance in Aspen Plus. In addition to this, it was desirable to examine regeneration of the solvents.

1.3 Increased efficiency in subsea operation

In offshore processing; hydrate inhibition, acid gas removal and gas dehydration are typically carried out in three different units. This gives one injection system for hydrate inhibition, and two absorption systems for acid gas and fine removal of water, including regeneration of the chemicals. The latter are typically parts of the topside facility. Before the gas enters the topside facility, MEG is typically injected into the pipelines for flow assurance and hydrate inhibition. Arriving at the platform, MEG-water and condensed liquids are separated from the gas, before the gas is sent to an acid gas absorption unit where amines are utilized. The last step is fine removal of water by absorption, which typically uses triethylene glycol (TEG) as the solvent.

All these processes are well known and widely used. Designing a process where these systems can be combined may give more efficient and compact processing units. Designs for gas processing equipment are continuously improved and gas and oil companies are now aiming for complete subsea processing of some reservoirs. Statoil is a leading oil and gas company and has developed more than 500 subsea wells the last 25 years. It is just one of the companies that now are doing research towards subsea processing, and they are targeting a complete subsea factory by 2020 [4]. The newest project towards subsea processing, is SUBPRO (Subsea production and processing), which is a collaboration work between NTNU, Centre for Research-based Innovation (SFI) and seven industrial partners, Statoil being one of them. They are aiming to be a leading international research center within subsea technology that can solve future challenges within subsea processing [5].

One ultimate goal in the future is to design a processing unit that removes acid gas and water simultaneously that can be installed for subsea gas processing. Utilizing subsea production facilities may decrease the number of employees offshore, and may be more cost effective in the long term. In this thesis it was therefore desirable to examine how well a combined processing unit could be simulated in Aspen Plus. Analysing type of contactor or sizing of equipment was not a part of this work.

1.4 Fossil fuel demand

Natural gas is a fossil fuel and origins from anaerobic decomposition of animal and plant material over millions of years, and is an important source of energy in a world with increasing energy demands. Natural gas is also a better fuel option compared to liquid oil and coal, because it has a higher fuel efficiency and burns cleaner [6]. From 1971 to 2013 the world's energy demand has increased significantly, and in 2013 natural gas was the second largest fuel source, the largest being oil with respect to consumption. Figure 1.4.1 shows how

the fuel consumption has developed since 1971 and the distribution of different fuel sources in million tonne of oil equivalent [7].

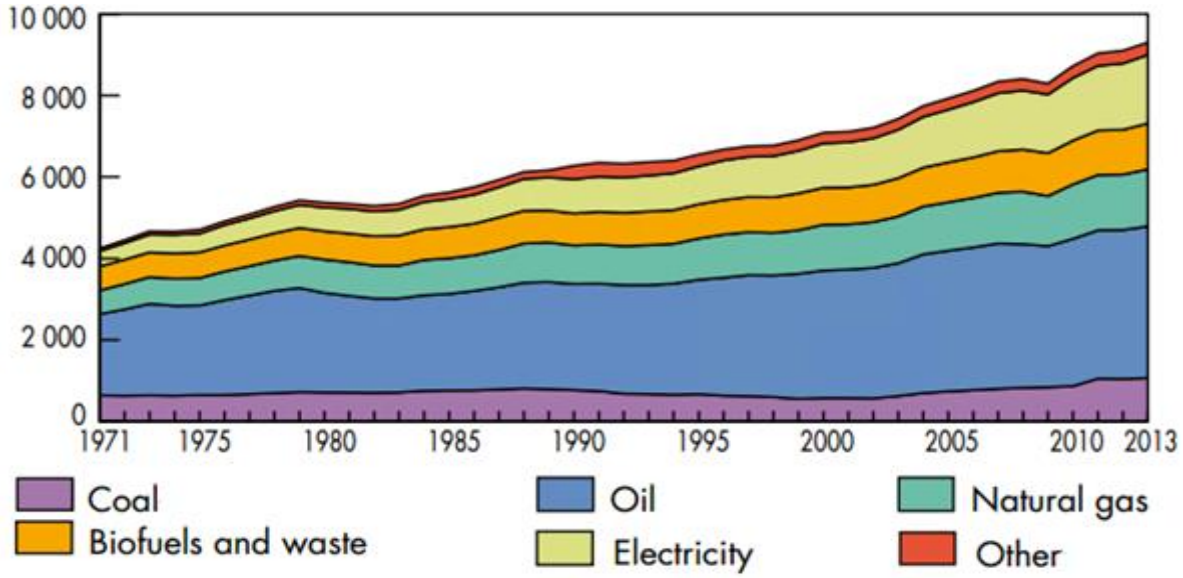

Figure 1.4.1: World fuel consumption, in million tonne of oil equivalent [Mtoe], from 1971 to 2013 [7].

Climate changes and global warming, as a result of greenhouse gas emissions is a major concern, but the world's energy demand is still increasing and there will still be need for natural gas as an energy source. From 2012 to 2040 it is expected an increase in natural gas consumption from 120 to 203 trillion cubic feet. Figure 1.4.2 gives an overview of the world's predicted natural gas consumption up to 2040 [8].

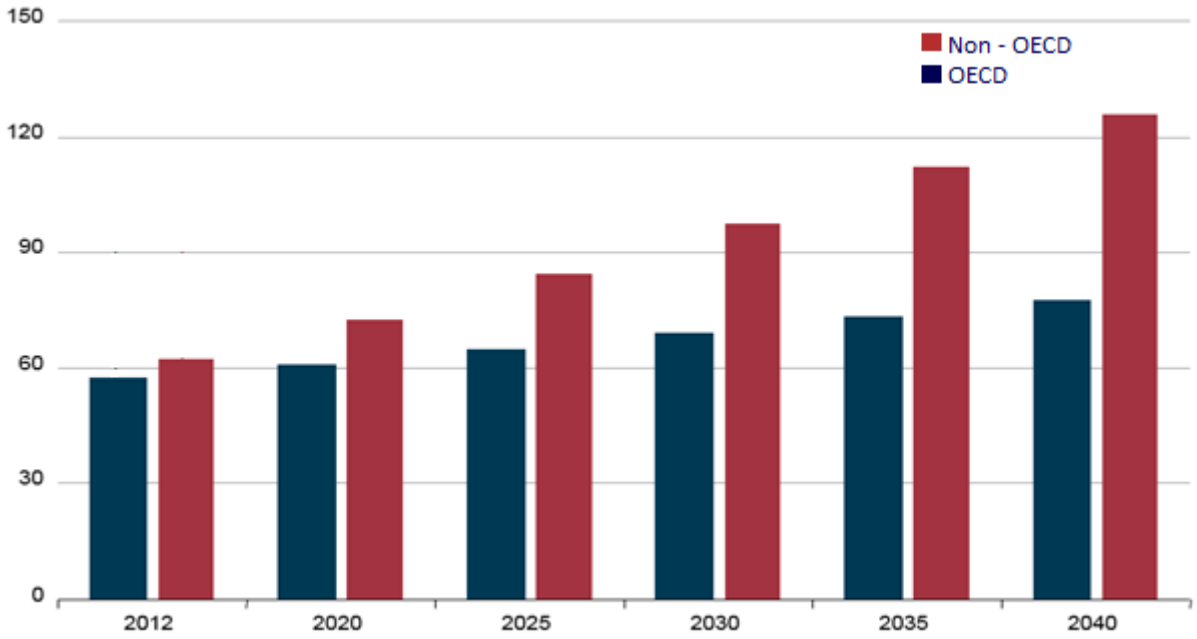

Figure 1.4.2: Predicted world natural gas consumption, in trillion cubic feet, up to year 2040. Demand in countries that are not part of the Organization for Economic Cooperation and Development (non-OECD), is predicted to increase by 2.5% per year from 2012 to 2040. OECD nations are predicted to have an increase in demand of 1.1% per year in the same time period [8].

1.5 Outline of Thesis

An introduction and motivation for investigating combined acid gas removal and gas dehydration of natural gas are given in Chapter 1. Chapter 2 gives an overview of why removal of acid gas and water is important before natural gas is sent for pipeline transportation. There is also a general process description of an acid gas removal unit using MDEA and a hydrate injection system using MEG, including the regeneration units. Theory of MDEA and MEG as absorbents and chemical reactions that need to be considered is also provided. An overview of VLE data available in literature, used for validating the template model in Aspen Plus is also presented in Chapter 2.

In Chapter 3, the VLE models retrieved from Aspen Plus compared to literature data are presented and discussed. Solubility of H_2S, CO_2 and methane (CH_4) in different MDEA solutions at different temperatures were examined. Solubility of H_2S, CO_2, CH_4 and H_2O in pure MEG at different temperatures were also evaluated. Average absolute deviation and absolute average deviation between literature data and the Aspen Plus model were calculated for all the systems that were analysed. In addition, a discussion about H_2S and CO_2 solubility in a mixed MDEA-MEG-H_2O solvent is provided.

The natural gas compositions that were examined are given in Chapter 4, including a preliminary analysis of the absorption process using aqueous MDEA as the solvent. Chapter 5 gives simulation results of the combined process, using MDEA-MEG solvents. Chapter 6 is divided in two, where acid gas removal and gas dehydration were simulated separately. The processes simulated in Chapter 6 include regeneration of MDEA and MEG as well. The results from simulations are given and discussed consecutively. Chapter 7 concludes the work performed in this thesis and gives recommendations for further work. Supplementary information relevant to the thesis is given in Appendices. The most important simulation files and calculations of average deviation and absolute average deviation for all data points that were validated in Chapter 3 can be provided by Hanna Knuutila upon request (e-mail: hanna.knuutila@ntnu.no).

Chapter 2 Acid gas removal and hydrate control

2.1 Importance of H_2S and CO_2 removal

Pipelines are widely used for natural gas transportation over long distances and there are strict requirements for the gas quality. Acid gas removal units, often called gas sweetening, are implemented in different industrial plants because of product specifications and strict emission requirements. Acid gas is used as a collective term for H_2S and CO_2 in this work. Natural gas is often contaminated with CO_2, and some reservoirs also contain H_2S. The concentration of acid gas depends on the reservoir source, and can typically contain up to 8% CO_2 and up to 5% H_2S [6]. Being able to remove H_2S and CO_2 simultaneously from the gas is a crucial part of the process for reaching transportation specifications for rich gas. Rich gas is commonly used as a term for gas leaving an offshore facility and sent for further processing. As mentioned, typical rich gas specifications are 2-3% CO_2 and 4 ppm H_2S.

H_2S is toxic and reacts to form weak acids in aqueous solutions, which are corrosive. The latter is also the case for CO_2. The rate of corrosion in equipment depends on processing temperature, amount of water and what type of chemicals that are used. For acid gas removal, absorption is widely applied by utilizing amines, which vary in corrosiveness. Tertiary amines are in general regarded as less corrosive than primary amines [9]. One of the main reasons for removing CO_2, which is non-flammable, is to increase the fuel heating value [10].

2.2 Natural gas dehydration for controlling hydrate formation

Flow assurance is one of the most important parts of the value chain in natural gas processing. Issues regarding flow assurance may result in production shut down if the problems are not detected early. The main issue concerning flow assurance engineers is formation of gas hydrates in the pipeline which can cause plugging. Gas hydrates are formed at low temperatures and high pressures if water and natural gas are both present in the pipeline. They are crystalline compounds where gas molecules, typically CH_4, CO_2 or H_2S, are captured within a water lattice structure which is hydrogen bonded. Usually, the type of hydrate is divided into different categories, which are structure I and structure II hydrates. The latter vary in how the water lattice is formed [11].

For controlling hydrate formation in pipelines before the gas arrives at the processing facility there are three different gas hydrate inhibitors that can be chosen. These are kinetic inhibitors, thermodynamic inhibitors or antiagglomeration inhibitors. MEG is an example of a thermodynamic inhibitor and is widely used because of its capability of being regenerated. Injecting MEG into the pipeline will shift the hydrate formation conditions to lower temperatures, which inhibit formation because the hydrate VLE curve is shifted to the left [12].

When the gas arrives at the production facility, it is usually sent to a dehydration unit for fine removal of water. This is important to meet transport pipeline specifications, to assure that no water will condense during transportation. As mentioned, typical dew point specifications on the Norwegian Continental shelf is -18^{o}C at 70 bara [3]. This minimizes the possibility of gas hydrate formation and increased corrosion rates in equipment.

2.3 Absorbents

For removing adequate amounts of H_2S and H_2O from a gas stream, suitable absorbents need to be considered. A suitable absorbent should fulfil some of the property requirements listed below [10, 13]

i. High selectivity for the desired components to remove.
ii. High loading capacity: Required circulation rate will determine operating costs and the size of the equipment.
iii. Easy to regenerate: Energy requirements for regeneration influences operating costs.
iv. Do not degenerate easily
v. Non corrosive
vi. Low vapor pressure (non-volatile): Minimizes loss of solvent material and high solvent concentrations can be used
vii. Low hydrocarbon solubility
viii. Minimal formation of corrosive by-products

2.3.1 Methyldiethanolamine

Amines are often categorized based on how many hydrogen atoms that are bound to the nitrogen atom. A primary amine has two hydrogen atoms and one hydrocarbon chain attached to the nitrogen (R_1NH_2), while a tertiary amine has three hydrocarbon groups connected to the nitrogen ($R_1R_2R_3N$). MDEA is a tertiary alkanolamine. Alkanolamines have at least one hydroxyl group (OH^-) connected one of the hydrocarbon groups. MDEA has two ethanol groups (-CH_2-CH_2-OH) and one methyl group (-CH_3) attached to the nitrogen [2]. An illustration of the MDEA molecule is shown in Figure 2.3.1.

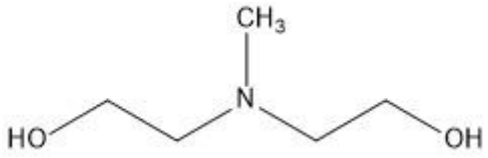

Figure 2.3.1: Illustration of the MDEA molecule.

MDEA is widely used as a solvent for chemical absorption of acid gas, and is often used to process gas which contains both H_2S and CO_2 because it has the ability to selectively remove H_2S. Another advantage with MDEA is that one does not need to consider carbamate formation in the absorption process. The absorption reactions are explained in detail in Chapter 2.5.

MDEA was one of the last alkanolamines commercialized because of the cost compared to other amines. However, the energy requirement for regenerating MDEA is lower compared to primary and secondary amines. The reason for this is mainly because the heat of absorption, when H_2S and CO_2 are absorbed, is lower for MDEA [14]. MDEA is also robust with respect to thermal degradation and can handle high temperatures in the regeneration unit. When H_2S and CO_2 is present, degradation of MDEA will occur at a faster rate, but it is reported to be lower than other amines [15]. In general, it is not recommended to have temperatures higher than 130 ^oC in the regeneration unit [16]. However, plant data from an acid gas removal unit using MDEA have been reported to operate with 132.1 ^oC in the reboiler [17].

Another advantage is that MDEA has a low vapour pressure which means that high concentrated solutions can be used without having any significant losses during operation [13]. H_2S and CO_2 are both acidic gases which promote corrosion. As mentioned, amines vary in corrosiveness, but tertiary amines are in general regarded as less corrosive than secondary and primary amines. This is because tertiary amines are regenerated more easily, and H_2S and CO_2 are more easily stripped from the rich solvent. The amount of acid gas absorbed in the solvent have an effect on the corrosion rate, and primary amines are more corrosive because of higher acid gas concentrations in the hot areas of the process. An additional advantage is that MDEA does not form carbamate, when reacting with CO_2, which has been reported to increase corrosivity [2]. Solution concentration may also have an impact on corrosiveness, and MDEA concentrations above 50-55 wt% is not recommended [2, 9, 13]. MDEA has a higher viscosity compared to monoethanolamine (MEA), and increases with increasing concentrations [10]. Using higher concentrations will therefore affect pumping costs. Increasing the lean MDEA temperature decreases the viscosity, but H_2S and CO_2 solubility decreases with increasing temperatures and needs to be considered when lean MDEA concentration and temperature are set.

2.3.2 Monoethylene glycol

Using a MEG injection system is one of the most widely used processes for continuous flow assurance control. Glycols are the most common chemicals that are used for dehydration and hydrate inhibition. MEG is traditionally used for hydrate inhibition in pipelines, and TEG is mostly utilized in topside dehydration systems. Common for all the glycols are that they are hygroscopic[1] and physically absorbs water [13]. In this thesis, natural gas dehydration was examined to prevent hydrate formation using MEG as the dehydration solvent. MEG has two hydroxyl groups (OH^-) connected to a hydrocarbon chain. An illustration of the MEG molecule is shown in Figure 2.3.2.

Figure 2.3.2: Illustration of the molecular structure of MEG.

[1] Glycols have high affinity for water, thus glycols are hygroscopic [13].

As for MDEA, MEG has the capability of being regenerated. A typical injection concentration is 90% MEG for hydrate inhibition. One of the disadvantages may be that higher concentrations will be needed for reaching desired water pipeline specifications, and regenerating to concentrations above 96% may be difficult [13]. The reason for choosing MEG in this work is because it is less viscous than TEG, and may be a better choice in colder climate areas [13]. MEG is a good alternative to inhibit hydrate formation, but does not degrade hydrates that are already formed. Hydrate formation before the injection point can therefore cause problems [10]. The decomposition temperature for MEG has been reported to be 165 ^{o}C [18].

2.4 Process description of purification and dehydration units

2.4.1 Chemical absorption of H_2S and CO_2 in MDEA

A typical process flow diagram (PFD) for chemical absorption of H_2S and CO_2 using a MDEA solvent, including the amine regeneration unit, is given in Figure 2.4.1. In the PFD, 'sour gas' is defined as natural gas contaminated with CO_2 and H_2S. 'Sweet gas' refers to the processed gas leaving the absorber column, and 'acid gas' is mainly CO_2 and H_2S removed from the system.

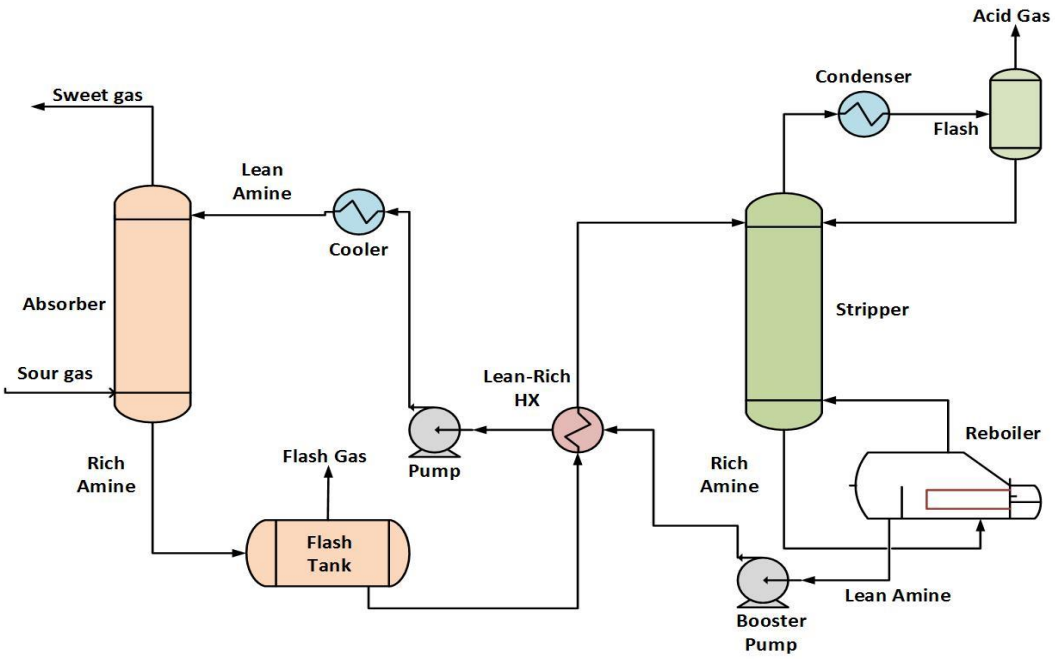

Figure 2.4.1: Simplified Process Flow Diagram (PFD) for a typical amine absorption process. The PFD shows the absorption column and the amine regeneration system. H_2S and CO_2 is recovered in the 'Acid gas' stream [13].

Sour gas, is taken into the bottom of the absorber and contacted counter-current with a lean aqueous MDEA solvent. The inlet temperatures of the absorber are quite low, typically around 30-40 ^{o}C, but the temperature in the column varies because of the exothermic absorption reactions. The temperature profile of the column is often shaped like a bulge, and the bottom temperature is usually higher than in the top. The purified gas, sweet gas, is taken

out of the top of the column and sent for further processing. Typically, a dehydration process follows the sweetening unit. This is because aqueous MDEA solutions are used, and the sweet gas will therefore contain water. The gas leaving the contactor is often called 'sweet gas' because the acidic components, H_2S and CO_2, have been removed.

Rich amine, rich in acid gas components, is taken out of the bottom of the absorber and flows to the regeneration unit. The pressure is first reduced in a flash tank to remove any co-absorbed hydrocarbons. The amount of acid gas components leaving with the flash gas is usually low. A lean-rich heat exchanger is used to preheat the rich amine solution, and is partially stripped before it flows into the stripping column. Stripper pressures are usually low, down to 1 bar, and a depressurizing valve can be utilized upstream the column.

The stripper column is the main component in the regeneration unit, and the reboiler provides both sensible heat and heat for reversing the reactions between acid gas and the amine. The amine solution is contacted counter-current with steam, which strips the amine of H_2S and CO_2. Stripping steam is generated because the amine solution is heated in the reboiler and because condensed water coming in as reflux is heated. Mainly H_2O, H_2S and CO_2 leave the top of the column which enables recovery of acid gas, by sending the condensed water back to the column.

The hot lean amine solution is taken out of the stripper and flows through the lean-rich heat exchanger. It is then pumped up to the absorber pressure, and cooled before contacted with the sour gas again [13]. The temperature of the lean amine entering the absorber is usually 5 ^oC higher than the sour gas to prevent co-absorption and condensation of hydrocarbons [17].

2.4.2 Physical absorption of H_2O in MEG

As mentioned earlier, topside dehydration is normally done by TEG absorption. However, since MEG is the solvent that is examined in this work, a process description using MEG for hydrate inhibition is explained in this chapter. A simple illustration of a MEG injection and regeneration loop is given in Figure 2.4.2 [19]. Lean MEG is injected into the pipeline to inhibit hydrate formation. At the processing plant, the rich MEG is regenerated and reinjected into the pipeline again. Water and waste are taken out of the processing plant.

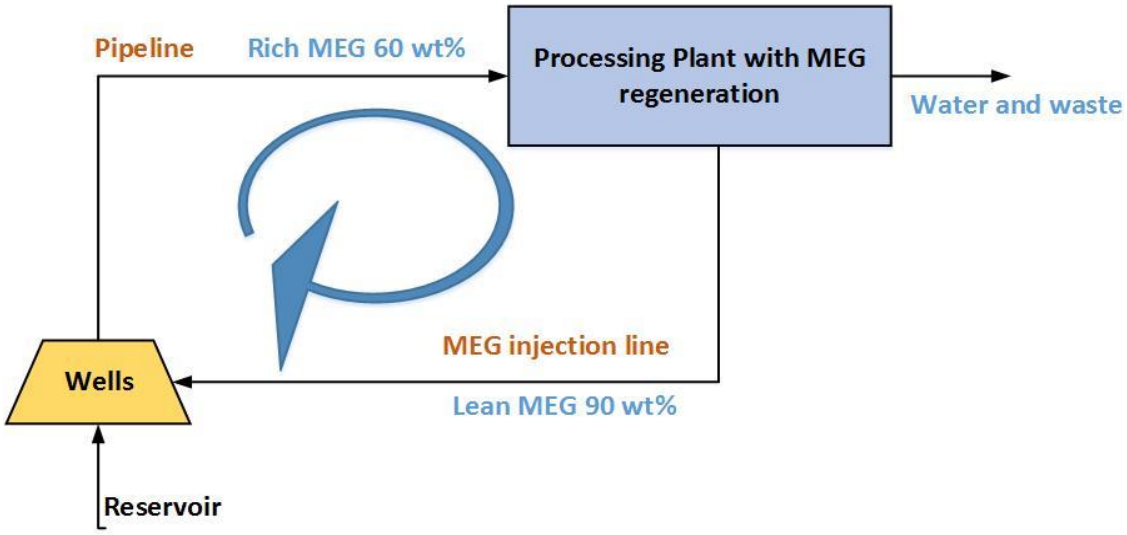

Figure 2.4.2: Illustration of the MEG injection and regeneration loop [19].

MEG regeneration can be done multiple ways. The main differences are between MEG regeneration and MEG reclamation. MEG regeneration is the process where only water is evaporated, and MEG flows through the processing unit as liquid. The downside with this configuration, is that any salts or chemicals are not separated from lean MEG, which means that MEG may be polluted over time. MEG reclamation is a configuration where both water and MEG are evaporated, and salts and pollutants are taken out in a liquid phase [19]. An illustration of a simple MEG regeneration and a MEG reclamation process are illustrated in Figure 2.4.3. Only simple regeneration was considered in this work.

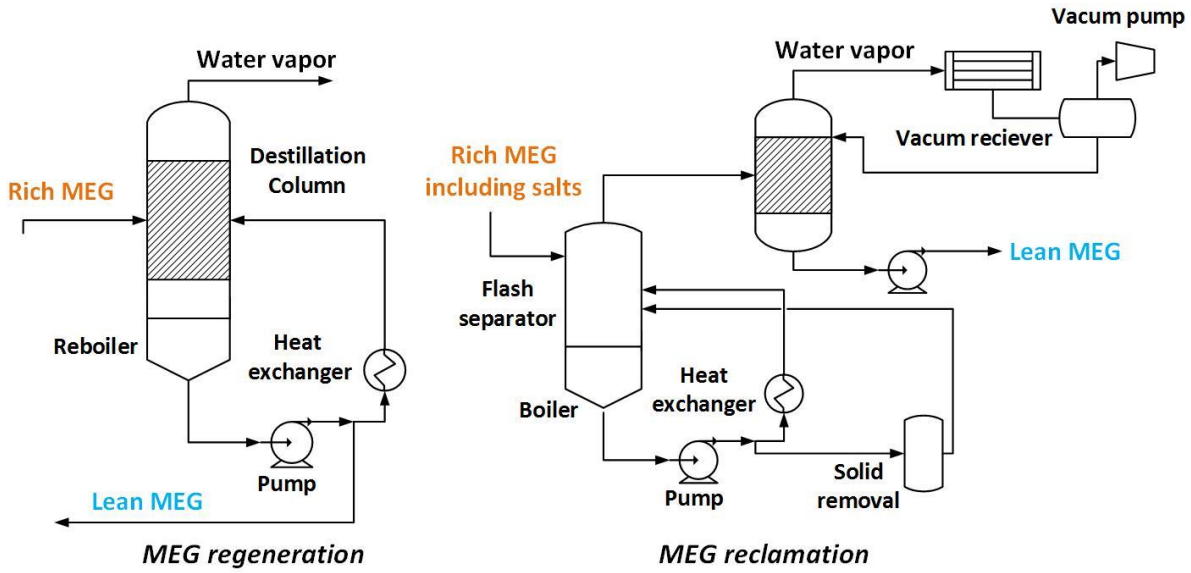

Figure 2.4.3: Illustration of MEG regeneration (left) and MEG reclamation (right) processes [19].

2.4.3 Combined gas purification and dehydration – a literature study

Literature studies addressing combined acid gas removal and dehydration system are limited. In acid gas absorption systems, the alkanolamines are used as absorbents in aqueous solutions, which means that the treated gas will be saturated with water vapor. This is why most gas processing systems have a dehydration system downstream the acid gas removal unit. According to Campbell [13], a combined process will work for acid gas removal but it can be difficult to reach water specifications, which again can cause a problem with respect to corrosion. Designing a combined purification and dehydration system can make the gas processing more effective and compact, and some process descriptions found in literature are presented in this chapter.

The first patented process for simultaneous acid gas removal and dehydration was suggested by Hutchinson [20] in 1939. The process was designed to use a combination of solvents, where one was for absorbing acid gas and the other for absorbing water, regenerating both of them. The process was patented for using a combination of glycol and amine as solvents, and it was recommended to use glycol in excess of the amine. A PFD of the process is given in Figure 2.4.4. The gas to be treated (stream *10a*) enters the absorber (*14*), where it is contacted counter current with the lean solvent mixture (*15*). The treated gas (*16*) is then condensed to recover solvent carry over, and the gas is then taken out (*21*). The regeneration system works in the same way as described in Chapter 2.4.1.

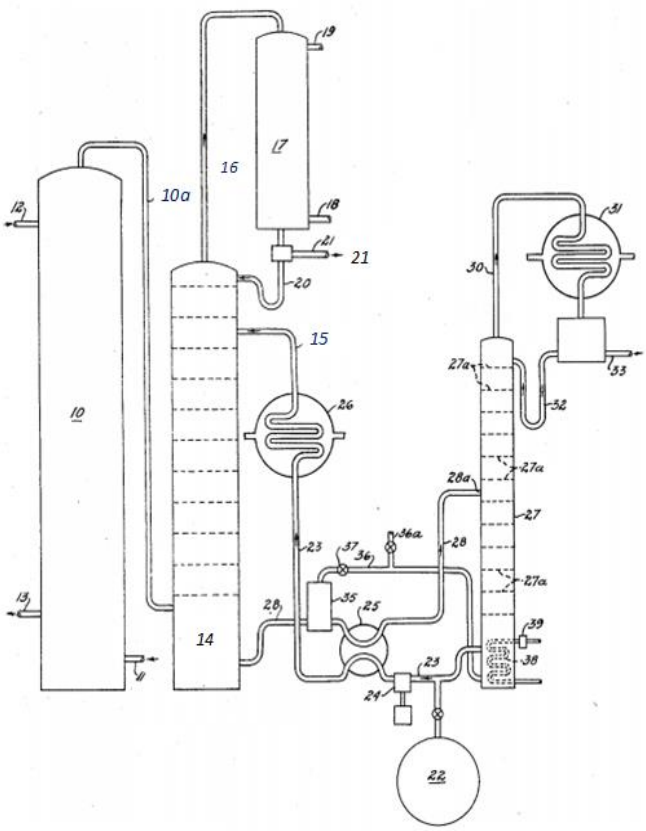

Figure 2.4.4: PFD of the gas treating process patented by Hutchinson [20] in 1939. The system is designed for combined acid gas removal and dehydration.

In 1948, a new improved process was suggested by McCartney [21]. The process proposed by Hutchinson [20] in 1939 was based on using high concentrations of glycol (50% to 90% by volume) and keeping the amine concentration fairly low (2% to 20% by volume). The problem with this process, according to McCartney, was that it would require large solvent circulation rates. The reason for this was that much smaller concentrations of amine could be used, compared to normal aqueous amine treatments units, to assure that amine losses were kept constant. He therefore proposed a process where the gas was contacted counter current with an amine solution in the lower part of the absorber where H_2S and CO_2 could be removed. Water removal was suggested in the top of the column, feeding the glycol solvent into the top of the absorber. The PFD of the patented process is shown in Figure 2.4.5, and was redrawn in this work based on the original patent.

The glycol solvent is taken out of the absorber (*18*) above the lean amine inlet stage (*19*), and regenerated by heating up the rich solvent. Acid gas and water vapor is taken out of the top of the glycol stripper (*34*), and sent to the amine stripper (*23*). The rich amine solution is taken out of the bottom of the absorber (*20*) and regenerated in the conventional way.

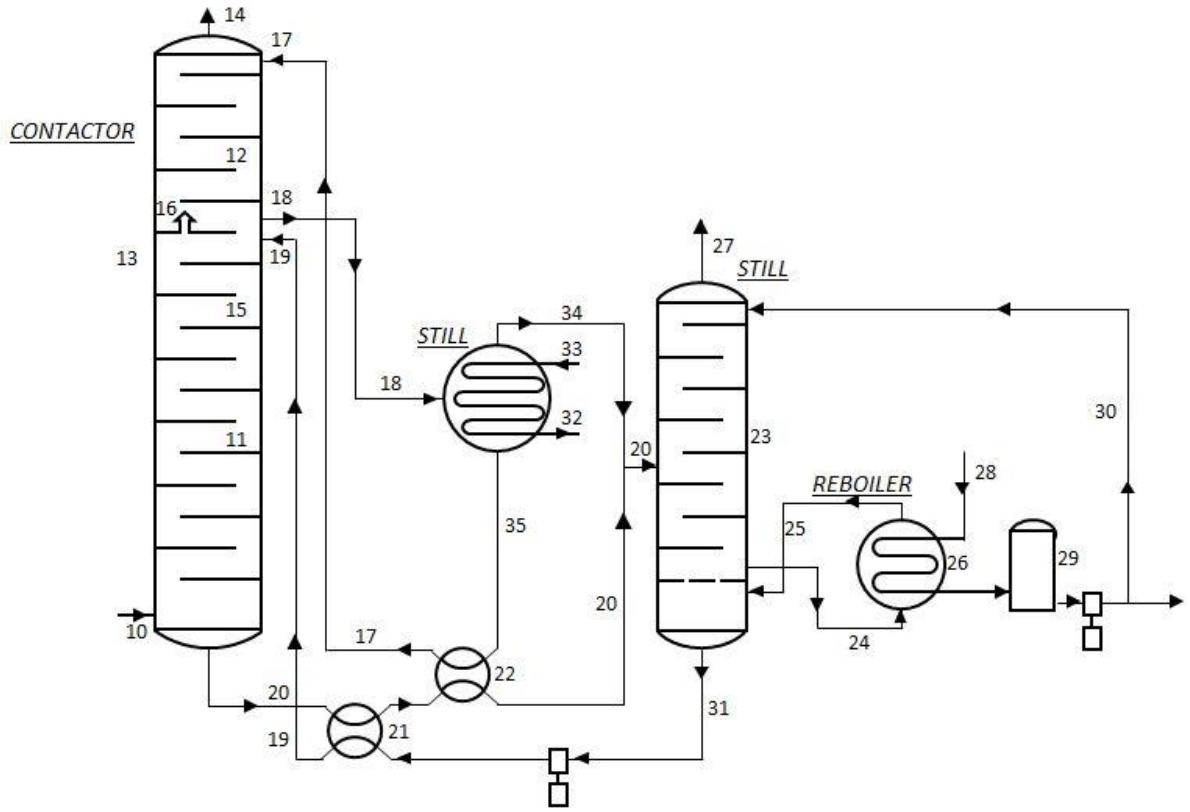

Figure 2.4.5: PFD of the gas treating process patented by McCartney [21] in 1948.

Chapin [22] patented a new process in 1950 based on the process proposed by McCartney. The problem Chapin found in McCartney's process was the possibility of vaporization and carry-over of the glycol solvent into the amine solvent, which in turn could lead to depletion of the glycol solvent. He therefore proposed a process where the loss from the glycol stripper was compensated for. A PFD of the patented process is given in Figure 2.4.6. The gas flows into the column (*10*) and is contacted counter current with a amine-glycol-solvent (*12*). Gas

dehydration takes place in the top of the column (*23*) where it is contacted with a glycol solvent (*26*). The rich solvent is taken out, loaded with water and amine-carry over, and sent for regeneration (*27*). The solvent is recovered in a reboiler (*29*) and sent to an accumulator (*32*). To handle the problem of glycol carry-over in stream (*30),* Chapin suggested using the lean amine-glycol solution as make up for the dehydration solvent. These make-up streams can be seen as streams (*38)* and (*42),* and is controlled by a level controller (*40*).

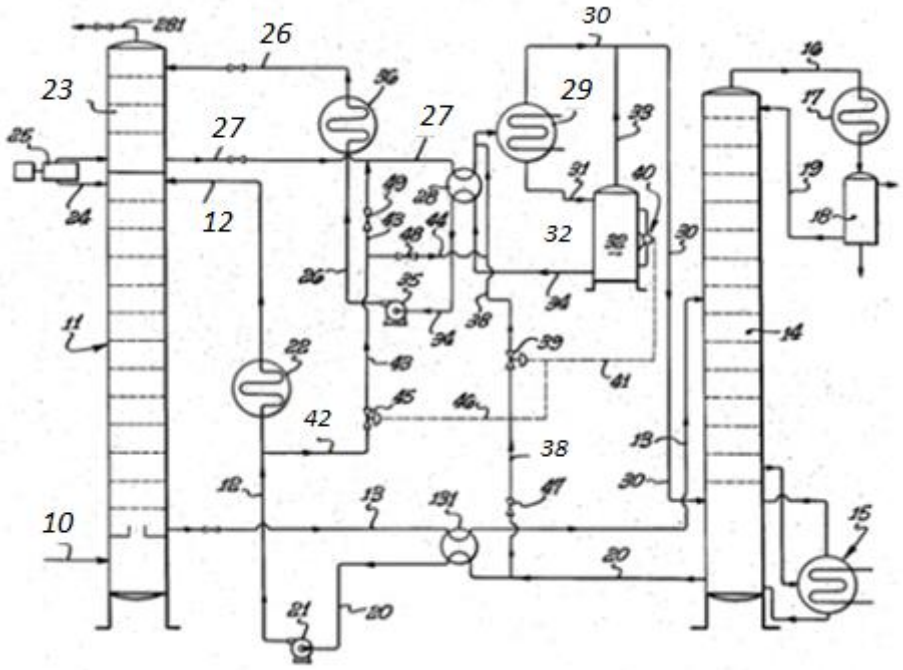

Figure 2.4.6: Process flow diagram of the gas treating process patented by Chapin [22] in 1950.

After this, in 1951, McCartney [23] proposed an improved process to handle the issues discussed by Chapin in 1950, regarding glycol solvent depletion. A PFD of the patented process is given in Figure 2.4.7. The gas (*10*) is contacted with an amine-glycol solvent (*12*). The rich solution (*13*) is regenerated normally in a still column (*15*). The gas in then contacted with a glycol solution (*28*) for water dehydration. To account for glycol carry-over in stream (*35),* condensate from the upper trays in still (*15)* is used as reflux, assuring condensation of glycol vapor.

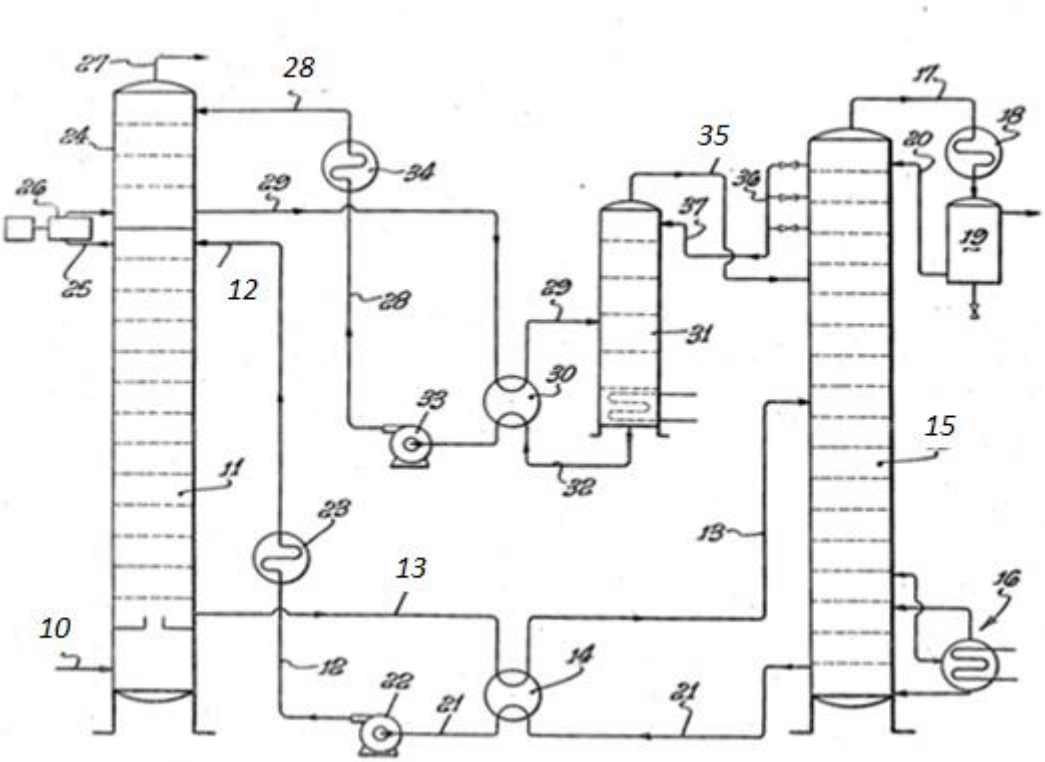

Figure 2.4.7: Process flow diagram of the gas treating process patented by McCartney [23] in 1951.

Dag Eimer [24] developed a process for simultaneous removal of water and H_2S from natural gas as a part of his PhD thesis at NTNU in 1994. This process was based on using TEG for water absorption and MDEA for H_2S absorption. He found that the process was satisfying with respect to absorption rate of H_2S and water. However, it required high circulation rates compared to typical glycol dehydration units. Analysis also showed that the solvent capacity for water was lower in the presence of MDEA.

2.5 Chemical absorption reactions

The chemical absorption reactions for H_2S and CO_2 in MDEA are given in Table 2.5.1. The reactions are presented as defined in the 'ElecNRTL_Rate_Based_MDEA_model' template in Aspen Plus version 8.6. MDEA chemically absorbs H_2S and CO_2, and the process is called chemisorption. There are no reactions defined for the H_2O-MEG system, because MEG physically absorbs H_2O and is called physisorption. Net absorption reactions for H_2S and CO_2 in MDEA are given in Table 2.5.2.

Table 2.5.1: Chemical reactions for the H_2S-CO_2-MDEA system defined in Aspen Plus version 8.6. Reactions retrieved from the 'ElecNRTL_Rate_Based_MDEA_model' template.

Reaction	Type	Stoichiometry
1	Equilibrium	$MDEAH^+ + H_2O \leftrightarrow MDEA + H_3O^+$
2	Equilibrium	$2\,H_2O \leftrightarrow H_3O^+ + OH^-$
3	Equilibrium	$HCO_3^- + H_2O \leftrightarrow CO_3^{2-} + H_3O^+$
4	Kinetic	$CO_2 + OH^- \rightarrow HCO_3^-$
5	Kinetic	$HCO_3^- \rightarrow CO_2 + OH^-$
6	Equilibrium	$H_2S + H_2O \leftrightarrow HS^- + H_3O^+$
7	Equilibrium	$HS^- + H_2O \leftrightarrow S^{-2} + H_3O^+$
8	Kinetic	$MDEA + CO_2 + H_2O \rightarrow MDEAH^+ + HCO_3^-$
9	Kinetic	$MDEAH^+ + HCO_3^- \rightarrow MDEA + CO_2 + H_2O$
10	Equilibrium	$CO_2 + 2\,H_2O \leftrightarrow HCO_3^- + H_3O^+$

Table 2.5.2: Net absorption reactions for the H_2S-CO_2-MDEA system [25].

Reaction	Type	Stoichiometry
11	Equilibrium	$MDEA + H_2S \leftrightarrow MDEAH^+ + HS^-$
12	Kinetic	$MDEA + CO_2 + H_2O \leftrightarrow MDEAH^+ + HCO_3^-$

Protonation of MDEA is given by reaction 1. Reaction 2 represents the dissociation of water. Reaction 4 gives the dissociation of CO_2 to HCO_3^- (bicarbonate). The equilibrium reaction for this is shown as reaction 10. The second dissociation reaction for CO_2, forming CO_3^{2-} (carbonate), is given by reaction 3. Reaction 5 is simply reaction 4 reversed. Reaction 6 gives the dissociation of H_2S to HS^- (bisulfide), while reaction 7 gives the dissociation of HS^- to S^{2-} (sulfide). The net reaction between MDEA and CO_2 is given as reaction 8. Reaction 9 is reaction 8 reversed.

For processing gas that contains both H_2S and CO_2, MDEA is regarded as a good choice of solvent. The main reason for this is because MDEA can provide selective removal of H_2S. Because MDEA is a tertiary alkanolamine and has a methyl group connected to the nitrogen atom, as seen in Figure 2.3.1, CO_2 will not react with MDEA and form carbamate. H_2S is known to react with MDEA by a proton transfer as seen in reaction 11, and this reaction is fast. CO_2 is first dissolved in water and then reacts to form bicarbonate. This is often the rate determining step for the absorption process and is a slow kinetic reaction. CO_2 does not react directly with MDEA as seen from reaction 12 or reaction 8, and is first dissolved in water. Absorption of CO_2 is therefore slow, and allows selective chemisorption of H_2S. Reaction 3 is also slow [25]. When both H_2S and CO_2 are present in the gas stream, MDEA often gives a bulk removal of CO_2 and may result in higher CO_2 concentrations in the sweet gas than desired, dependent on the initial gas concentrations [10].

The absorption reactions are exothermic, and will increase the temperatures in the absorption column. Regeneration of the rich MDEA solution is therefore energy demanding because the reactions need to be reversed. The heat of absorption is not constant, but dependent on the

acid gas loading in the liquid phase. Loading of component *i*, α_i, is defined as moles of component *i* absorbed per mole amine. The heat of absorption is typically nearly constant up to a certain load, and after that decreasing for increasing loadings. The heat of absorption for MDEA is lower than for primary amines, such as monoethanolamine (MEA). This is regarded as an advantage with respect to regeneration, because reversing the reactions will require less energy. An additional advantage is that H_2S has a lower heat of reaction in MDEA than CO_2 [14].

2.6 Literature VLE data

A list of literature solubility data for H_2S, CO_2, CH_4 and H_2O in MDEA and MEG is given in Table 2.6.1. This is VLE data for the system specified and was used for the VLE validations which are examined in Chapter 3. The table shows solvent concentration, c_s, temperature range, pressure range and the VLE data unit. Most of the sources listed in Table 2.6.1 report solubility data for binary systems. Available VLE data for the ternary system of interest, H_2S-MDEA-MEG, are limited. Solubility of CO_2 and H_2S mixtures in a MDEA-MEG-H_2O solvent have been reported by Xu et al. [26]. The VLE data was measured at 40 ^oC, 60 ^oC and 90 ^oC with partial pressures of H_2S ranging from 0.34 to 38.8 kPa. However, there are only reported five data points for each temperature.

Table 2.6.1: Experimental solubility data for different gas-MDEA and gas-MEG systems.

Source	**System** ***g-s***	**Concentration** c_s	**Temperature** **T**	**Pressure range** P_g	**Type of solubilitydata**
Jou et al. [14]	H_2S-MDEA CO_2-MDEA	1.0, 2.0, 4.28 kmol MDEA/m^3	25-120 ^oC	0.001-6600 kPa	mol/mol MDEA
MacGregor and Mather [25]	H_2S-MDEA CO_2-MDEA	2.0 mol MDEA /dm^3	40 ^oC	0.52-3770 kPa	mol/mol MDEA
Jou et al. [27]	CO_2-MDEA	3.04 kmol MDEA/m^3	40 ^oC 100 ^oC	0.004-236 kPa	mol/mol MDEA
Jou et al. [28]	CH_4-MDEA C_2H_6-MDEA	3 kmol MDEA/m^3 (34.7 wt%)	25-130 ^oC	0-13000 kPa	Mole fraction
Jou et al. [29]	H_2S-MEG CO_2-MEG	99.5% MEG 0.5% H_2O	25-125 ^oC	0-6700 kPa 0-20000 kPa	Mole fraction
Galvão and Francesconi [30]	CH_4-MEG CO_2-MEG	99.8% MEG	30-150 ^oC	0-14000 kPa	Mole fraction
Zheng et al. [31]	CH_4-MEG CO_2-MEG N_2-MEG	99.9% MEG	50-125 ^oC	0-40000 kPa	Mole fraction
Horstmann et al [32]	H_2O-MEG	99.99% MEG	60-80 ^oC	0.22-47.44 kPa	Mole fraction
Gonzales and Van Ness [33]	H_2O-MEG	99.5% MEG	50 ^oC	0.316-12.082 kPa	Mole fraction
Villamañan et al. [34]	H_2O-MEG	99%MEG	60 ^oC	0.214-19.931 kPa	Mole fraction
Xu et al. [26]	CO_2/H_2S-MDEA-MEG	30 wt%MDEA+ 65 wt%MEG + 5 wt% H_2O	40-90 ^oC	2.91-70.75 kPa	mol/mol MDEA

Chapter 3 Vapor-liquid equilibrium validation

This chapter gives assumptions for the VLE validation and information about the template model that was used as a basis for the simulations. All the VLE systems that were analysed are represented and discussed in this chapter.

3.1 Assumptions

A vapor-liquid equilibrium (VLE) validation was performed to analyse the accuracy of the VLE model available in Aspen Plus, compared to literature data. This gives an indication of how reliable the model in Aspen Plus is, which is important for absorption and stripper simulations. The VLE curves were simulated using a simple flash at the same operating conditions as in literature. An illustration of the flash setup used for all VLE simulations is given in Figure 3.1.1.

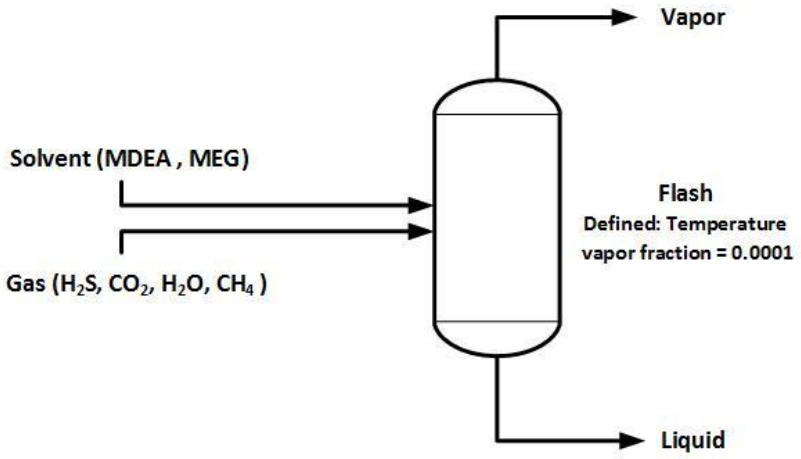

Figure 3.1.1: Flash setup used in Aspen Plus for the VLE simulations.

The VLE results are presented by the partial pressure of gaseous component *i*, P_i, as a function of loading, α_i, in mole per mole solvent or mole fraction (dimensionless). Partial pressure of component *i* was calculated from Raoult's law [35], as given in Equation 1. Mole fraction of component *i* in the vapor phase is denoted by y_i, and P_{tot} is the total pressure.

$$P_i = y_i P_{tot} \tag{1}$$

To analyze the VLE data from Aspen Plus and compare it with literature data, the percentage deviation, $\%\Delta_i$, was calculated from Equation 2. This equation gives the percentage deviation between simulated partial pressures, P_{sim}, and experimental partial pressures, P_{exp}, for a given loading or mole fraction. The average absolute deviation for the loading range, defined as AD in this work, was calculated from Equation 3. Average deviation, $\overline{\%\Delta}$, was calculated by Equation 4, and used to find the absolute average deviation, AAD, given by Equation 5. In the equations, *n*, is the number of data points in the loading range. The simulated partial pressures corresponding to the experimental loadings were found by linear interpolation and calculated

by Equation 6, where the partial pressure was estimated between point 1 and 2 at a given experimental loading, α_{exp}. Average absolute deviation, AD, and absolute average deviation, AAD, are used to discuss the Aspen Plus model compared to literature data in this work.

$$\%\Delta_i = \frac{P_{sim} - P_{exp}}{P_{exp}} \cdot 100\% \tag{2}$$

$$AD = \frac{1}{n}\sum_{i=1}^{n} |\%\Delta_i| \tag{3}$$

$$\overline{\%\Delta} = \frac{1}{n}\sum_{i=1}^{n} \%\Delta_i \tag{4}$$

$$AAD = \frac{1}{n}\sum_{i=1}^{n} |\%\Delta_i - \overline{\%\Delta}| \tag{5}$$

$$P_{sim} = P_1 + (P_2 - P_1)\left(\frac{\alpha_{exp} - \alpha_1}{\alpha_2 - \alpha_1}\right) \tag{6}$$

3.2 Aspen Plus template model

All the simulations conducted in this work were performed in Aspen Plus version 8.6, and the template 'ElecNRTL_Rate_Based_MDEA_model' was used as a basis. Elec-NRTL is a property method that can be used for acid gas absorption systems utilizing amines. It is the most versatile electrolyte property method, and can handle a wide range of concentrations of aqueous and mixed solvents. It uses the Redlich-Kwong equation of state for calculating vapor phase properties, and binary and pair parameters, in addition to equilibrium constants based on experimental data, are stored in databanks in Aspen Plus [36].

The chemical reactions defined in the template model are already discussed and given in Table 2.5.1. For equilibrium reactions, the equilibrium constant, K_{eq}, can be calculated from Gibbs energies or from a built-in expression which gives the temperature dependency. The temperature dependency of the equilibrium constants in Aspen Plus is calculated from Equation 7.

$$ln\, K_{eq} = A + \frac{B}{T} + C ln T + DT \tag{7}$$

Temperature, *T*, is given in degrees Kelvin. Coefficients *A*, *B*, *C* and *D* are based on experimental equilibrium data and retrieved from databanks, but can also be user defined. In the original template model, the temperature dependency is defined for reaction 6 and 7 (see Table 2.5.1), and the coefficients are given in Table 3.2.1. Coefficients defined for reaction 6 in Aspen Plus were found to be based on Austgen et al. [37]. Finding the source of the coefficients for reaction 7 was not successful, and are given as defined in the template model.

Table 3.2.1: Temperature dependency of equilibrium constants, $ln\,K_{eq} = A + \frac{B}{T} + ClnT + DT$, for the given reaction. Coefficient values given as defined in the Aspen Plus template 'ElecNRTL_Rate_Based_MDEA_model'.

Rx. number	Reaction	A	B	C	D
6	$H_2S + H_2O \leftrightarrow HS^- + H_3O^+$	214.582	-12995.4	-33.5471	-
7	$HS^- + H_2O \leftrightarrow S^{-2} + H_3O^+$	-9.742	-8585.47	-	-

3.3 VLE validation

A brief overview of all the binary VLE systems and which data source they were compared with are given in Table 3.3.1. It also gives the solvent concentration range, c_s, temperature range, partial pressure- and loading range for the given component, *g*, and number of data points analysed from the given source. AD and AAD were calculated for the whole range of data, and minimum and maximum values are given here. VLE curves for the binary systems given in Table 3.3.1 are shown and more thoroughly discussed in Chapter 3.3.1 to Chapter 3.3.8. The validations were performed by using a sensitivity analyser in Aspen Plus, with maximum 1,000 data points for each run. In total, 500 experimental data points were evaluated.

As seen from the table, the experimental data are obtained over large intervals, and the partial pressures intervals are wide. AD's between experimental partial pressures and simulated pressures range from 3.5% to 218.6%. The ElecNRTL model in Aspen Plus should give accurate results for vapor phase calculations up to medium pressures, but it is recommended that binary interaction parameters are fitted to the operational window [36]. This was not within the scope of this thesis, but the model can be fitted to the relevant area of operation to assure better predictions.

Table 3.3.1: Overview of VLE validations of different gas-solvent (*g*-*s*) systems. Average absolute deviation (AD) and absolute average deviation (AAD) were calculated between experimental data and the VLE model available in Aspen Plus. Aqueous concentration of solvent *s* is given as c_s. Minimum and maximum values of the pressure and loading range, $P_{g,exp}$ and $\alpha_{g,exp}$, from the respective source are given. The number of experimental data points that were validated for each source is denominated as *n*.

System *g*-*s*	Data source	c_s [wt%]	T_{exp} [°C]	$P_{g,exp}$ [kPa]	$\alpha_{g,exp}$ [mol g/mol s]	*n*	AD [%]	AAD [%]
CO_2-MDEA	[14]	23.7 – 50.1	25-120	0.000217-6570	0.00037-1.833	100	23.2-100.1	6.4-68
	[25]	23.7	40	1.17-3770	0.124-1.203	5	47.0	6.4
H_2S-MDEA	[14]	11.9 – 50.1	25-120	0.0013-5840	0.00129-2.902	91	12.2-174.8	11.1-174.6
	[25]	23.7	40	0.52-1600	0.13-1.725	27	21.7	18.7
CH_4-MDEA	[28][a]	34.7	25-130	95-13210	0.000042-0.00326	30	49.5-112.5	9.1-47.6
CO_2-MEG	[29][a]	99.5	25-125	29.3-20290	0.000693-0.1388	31	22.1-100.5	18.2-52.6
	[30][a]	99.8	50-125	425.5-5421	0.0045-0.0508	12	15.5-72.9	15.5-32.5
	[31][a]	99.9	50-125	895-38400	0.0049-0.1724	30	39.7-218.6	33.7-11.4
H_2S-MEG	[29][a]	99.5	25-125	3.2-6750	0.00011-0.482	38	14.6-43.6	17.2-38.9
CH_4-MEG	[30][a]	99.8	30-150	1367.4-13726.4	0.0015-0.0291	25	11.9-47.4	6.7-15.6
	[31][a]	99.9	50-125	200-39617	0.0003-0.00421	31	7.9-26.9	2.2-3.5
H_2O-MEG	[32][a]	99.99	60	0.28-19.92	0.00327-0.99968	37	6.8	9.8
	[34][a]	99	60	0.543-19.428	0.0188-0.9797	22	3.5	3.6
	[33][a]	99.5	50	0.316-12.082	0.0185-0.9803	21	4.2	3.6

[a]Solubility data for component *g* in solvent *s* given in mole fraction, x_i, not loading, α_i.

As mentioned in Chapter 2.6, solubility data for H_2S and CO_2 in the mixed solvent of interest, MDEA-MEG, are very limited. A VLE validation of H_2S-CO_2 mixtures in a 30 wt% MDEA + 65 wt% EG + 5 wt% H_2O solvent was conducted against the reported data by Xu et al. [26]. AD and AAD between the Aspen model and experimental data are given in Table 3.3.2. The VLE validation for this system is discussed in Chapter 3.3.9, but it can be noted already here that simulated partial pressures experience large deviations from the experimental values.

Table 3.3.2: AD and AAD between experimental VLE data and Aspen Plus VLE values for H_2S-CO_2 mixtures in a 30 wt% MDEA + 65 wt% EG + 5 wt% H_2O solvent at 40 °C, 60 °C and 90 °C [26]. The number of experimental data points that were validated is denominated as *n*. Minimum and maximum values of the pressure and loading range, P_i and α_i, for the different temperatures are given.

T [°C]	P_{CO_2} [kPa]	α_{CO_2} [mol CO_2/mol s]	P_{H_2S} [kPa]	α_{H_2S} [mol H_2S/mol s]	*n*	AD_{CO_2} [%]	AD_{H_2S} [%]	AAD_{CO_2} [%]	AAD_{H_2S} [%]
40	3.55-63.62	0.0154-0.106	1.1-37.97	0.0199-0.223	5	414.0	2308.5	204.9	1177.1
60	13.82-70.75	0.0128-0.0532	1.43-15.16	0.0173-0.0984	5	621.9	2263.8	135.7	470.0
90	17.52-69.45	0.00954-0.0201	1.78-40.37	0.0110-0.0748	5	389.8	1776.6	138.3	670.2

3.3.1 Solubility of CO_2 in aqueous MDEA solutions

Figure 3.3.1 and 3.3.2 give the VLE curves retrieved from Aspen Plus for CO_2 in 50.1 wt% and 23.7 wt% aqueous MDEA at 25 °C, 40 °C, 70 °C and 120 °C, compared to experimental data. AD and AAD between P_{exp} and P_{sim} over the experimental loading range for each MDEA concentration and temperature are given in Appendix A.1. This applies for all the VLE validations discussed in the next chapters.

At 25 °C and 40 °C the AD's are 32.1% and 33.1%, respectively, in a 50.1 wt% MDEA solution. AAD's are 29.8% and 21.4% at the same temperatures. At 70 °C, AD is as high as 100.1%, and Aspen Plus gives percentage deviations up to 292.9% (α_{CO_2}= 1.232). However CO_2 loadings above 1 (α_{CO_2}> 1), will most likely not need to be considered in further simulations, nor recommended in acid gas removal systems because of possibilities of increased corrosion rate [2]. For α_{CO_2}< 0.8, AD's are 20.8%, 30.5% and 46% for 25 °C, 40 °C and 70 °C respectively. Aspen Plus model values fit better to experimental data at lower loadings (α_{CO_2}< 0.8), compared to the whole range reported.

For stripper simulations, reboiler temperatures up to 130 °C can be expected [16]. At 120 °C, Aspen Plus gives AD's of 80.9% and 57.9 %, in 50.1 wt% and 23.7 wt% MDEA respectively. In further simulations, it is therefore expected high recoveries of CO_2 because Aspen Plus under-predicts solubility at high temperatures. This can be seen from Figures 3.3.1 and 3.3.2, where the Aspen plus VLE curve over-predicts partial pressures compared to the experimental points.

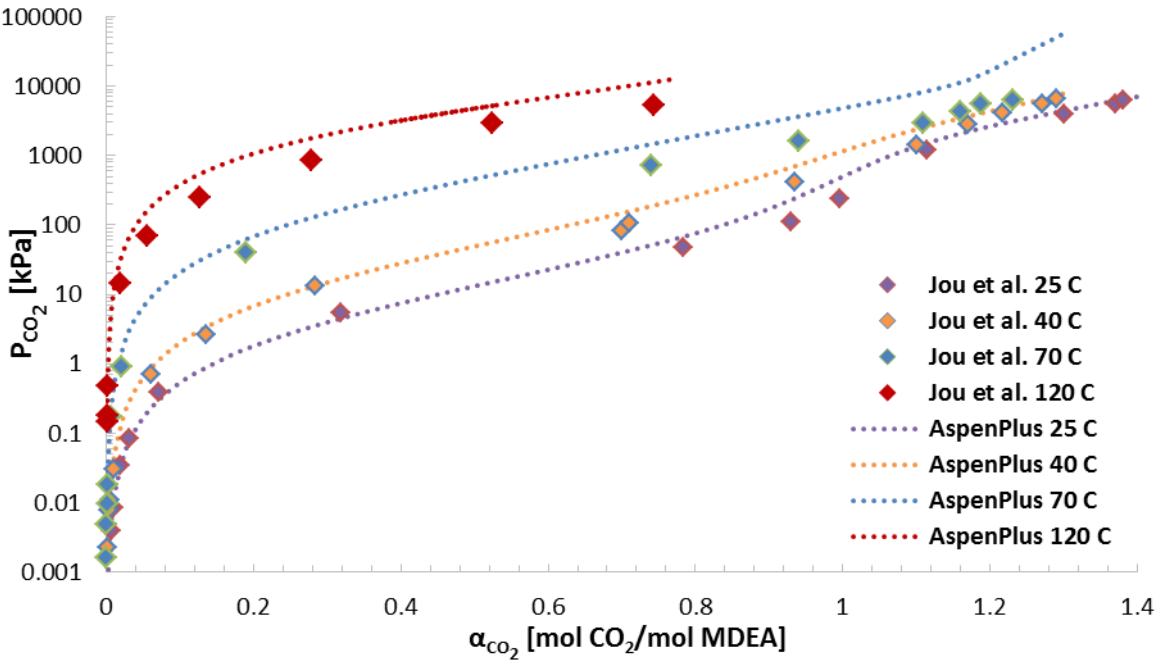

Figure 3.3.1: Partial pressure of carbon dioxide, P_{CO_2}, on a log scale as a function of loading, α_{CO_2}, in the liquid phase. The figure shows the VLE models retrieved from Aspen Plus for CO_2 in a 50.1 wt% aqueous MDEA solution at 25 °C, 40 °C, 70 °C and 120 °C, compared to experimental data reported by Jou et al. [14].

At 25 °C and 40 °C, the AD's are 23.2% and 28.4% in a 23.7 wt% MDEA solution, which are lower, compared to the retrieved results in a 50.1 wt% MDEA solution. AAD's are 19.5% and 26.7% at the same temperatures. At 70 °C, AD is 32.5%, which also shows a better fit than using a 50.1 wt% MDEA solution. Solubility of CO_2 decreases as the MDEA concentration is increased, and can be seen from Figure A.2.1 in Appendix A.2, where the CO_2 solubility in a 50.1 wt% MDEA solution is compared to 23.7 wt% MDEA.

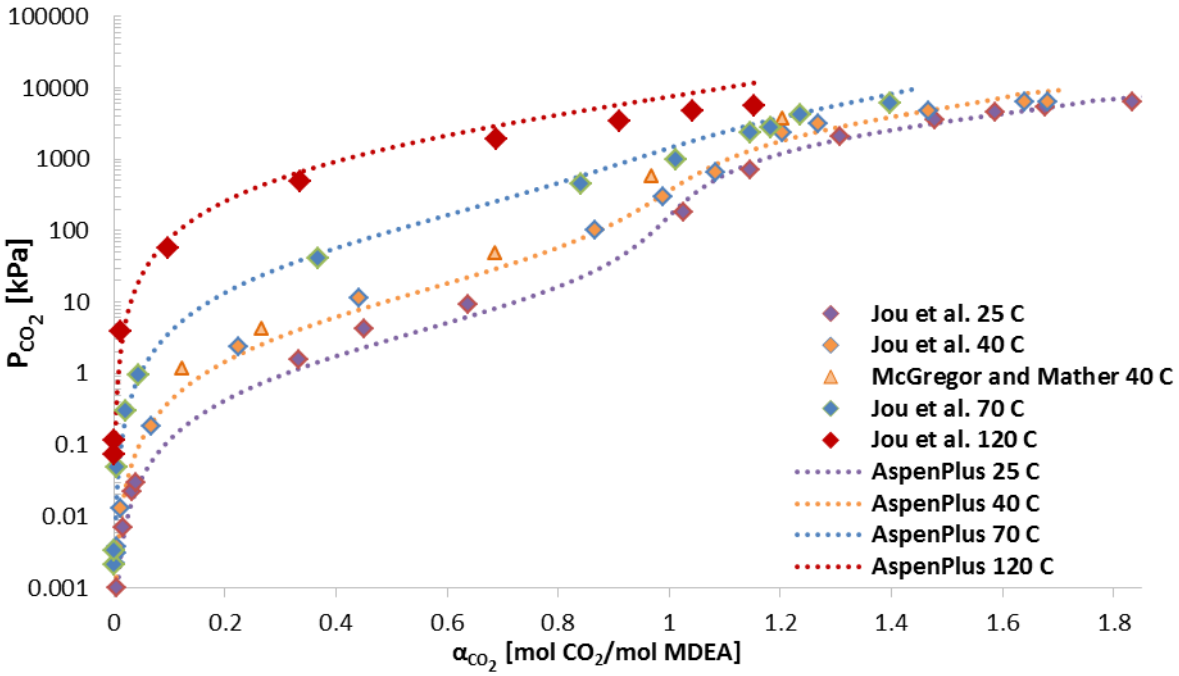

Figure 3.3.2: Partial pressure of carbon dioxide, P_{CO_2}, on a log scale as a function of loading, α_{CO_2}, in the liquid phase. The figure gives the VLE models retrieved from Aspen Plus for CO_2 in a 23.7 wt% aqueous MDEA solution at 25 °C, 40 °C, 70 °C and 120 °C, compared to experimental data reported by Jou et al. [14] and MacGregor and Mather [25].

3.3.2 Solubility of H_2S in aqueous MDEA solutions

Figures 3.3.3 and 3.3.4 give the VLE curves retrieved from Aspen Plus for H_2S in 50.1 wt% and 23.7 wt% aqueous MDEA solutions at 25 °C to 120 °C, compared to experimental data. Figure 3.3.5 shows Aspen Plus VLE curves at 40 °C compared to experimental data for 50.1 wt%, 23.7 wt% and 11.9 wt% MDEA solutions.

AD in a 50.1 wt% MDEA solution is lowest at 120 °C, with 96.5%, and the poorest result is at 40 °C with an AD of 174.8%. Percentage deviations are below 63% at loadings above 0.5. However $\alpha_{H_2S} > 0.5$ will not need to be considered in this thesis. Up to this point, the AD is up to 302% (at 70 °C). In general, Aspen Plus under-predicts the solubility of H_2S in a 50.1 wt% MDEA solution up to $\alpha_{H_2S} = 0.5$, and absorption simulations may require higher amine flowrates compared to reality.

The results using a 23.7 wt% MDEA solution, gives AD's of 15.6% at 40 °C and 12.2% at 100 °C. Aspen Plus gives a model that fits well with experimental data for lower MDEA concentrations, as it can be seen from Figure 3.3.4.

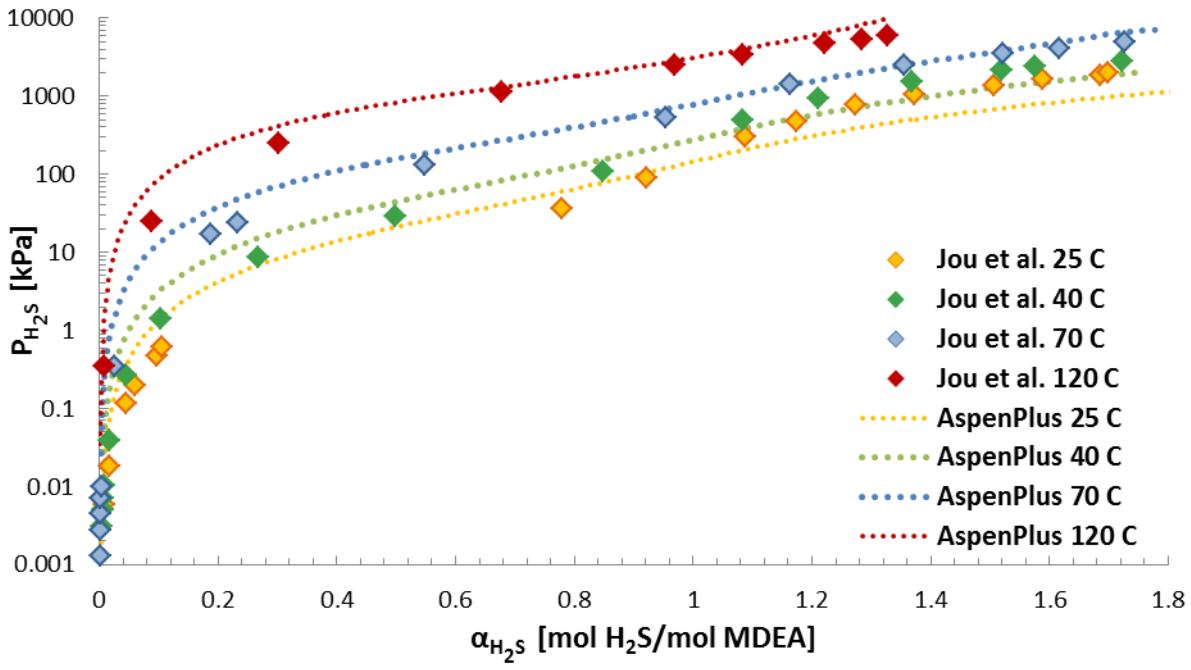

Figure 3.3.3: Partial pressure of hydrogen sulfide, P_{H_2S}, on a log scale as a function of loading, α_{H_2S}, in the liquid phase. The figure shows the VLE models in Aspen Plus for H_2S in a 50.1 wt% aqueous MDEA solution at 25 °C, 40 °C, 70 °C and 120 °C, compared to experimental data reported by Jou et al. [14].

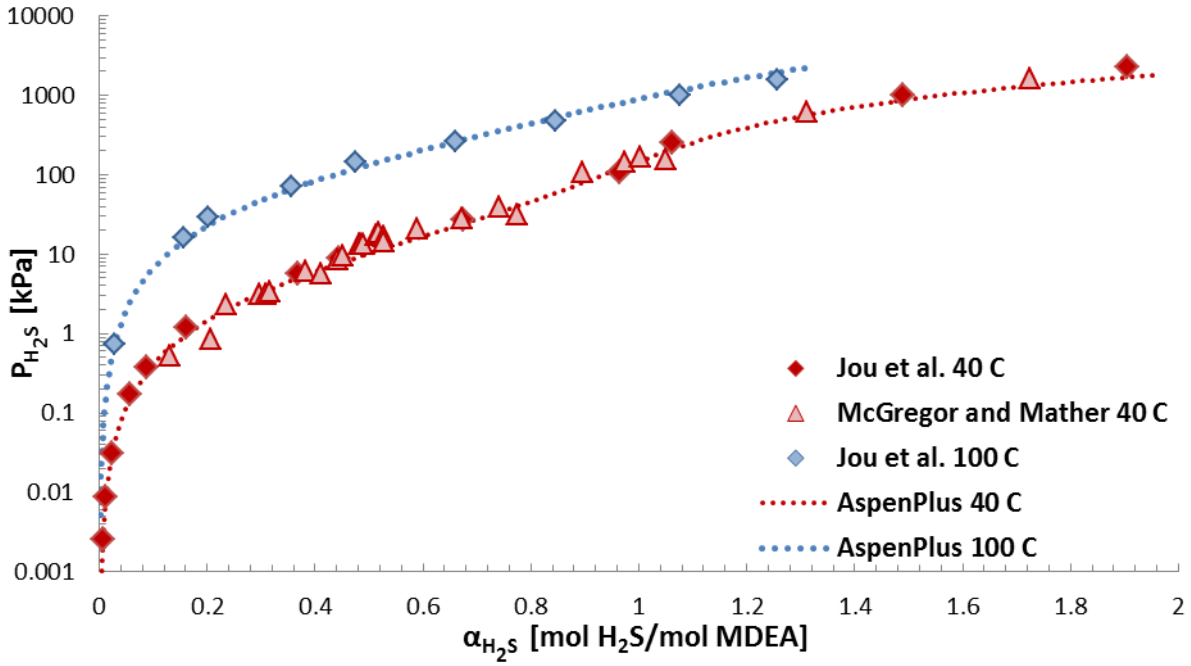

Figure 3.3.4: Partial pressure of hydrogen sulfide, P_{H_2S}, on a log scale as a function of loading, α_{H_2S}, in the liquid phase. The figure shows the VLE models in Aspen Plus for H_2S in a 23.7 wt% aqueous MDEA solution at 40 °C and 100 °C compared to experimental data reported by Jou et al. [14] and McGregor and Mather [25].

Figure 3.3.5 shows how the MDEA concentration affects the solubility of H_2S at 40 °C, and it can be seen that H_2S is more soluble in a 11.9 wt% MDEA solution compared to 23.7 wt% and 50.1 wt% MDEA. AD for a 11.9 wt% MDEA solution is 21.9%. The results in a

23.7 wt% and a 11.9 wt% MDEA solution were considered to be precise, based on the low deviations.

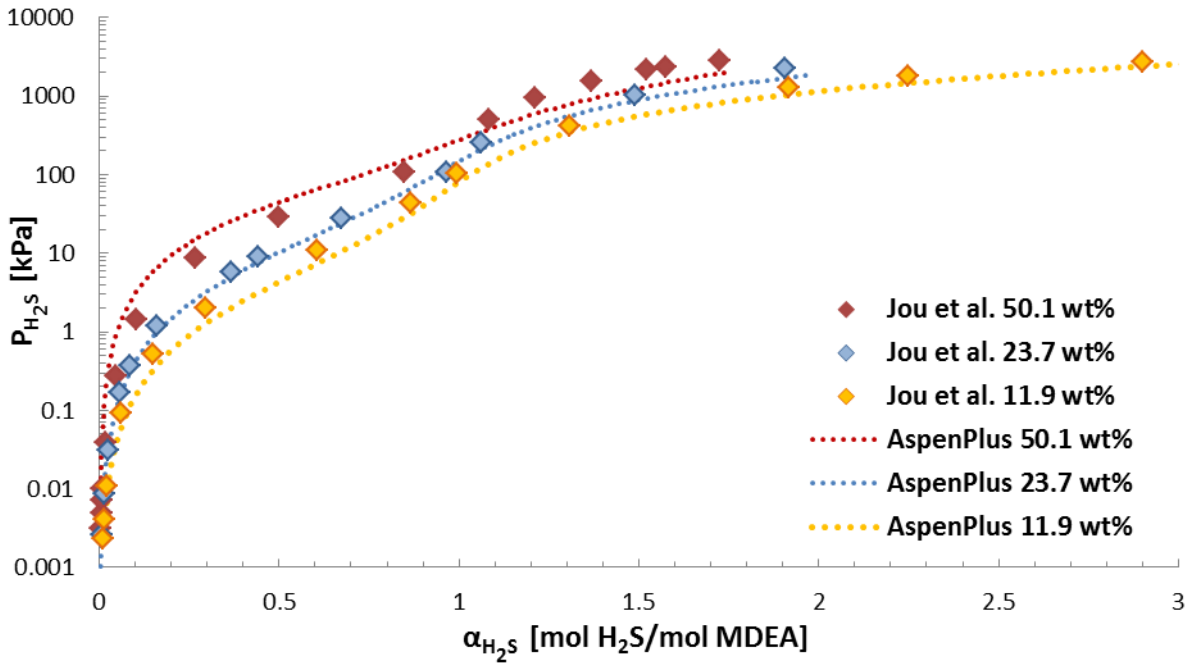

Figure 3.3.5: Partial pressure of hydrogen sulfide, P_{H_2S}, on a log scale as a function of loading, α_{H_2S}, in the liquid phase. The figure shows the VLE models in Aspen Plus for H_2S at 40 ^oC for different aqueous MDEA concentrations compared to experimental data reported by Jou et al. [14].

It can also be noted that AD in a 23.7 wt% MDEA solution, is lower for H_2S than for CO_2 at all temperatures. The VLE model predictions for the 50.1 wt% solution does not fit experimental data as well as for lower concentrations, and AD's for CO_2 are lower than for H_2S in this case (see Appendix A.1).

For acid gas loadings up to 0.4, solubility of CO_2 is higher in a 50.1 wt% MDEA solution compared to H_2S, at 25 ^oC and 40 ^oC. However, At 70 ^oC and 120 ^oC, H_2S is more soluble, which may indicate that CO_2 will be easier to strip than H_2S. This can be seen from Figure A.2.2 in Appendix A.2.

Designing an absorber, one would expect that increasing the MDEA concentration would lower the circulation rate required to reach outlet gas specifications, which in turn may reduce operating costs. The answer is, however, not that straightforward. As it can be seen from Figure 3.3.5, the partial pressures of H_2S are higher for increasing MDEA concentrations for the same respective loadings. This can also be seen for CO_2 in Figure A.2.1 in Appendix A.2. Using low MDEA concentrations may result in more water leaving with the sweet gas as well. Using a high concentrated MDEA solution may decrease the circulation rates needed for absorbing acid gas, but it is important to analyse the temperature of the solvent since higher temperatures decreases the solubility. The exothermic reactions can also increase the solution temperature to an extent where the acid gas vapor pressure is increased over the solution through the column if the circulation rate is sufficiently low [2].

3.3.3 Solubility of CH_4 in aqueous MDEA

Figure 3.3.6 shows the VLE curves retrieved from Aspen Plus for CH_4 in a 34.7 wt% aqueous MDEA solution at 25 °C to 130 °C, compared to experimental data.

In general, the VLE model in Aspen Plus gives higher partial pressures for all temperatures compared to data reported by Jou et al. [28]. The trend Aspen Plus gives, shows that it under-predicts the solubility of CH_4 in MDEA. AD's are lowest at 25 °C and 40 °C with 50.5% and 49.5%, respectively. AAD for these temperatures are low, 10.8% and 9.1%, respectively.

At 130 °C the AD is 112.5% and AAD is 47.6%. This is because of high percentage deviations for x_{CH_4} > 0.001. For desorption simulations, required energy to strip CH_4 from aqueous MDEA is expected to be lower compared to reality. Most likely, most of the CH_4 can be removed from rich MDEA with pressure relief, because of low loadings. It can also be noted that the solubility of CH_4 in 34.7 wt% MDEA has a low correlation to the temperature.

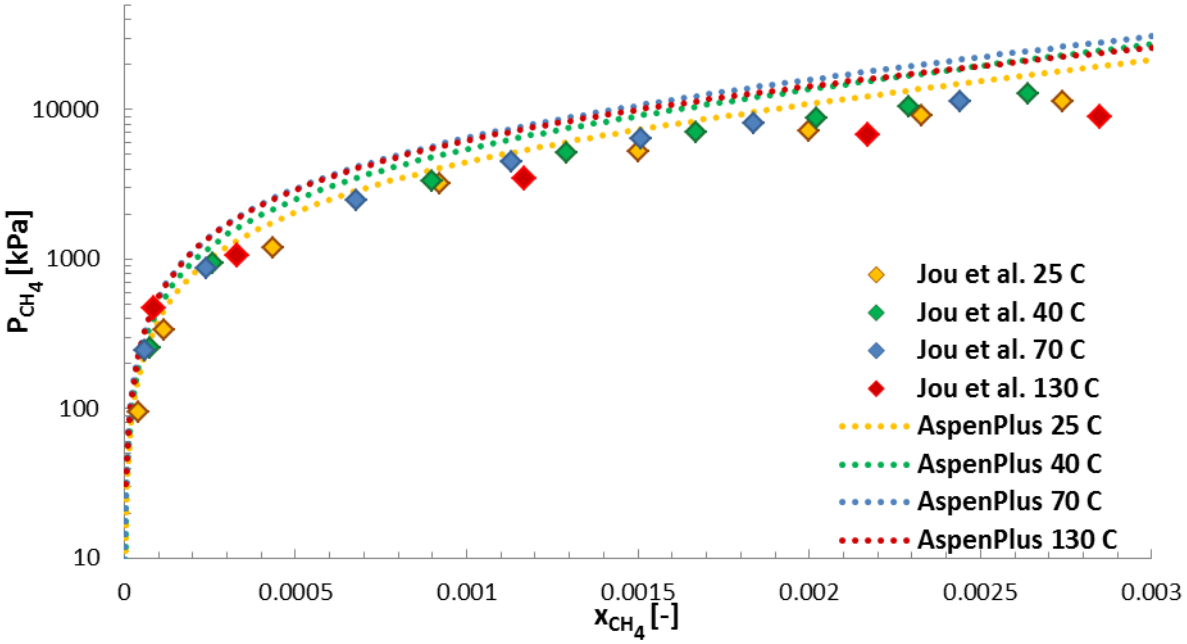

Figure 3.3.6: Partial pressure of methane, P_{CH_4}, on a log scale as a function of mole fraction, x_{CH_4}, in the liquid phase. The figure shows VLE models in Aspen Plus for CH_4 in a 34.7 wt% aqueous MDEA solution at 25 °C, 40 °C 70 °C and 130 °C, compared to experimental data reported by Jou et al. [28].

3.3.4 Solubility of CO_2 in MEG

Figures 3.3.7 and 3.3.8 give solubility curves for CO_2 in pure MEG (purity > 99.5%) at 25 °C to 125 °C, compared to experimental data.

AD is 22.1% at 25 °C, and up to 53% at 50 °C. However, up to x_{CO_2}= 0.09, the model in Aspen Plus fits the experimental data well. AD was calculated to be 9.6% at 25 °C (compared to Jou et al. [29]), and 10.4% at 50 °C (compared to Zheng et al. [31] for x_{CO_2}< 0.09. At 50 °C

the VLE curve has an unexpected behaviour for x_{CO_2}> 0.1, but experimental data tend to follow the same trend.

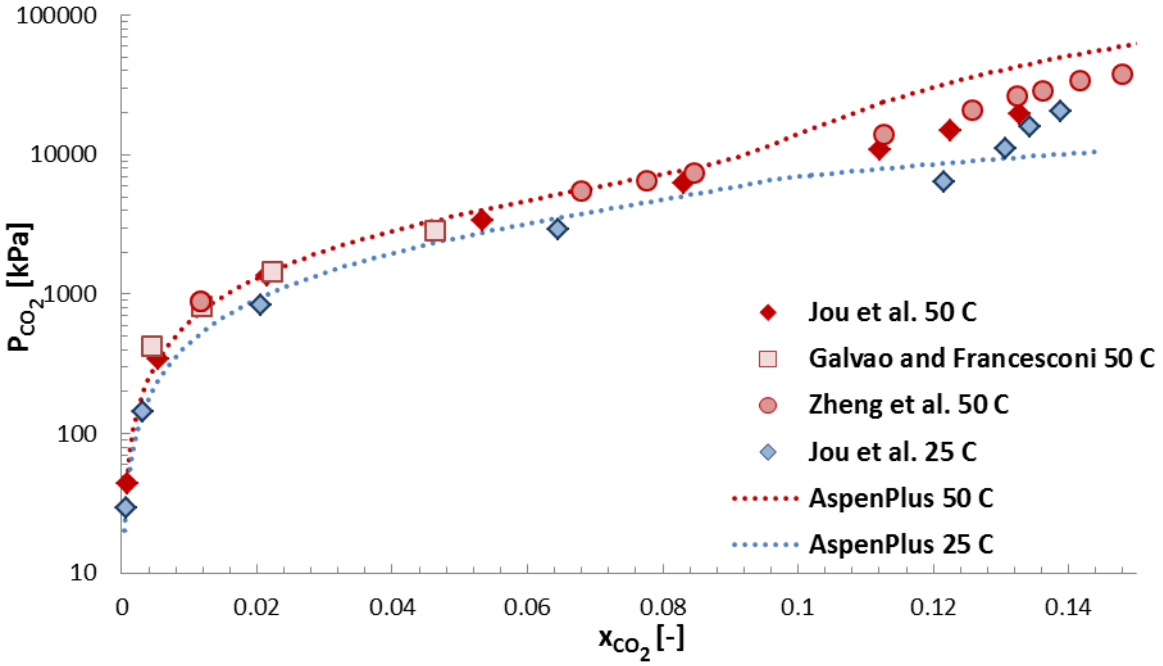

Figure 3.3.7: Partial pressure of carbon dioxide, P_{CO_2}, on a log scale as a function of mole fraction, x_{CO_2}, in the liquid phase. The figure shows the VLE models in Aspen Plus for CO_2 in pure MEG (purity > 99.5%) at 25 ^oC and 50 ^oC compared to experimental data reported by Jou et al. [29], Galvao and Francesconi [30] and Zheng et al. [31].

At 100 ^oC, Aspen Plus gives a good prediction up to x_{CO_2}= 0.05, where the lowest percentage deviation was calculated to be 15% (compared to Zheng et al. [31]). Over the whole loading range, Aspen Plus fits the data reported by Jou et al. [29] better compared to the other sources, with AD and AAD of 31.3% and 18.2%, respectively. From Figure 3.3.8 it can also be seen that the equilibrium curves predicted by Aspen Plus have a higher temperature dependency compared to measured data.

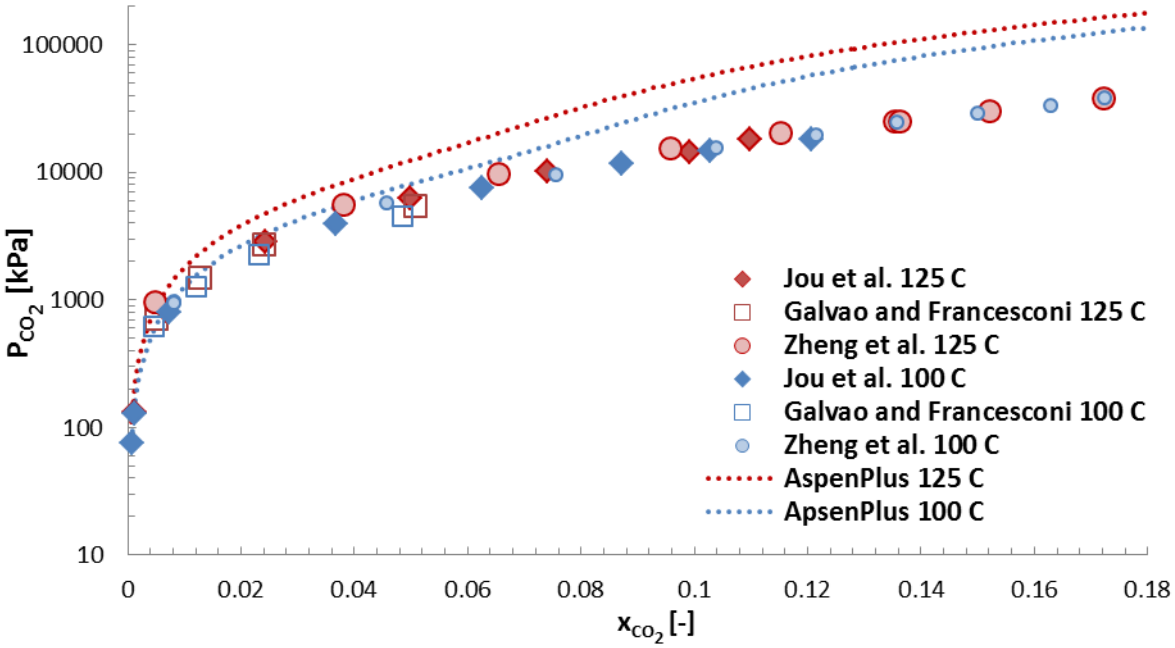

Figure 3.3.8: Partial pressure of carbon dioxide, P_{CO_2}, on a log scale as a function of mole fraction, x_{CO_2}, in the liquid phase. The figure shows the VLE models in Aspen Plus for CO_2 in pure MEG (purity > 99.5%) at 100 ^oC and 125 ^oC compared to experimental data reported by Jou et al. [29], Galvao and Francesconi [30] and Zheng et al. [31].

3.3.5 Solubility of H_2S in MEG

Figure 3.3.9 gives VLE models for H_2S in pure MEG (purity > 99.5%) at 25 ^oC to 125 ^oC compared to reported data by Jou et al. [29]. The VLE curves are plotted up to x_{H_2S} = 0.1, but there are solubility data reported up to x_{H_2S} = 0.45. Mole fractions above 0.1 are not relevant for this work. Solubility curves for the whole loading range reported, are given in Appendix A.3.

Lowest AD's occurs at 100 ^oC and 125 ^oC with 14.6% (3.7% for x_{H_2S} < 0.1) and 16.9%, respectively. For x_{H_2S} < 0.1, the AD's were calculated to be 21%, 14.7% and 5.2% for 25 ^oC, 50 ^oC and 75 ^oC, respectively. The diminishing AD's indicates that Aspen Plus gives a better fit to experimental data when temperature increases.

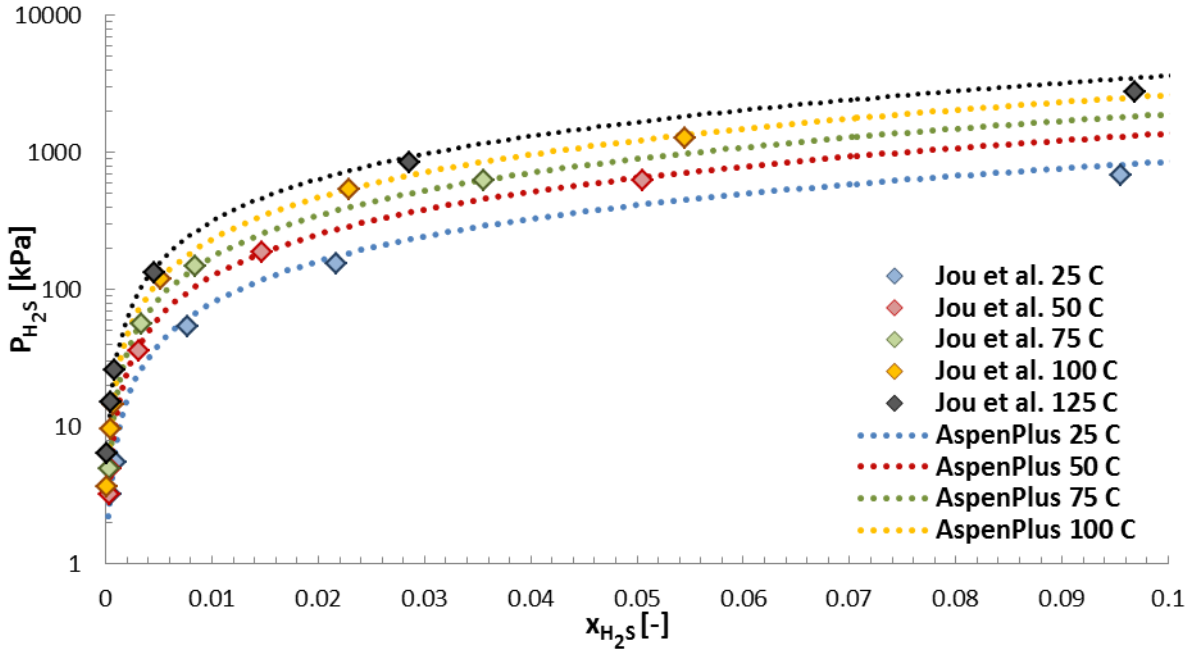

Figure 3.3.9: Partial pressure of hydrogen sulfide, P_{H_2S}, on a log scale as a function of mole fraction, x_{H_2S}, in the liquid phase. The figure shows the VLE models in Aspen Plus for H_2S in pure MEG (purity > 99.5%) at 25 ^oC to 125 ^oC compared to experimental data reported by Jou et al. [29].

3.3.6 Solubility of CH_4 in MEG

Figures 3.3.10 and 3.3.11 give VLE models for CH_4 in pure MEG (purity > 99.8%) at 30 ^oC to 150 ^oC compared to experimental data. Aspen Plus solubility curves fit well to experimental data at 30 ^oC and 50 ^oC, where the AD's are 16.5% and 11.9%, compared to Galvão and Francesconi [30]. At 125 ^oC, the VLE model in Aspen Plus have AD and AAD as low as 7.9% and 2.6%, compared to Zheng et al. [31]. From Figures 3.3.10 and 3.3.11, it can be seen that the solubility of CH_4 in MEG predicted by Aspen Plus, has a low correlation to the temperature.

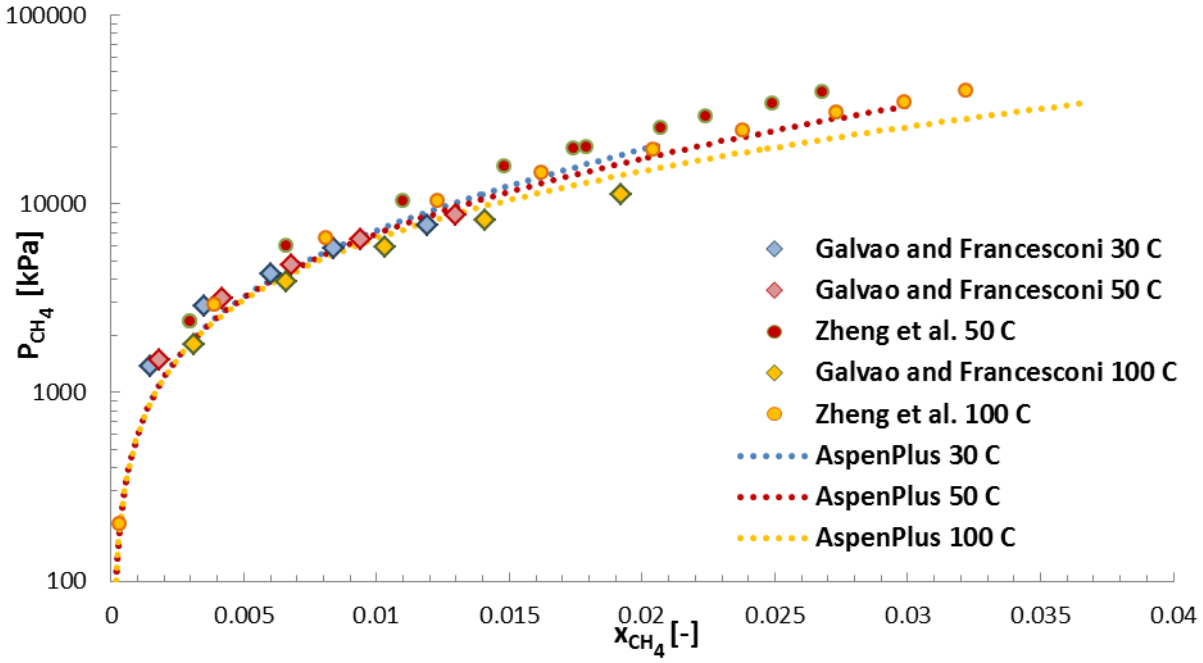

Figure 3.3.10: Partial pressure of methane, P_{CH_4}, on a log scale as a function of mole fraction, x_{CH_4}, in the liquid phase. The figure shows the VLE models in Aspen Plus for CH_4 in pure MEG (purity > 99.5%) at 30 ^oC, 50 ^oC and 100 ^oC compared to experimental data reported by Galvao and Francesconi [30] and Zheng et al. [31].

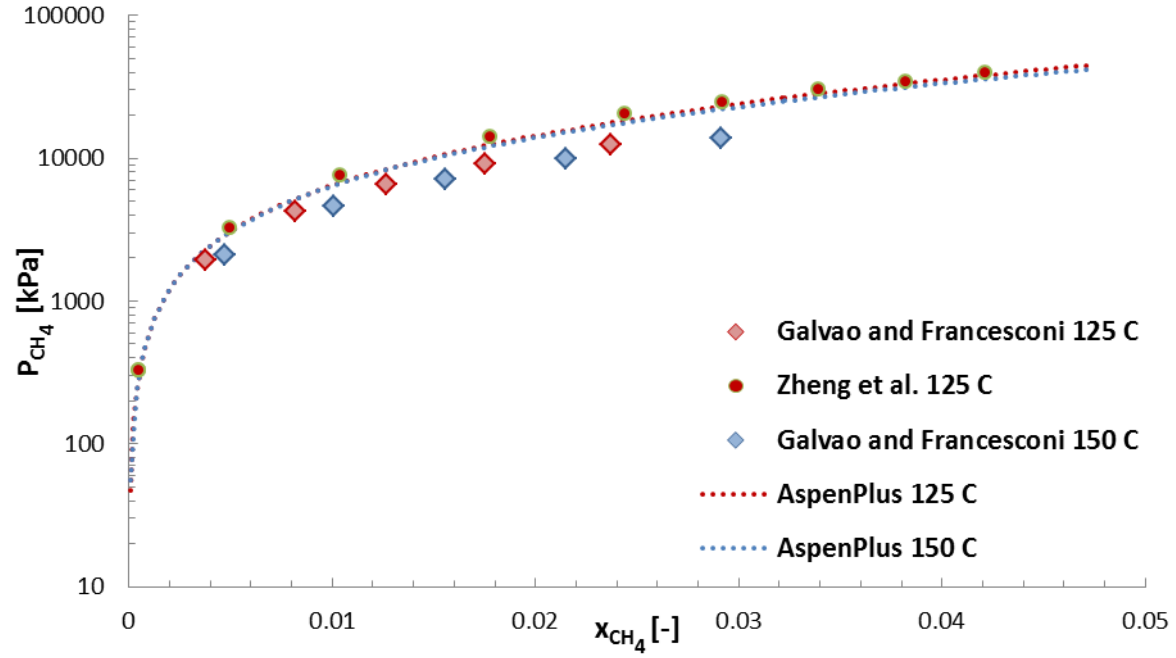

Figure 3.3.11: Partial pressure of methane, P_{CH_4}, on a log scale as a function of mole fraction, x_{CH_4}, in the liquid phase. The figure shows the VLE models in Aspen Plus for CH_4 in pure MEG (purity > 99.5%) at 125 ^oC and 125 ^oC compared to experimental data reported by Galvao and Francesconi [30] and Zheng et al. [31]

3.3.7 Solubility of H_2O in MEG

Figure 3.3.12 gives VLE models for H_2O in pure MEG (purity > 99.5%) at 50 ^oC and 60 ^oC compared to reported data.

In general, the Aspen Plus model gives a very good prediction of the VLE curves for H_2O in MEG. The highest AD and AAD are 6.8% and 9.8%, compared to Horstmann et al. [32] at 60 ^oC. Because MEG has high affinity for water, it gives low partial pressures at high loadings.

In conventional topside dehydration units, TEG is a widely used dehydration solvent. Figure A.4.1 in Appendix A.4 shows VLE models in Aspen Plus for H_2O in pure MEG, compared to TEG at 50 ^oC, 60 ^oC and 150 ^oC. Using the template model in Aspen Plus designed for acid gas removal in MDEA, gives the same solubility results for H_2O in MEG and TEG. Relative differences between the dehydration solvents were not reported because the marginal differences are small.

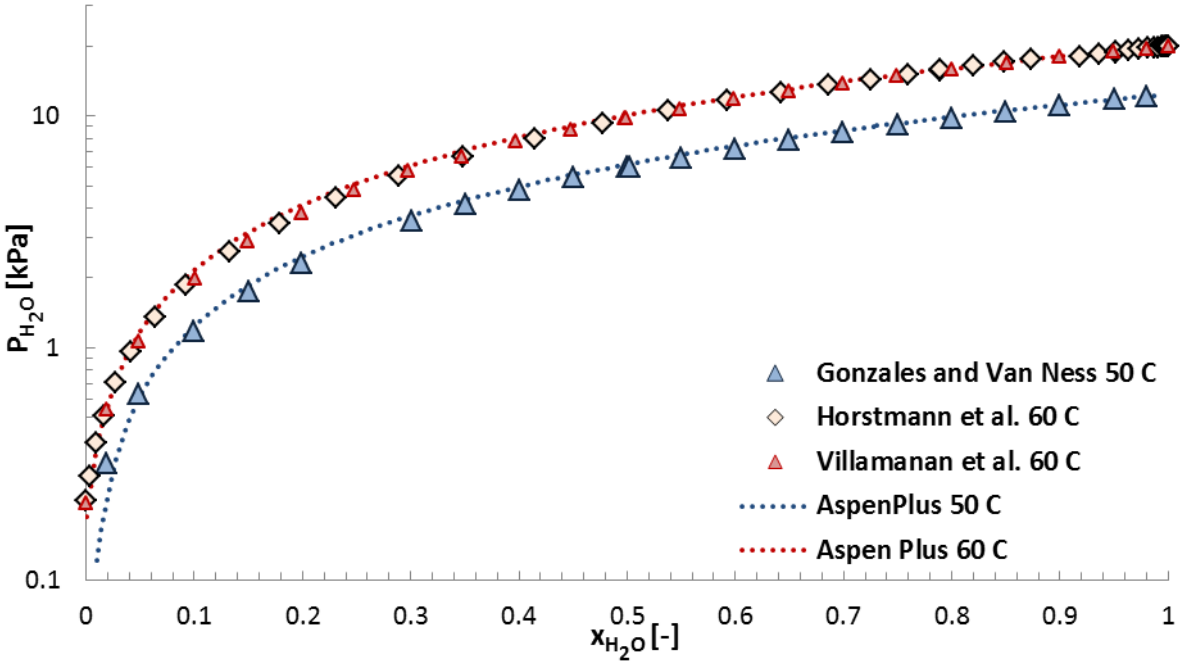

Figure 3.3.12: Partial pressure of water, P_{H_2O}, on a log scale as a function of mole fraction, x_{H_2O}, in the liquid phase. The figure shows the VLE models in Aspen Plus for H_2O in pure MEG (purity > 99.5%) at 50 ^oC and 60 ^oC compared to experimental data reported by Gonzales and Van Ness [33], Horstmann et al. [32] and Villamañãn [34].

3.3.8 Comparing solubility of H_2O, CH_4, H_2S and CO_2 in MEG

Figure 3.3.13 gives solubility curves for H_2O, CH_4, H_2S and CO_2 in pure MEG (purity > 99.5%) at 50 ^oC, 100 ^oC and 125 ^oC, predicted by Aspen Plus up to mole fractions equal 0.1. The figure shows how the solubility of the different components differ, and that MEG has highest affinity for H_2O compared to CH_4, H_2S and CO_2. CH_4 is least soluble in MEG and the solubility has a weaker temperature dependency than the other components.

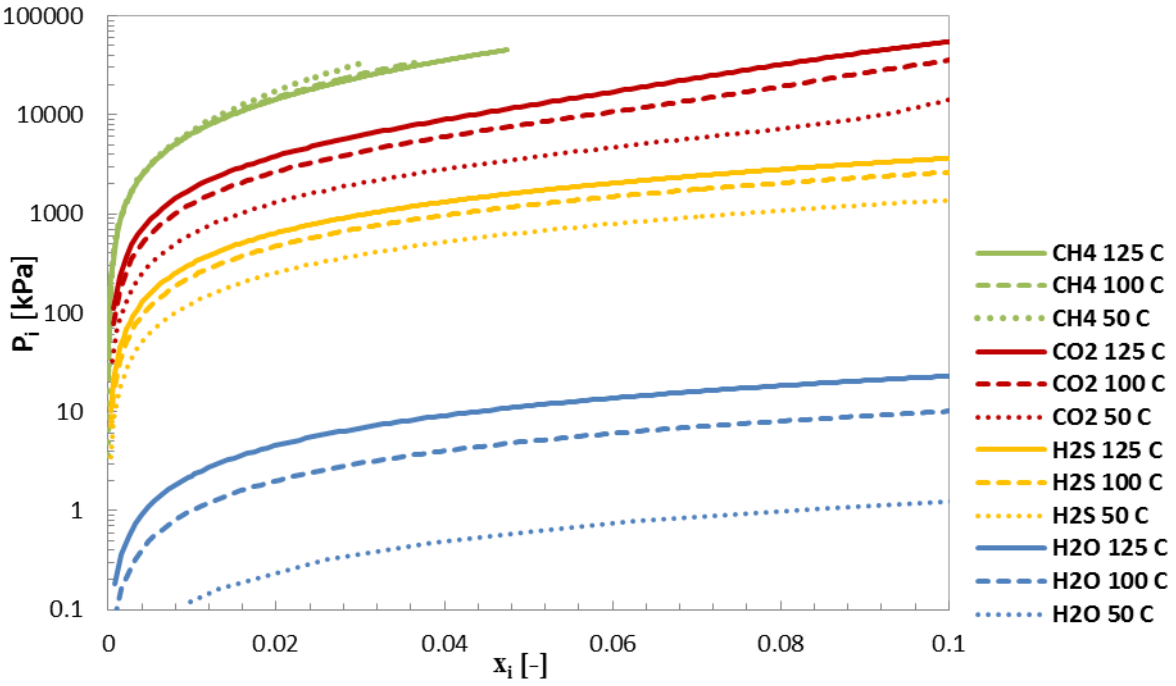

Figure 3.3.13: Partial pressure of component *i*, P_i, on a log scale as a function of mole fraction, x_i, in the liquid phase. The figure shows the VLE models from Aspen Plus for CH_4, CO_2, H_2S and H_2O in pure MEG (purity > 99.5%) at 50 ^oC, 100 ^oC and 125 ^oC.

3.3.9 Solubility of H_2S-CO_2 mixtures in a MDEA-MEG-H_2O solvent

The setup for running VLE analysis for H_2S and CO_2 mixtures in a MDEA-MEG-H_2O solvent is shown in Figure 3.3.14. The first solubility analysis performed, was in 30 wt% MDEA + 65 wt% MEG + 5 wt% H_2O at 40 ^oC, 60 ^oC and 90 ^oC because of the reported data by Xu et al. [26]. AD and AAD between simulated and reported data are given in Table 3.3.2. The simulated data retrieved from Aspen Plus was not consistent with the reported literature data. One of the issues for validating H_2S and CO_2 solubility in MDEA-MEG solvents is the lack of experimental data and published articles on this topic, and the VLE validation as a basis for further work was therefore challenging. The data reported by Xu et al. [26] have an acceptable temperature range, but the number of data points for each temperature are limited to five. The template model in Aspen Plus gives poor results for the mixed solvent, containing 65 wt% MEG, and AD of H_2S is as high as 2308.5% at 40 ^oC, compared to Xu et al. [26].

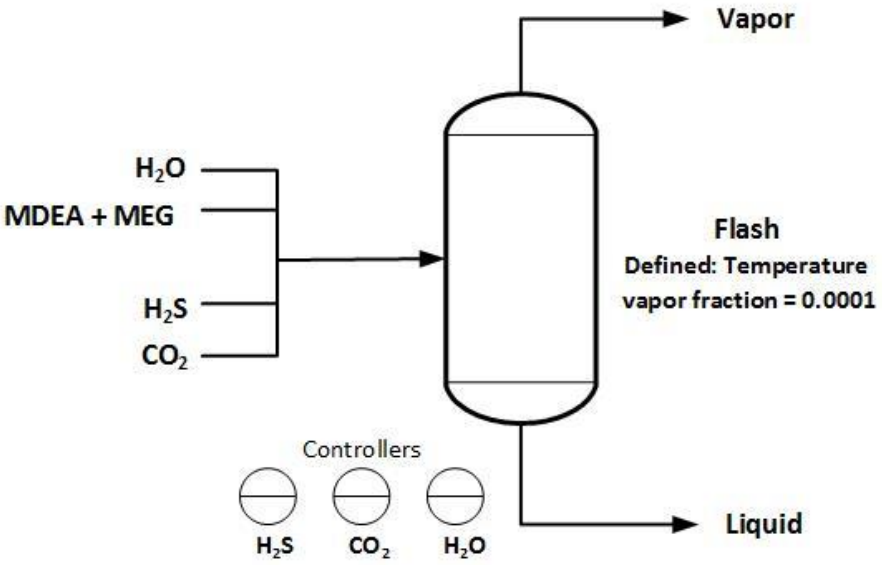

Figure 3.3.14: Aspen Plus setup for analysing solubility of H_2S-CO_2 mixtures in a MDEA+MEG+H_2O solvent. A flow controller was used to regulate the amount of water, to get the desired weight fraction of water in the liquid phase. Flow of H_2S and CO_2 was also regulated to correct loadings in the liquid phase and the partial pressures were calculated.

One reason for why the Aspen Plus model is giving poor results in this ternary solvent, may be that the amount of water present in the solvent is small (5 wt%). All the absorption reactions defined in the template model, are dissociation reactions in water (see Table 2.5.1). Literature reports advantages of using MDEA for absorbing H_2S because of a simple proton transfer reaction [14]. Because this reaction is not defined in the template model, simulating the absorption process will require aqueous solvents. This is also the case for CO_2, which requires water for the absorption reaction in MDEA to take place. Therefore, a decrease in CO_2 solubility in the mixed solvent is expected, when the aqueous solvent contains more MEG than H_2O. However, H_2S is known to react directly with MDEA, and replacing water with MEG should not have the same effect on solubility, compared to that of CO_2. This is therefore the main issue with the template model in Aspen Plus if an amine-glycol solvent, with a low water content, is to be used for simultaneous acid gas and water removal. The highest average deviation for CO_2 is 621.9% at 60 ^oC compared to Xu et al. [26]. Even if this is lower than for H_2S, it is still regarded as a high deviation.

A literature review of thermodynamic models on the MDEA-H_2S-CO_2 system has shown to be based on the same procedure as defined in Aspen Plus. All the equilibrium constants are based on dissociation in water, and there are several sources reporting different coefficient values for the equilibrium constant [37, 38, 39, 40, 41]. Finding literature that gives equilibrium coefficients for the direct reaction between H_2S and MDEA was not successful.

Xu et al. [26] also reported VLE curves for different MDEA-MEG-H_2O solvents at 40 ^oC, but the solubility data is not reported. These data points have been read of manually and were provided by Skylogianni [42]. Figure A.5.1 in Appendix A.5 gives the VLE curves retrieved from Aspen Plus for these solvents, compared to the experimental data. The issues discussed

can be confirmed by examining the solubility curves. The solubility of H_2S decreases considerably for increasing MEG concentration in the MDEA solvent.

In a second analysis, the amount of water in the system was increased. A water flow controller was used to regulate the weight percent water out in the liquid phase. The water out of the flash in the liquid phase was regulated to 5 wt%, 10 wt%, 20 wt% and 30 wt% at 40 ^oC, 60 ^oC and 90 ^oC. A 30 wt% MDEA + 65 wt% MEG + 5 wt% H_2O was used as the basis. Water weight percent out of the flash in the liquid phase, $wt\%\ H_2O$, was calculated by Equation 8.

$$wt\%\ H_2O\ = \frac{(\dot{n}\ Mm)_{H_2O} + (\dot{n}\ Mm)_{H_3O^+} + (\dot{n}\ Mm)_{OH^-} + (\dot{n}\ Mm)_{HCO_3^-}}{\sum_{i=1}^{n}(\dot{n}\ Mm)_i\ - ((n_{in}^{\cdot} - \dot{n}_{out})Mm)_{H_2S}\ - ((n_{in}^{\cdot} - \dot{n}_{out})\ Mm)_{CO_2}} \qquad (8)$$

Keeping the amount of water out at 5 wt% gave the same results as the original run (given in Table 3.3.2). The results for 10 wt% to 30 wt% excess water at 40 ^oC, 60 ^oC and 90 ^oC are given in Table 3.3.3, and was compared to Xu et al. [26]. The lowest AD for H_2S was 27.9%, when 30 wt% excess water is used at 40 ^oC.

The results show that solubility of H_2S increases when there is more water present in the solvent. This is important for absorption simulations, and using MDEA-MEG solvents with a low water content will most likely not give satisfying results with respect to absorption rate of H_2S. Because it is desirable to remove water and acid gas simultaneously, it will also be important to examine if the water content through the absorber increases even if MEG is present.

Table 3.3.3: AD and AAD between reported data by Xu et al. [26] and simulated solubility data retrieved from Aspen Plus, when more water is added in the solvent. The first column is weight percent water out of the flash in liquid phase. Original solvent concentrations: 30 wt%MDEA+65 wt% MEG+5 wt% H_2O.

w_{H_2O}	T	AD_{CO_2}	AD_{H_2S}	AAD_{CO_2}	AAD_{H_2S}
10 wt%	40 ^oC	137.3	1285.3	83.6	709.7
	60 ^oC	350.0	1735.7	88.4	320.8
	90 ^oC	404.0	1866.6	140.9	699.4
20 wt%	40 ^oC	49.9	204.1	13.4	119.8
	60 ^oC	21.7	424.0	18.7	62.1
	90 ^oC	287.0	1335.3	96.7	463.2
30 wt%	40 ^oC	83.8	27.9	3.5	27.0
	60 ^oC	66.4	51.8	4.8	14.1
	90 ^oC	43.2	355.4	24.6	115.8

3.3.10 Equilibrium constant analysis

The definition of the equilibrium constants, K_{eq}, in the template model are given in Table 3.2.1. Since H_2S and MDEA react directly with a proton transfer, it was desirable to define this reaction in the model. This was done by deleting reaction 6 (see Table 2.5.1) and defining

reaction 11 (see Table 2.5.2). The equilibrium constants were defined by the equation of Gibbs energy. Aspen Plus then calculates K_{eq} from the reference state, Gibbs free energy of the components [36]. The results were not improved when the net reaction was defined.

The next approach was combining the equilibrium constant expressions. Equilibrium constants for reaction 1 and 6 were combined to see how Aspen Plus responded, and the derivation of this is shown in Equations 9 to 13. Brackets in the equations indicate concentration of the given component. Coefficients A, B, C and D in Equation 7 was taken from Austgen et al. [37] for reaction 1 and 6, and the coefficients calculated for reaction 11 are given in Table 3.3.4. Based on how the temperature dependency of K_{eq} is defined, combining Equations 7 and 12, gives Equation 13.

$$K_1 = \frac{[MDEA][H_3O^+]}{[MDEAH^+][H_2O]} \tag{9}$$

$$K_6 = \frac{[HS^-][H_3O^+]}{[H_2S][H_2O]} \tag{10}$$

$$K_{11} = \frac{[HS^-][MDEAH^+]}{[H_2S][MDEA]} = \frac{K_6}{K_1} \tag{11}$$

$$ln\ K_{11} = ln\left(\frac{K_6}{K_1}\right) = ln\ K_6 - lnK_1 \tag{12}$$

$$ln\ K_{11} = (A_6 - A_1) + \frac{(B_6 - B_1)}{T} + (C_6 - C_1)\ lnT + (D_6 - D_1)T \tag{13}$$

Table 3.3.4: Temperature dependency of equilibrium constants, $ln\ K_{eq} = A + \frac{B}{T} + ClnT + DT$, for the given reaction. Coefficients A, B, C and D were calculated based on Austgen et al. [37].

Reaction	Rx. n	K_{eq}	A	B	C	D
$MDEA + H_2S \leftrightarrow MDEAH^+ + HS^-$	11	K_{11}	223.9985	-8760.42	-33.5471	0

A VLE analysis was performed using the calculated equilibrium coefficients for reaction 11 in Table 3.3.4 for H_2S and CO_2 in a 30 wt%MDEA + 65 wt% MEG + 5 wt% H_2O solvent, and the results were compared to the VLE analysis discussed in Chapter 3.3.9 and the reported data by Xu et al. [26]. The approach failed to give better results and was not taken any further. Defining all equilibrium coefficients for every reaction in Aspen Plus, based on Austgen et al. [37] gave the same simulation results as the original template model. Because of this, and because there are no literature data for the direct reaction, the original template model was used for all simulations.

3.3.11 How CO_2 affects H_2S solubility

Figure 3.3.15 gives the H_2S solubility curves in a 45 wt% aqueous MDEA solution at 40 ^oC and 120 ^oC, and shows how the VLE of H_2S is affected for increasing CO_2 contents. When the CO_2 content is 20% in the inlet gas (molar H_2S/CO_2 ratio = 4), the solubility of H_2S is not affected as much as when the CO_2 content is 50% (molar H_2S/CO_2 ratio =1). It can be seen that CO_2 has a higher influence on the H_2S solubility higher loadings (above 0.35) when the H_2S/CO_2 ratio is high.

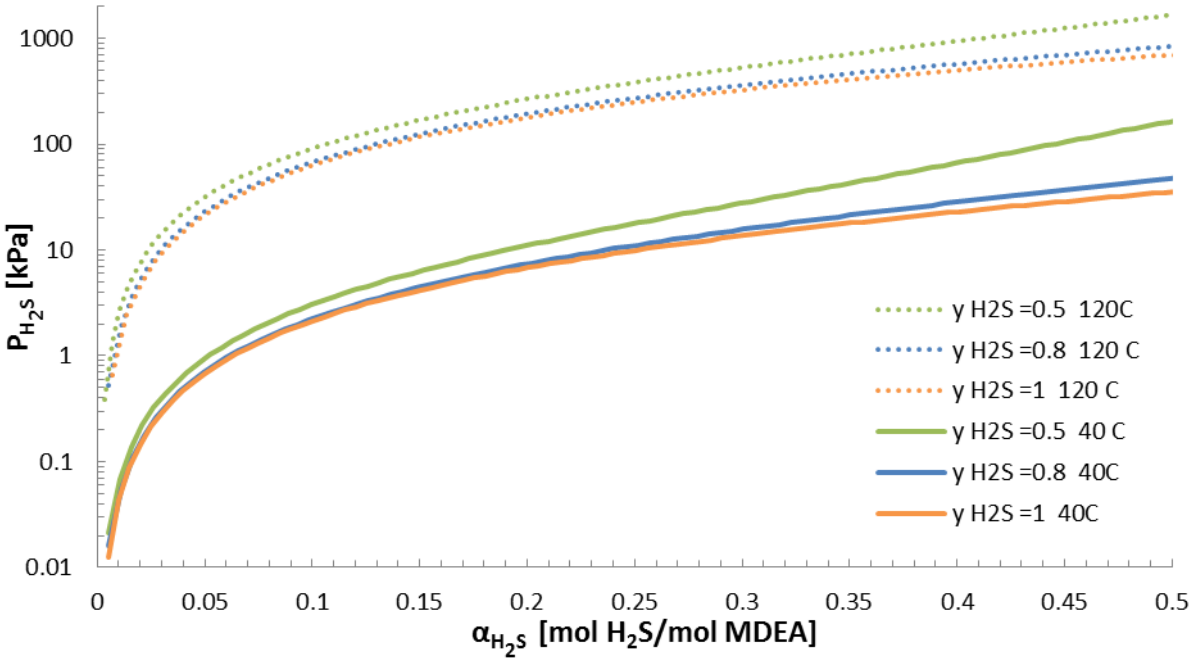

Figure 3.3.15: Simulated results for how CO_2 affects H_2S solubility in a 45 wt% aqueous MDEA at 40 ^oC and 120 ^oC. Mole fractions, y_{H_2S}, refers to the gas composition into the flash. This means that y_{H_2S} = 0.5 refers to 50% H_2S and 50% CO_2 in the inlet gas. Solubility curves were simulated in Aspen Plus.

Chapter 4 Basis for Aspen Plus simulations

4.1 Gas composition cases

The basis for the simulations was natural gas containing H_2S and CO_2, and was otherwise assumed to be only CH_4 saturated with water. Reservoir temperatures and pressures vary, and due to friction and heat transfer from pipe fluids to sea temperature, the temperature and pressure conditions will decrease along the pipeline. To simplify the simulations, it was assumed that natural gas enters the processing unit at 100 bar and 25 ^oC [43]. Three gas compositions were used for analysis, where the H_2S and CO_2 content varied. The operating conditions and compositions are given in Table 4.1.1. Aspen Plus was used to find the saturated compositions. The H_2S content in the sour gas range from 49.8 ppm to 4.5%, and the CO_2 content from 5.6% to 8%. All simulations discussed in the next chapters refer to these gas composition cases. All preliminary analyses were performed for Case 1 and 2, because Case 3 was decided on a later point in this work [43].

Table 4.1.1: Gas conditions used as a basis for the simulations. The natural gas is saturated with water at the given conditions.

Parameter	**Unit**	**Saturated natural gas**		
Temperature	[^oC]	25		
Pressure	[bar]	100		
Composition (molar basis)		**Case 1**	**Case 2**	**Case 3**
CH_4	[%]	94.3156	94.2708	87.403
CO_2	[%]	5.5873	5.5873	8.0
H_2S	[ppm]	49.8	498	45000[a]
H_2O	[%]	0.0921	0.0921	0.097

[a] 45000 ppm equals 4.5% H_2S

As mentioned in Chapter 1, a typical specification for rich gas leaving an offshore platform is maximum 4 ppm H_2S and 2-3% CO_2 (by volume). These values were therefore used as target values for the simulation [1, 2]. A water dew point specification for pipeline transportation is typically -18 ^oC at 70 bara [3]. Using a conversion table it was found that this gives a water content of 32 kg/10^6 std m^3 gas at standard conditions[2] [13]. In Aspen Plus it is easier to analyse stream data based on mole or mass fraction, and the specification was therefore calculated to be 42 ppm H_2O on a molar basis. Calculations are explained in Appendix B.1.

4.2 Preliminary absorber analysis

A preliminary analysis was performed to examine absorption of H_2S and CO_2 in MDEA, varying the molar liquid-gas ratio, L/G, into the absorber, as a function of absorber stages. This was to find the minimum number of stages and to examine the column performance for various L/G ratios. Molar L/G ratio as mole liquid solvent/mole gas, were used for all

[2] Standard conditions: 101.325 kPa and 15 ^oC [13]

simulations instead of molar flow and mass flow, respectively. All the absorber and stripper simulations in this work were based on equilibrium stage calculations in 'RadFrac' columns.

The analysis was performed for Case 1 using a 50 wt% aqueous MDEA solution at 30 ^oC. The setup used in Aspen Plus is shown in Figure 4.2.1. If subsea acid gas removal is implemented in the future, there may be limitations for what temperatures liquid solvents can hold because the seabed temperature is low, especially in cold climate areas. Typical acid gas absorbers use solvent temperatures above the inlet gas temperature to prevent co-absorption of hydrocarbons, and the MDEA temperature was therefore set to 30 ^oC [17]. Solubility of H_2S and CO_2 in MDEA increase at lower temperatures, as seen in Chapter 3.3.1 and 3.3.2, but other factors, such as viscosity of MDEA, must be considered as well. As mentioned earlier, viscosity of MDEA increases for higher concentrations and lower temperatures [10]. Using high concentrations of MDEA at low temperatures will, among others, affect the pumping costs. Lean loading of H_2S in the MDEA solvent, α_{H_2S}, was set to 0.004 and it was assumed zero loading of CO_2 [44]. This applies for all the absorption simulations where the regeneration unit is excluded. With respect to operation and equipment, maximum loading of acid gas in lean MDEA is recommended to lie between 0.004 and 0.010 [2].

The inlet streams to the absorber were defined to enter 'on-stage'. This enables both the liquid and vapor phase to enter the stage specified. If 'above-stage' feed is specified, the flow enters between two stages. The liquid phase will then flow to the specified stage, and the vapor phase will flow to the stage above. 'On-stage' feed streams were used for all the absorption and stripping simulations in this work.

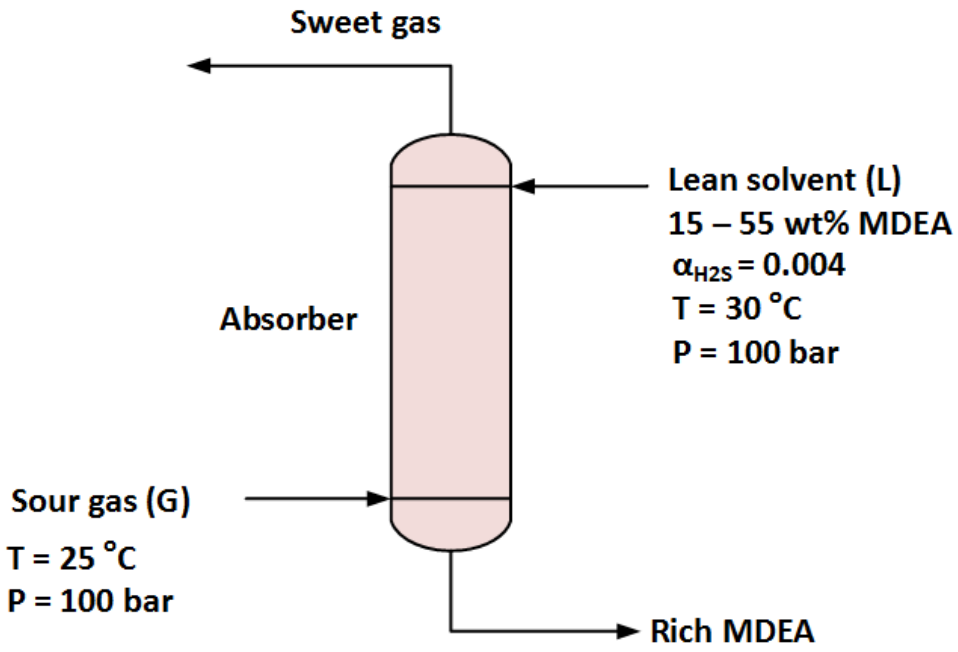

Figure 4.2.1: Setup in Aspen Plus for preliminary analysis of the absorber.

Figure 4.2.2 gives the H_2S content in the sweet, as a function of number of stages in the absorber, *n*, for different L/G ratios. As seen from the figure, using more than eight stages in

the absorber will not give any significant improvements on the purity of the sweet gas. For L/G ratios below 0.82, the H_2S content in the sweet gas increases above the initial value (49.8 ppm), which means that some of the H_2S in the lean MDEA solution is stripped in the absorption column.

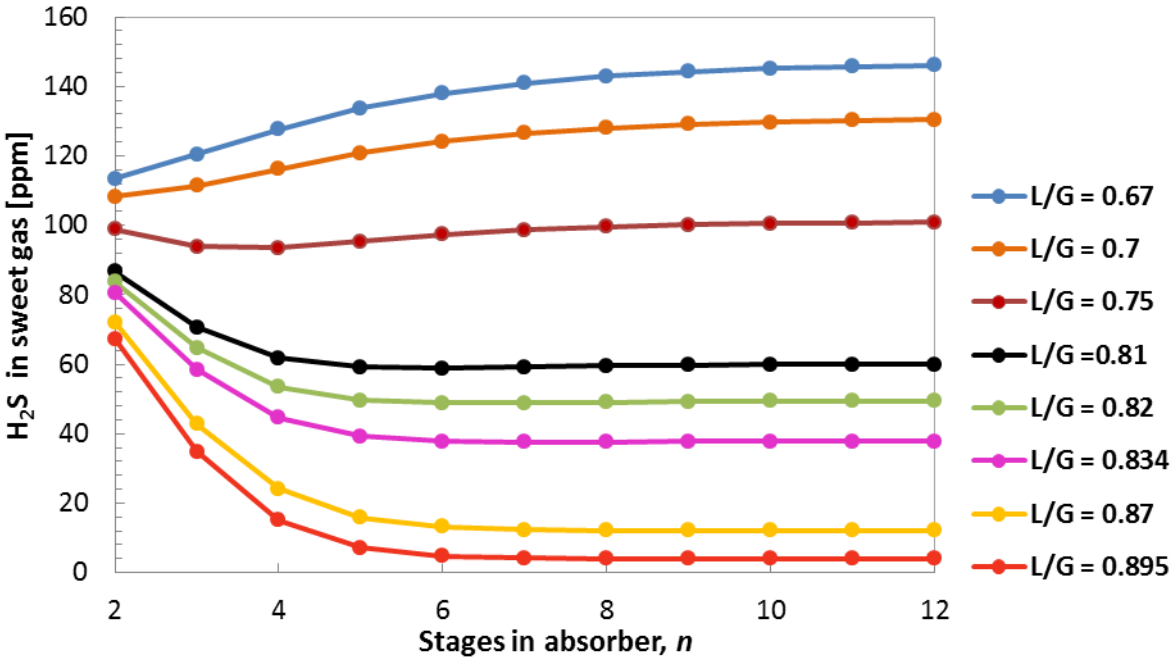

Figure 4.2.2: Amount of H_2S out of the absorber as a function of the number of stages, *n*, for different molar L/G ratios [mol/mol]. Analysis performed with 49.8 ppm H_2S initially in the gas, Case 1, and using a 50 wt% aqueous MDEA solution at 30 ^oC.

Figure 4.2.3 shows the temperature profiles for four different L/G ratios. Normally, the highest temperatures in the absorber are in the middle or lower middle part of the column, because the bulk removal of acid gas is in this area. As seen from the figure, the temperature profiles are quite broad, which are common for tertiary amines [2]. This may be because the concentration of CO_2 is higher than H_2S in the sour gas, and that CO_2 has a higher heat of reaction than H_2S in MDEA. The temperature bulge is slightly moved downwards and is sharper as the L/G ratio increases. For L/G = 0.67, the top-stage temperature is higher than the bottom temperature, which means that the gas leaving the column carries more of the reaction heat than the liquid, and is not preferred in operation. This can result in a shift of the H_2S equilibrium (see reaction 11, Table 2.5.2) to the left, which can be seen from Figure 4.2.2 where the H_2S content in the gas is increased through the absorber.

For L/G = 0.895, which yields 4 ppm H_2S in the sweet gas, the temperature in the bottom stage is higher than in the top of the column. The top temperature is 38 ^oC, and after this it increases rapidly in the first four stages. Examination of the composition profile of CO_2, showed that most of the CO_2 is removed in this area, having larger concentration changes from stage 2 through stage 5 compared to the bottom part of the column. The molar H_2S fraction in the gas phase had its peak at stage 5. After this, the temperature decreases again because the sour gas enters the column at 25 ^oC, but not as much as in the top of the column. The rich MDEA solution is carrying more of the reaction heat, and the flow rate of gas is not

sufficient to cool the rich solution. In the top, the opposite effect occurs, and the MDEA solvent entering at 30 °C cools down the gas in the top part of the column.

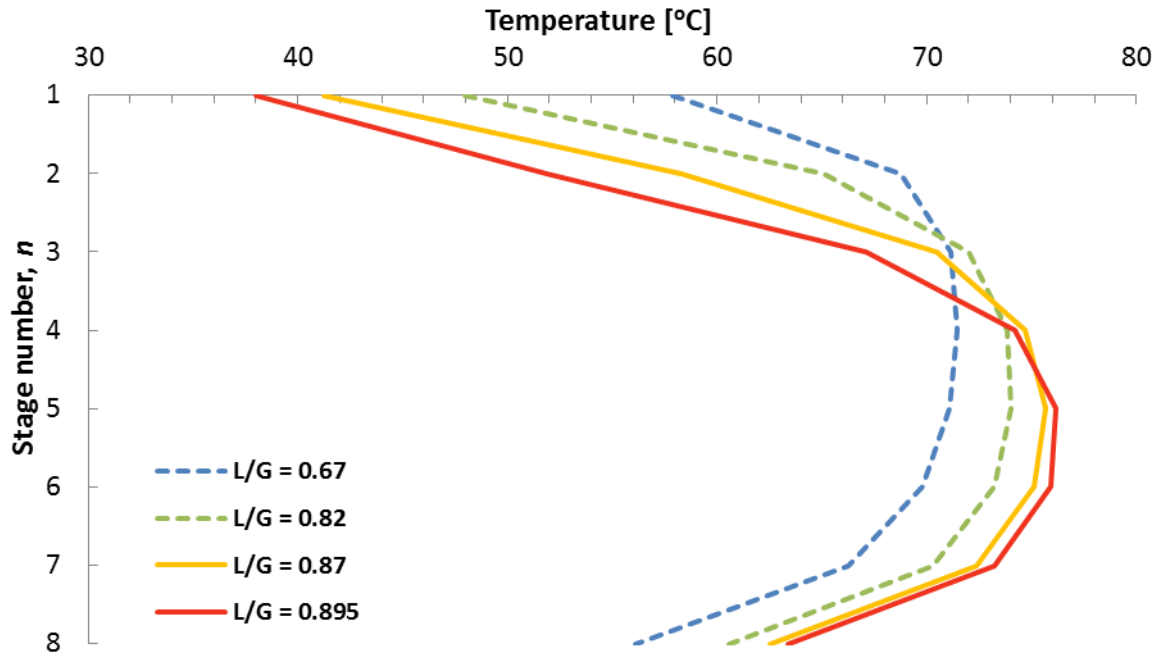

Figure 4.2.3: Temperature profiles in the absorber for different L/G ratios [mol/mol]. Stage 1 is the top of the column. Analysis done with 49.8 ppm H_2S initially in the reservoir gas (Case 1) and using a 50 wt% aqueous MDEA solution at 30 °C.

The loading of H_2S and CO_2 in the rich MDEA leaving the column as a function of the number of stages for the same L/G cases, given in Figure 4.2.2, are given in Appendix C.1. The results show that α_{H_2S} is equal to 0.004, or less, as the number of stages are increased when the L/G ratio is below 0.82, which is in agreement with the discussion above. Rich loading of CO_2 decreases when L/G ratios are increased, which is expected. For further simulations eight stages in the absorber are used.

Figure 4.2.4 shows L/G ratios as a function of MDEA concentration. This analysis examined Case 1 and 2, and the L/G ratio was adjusted to give a H_2S content of 4 ppm, on a dry basis, in the sweet gas. Because the preliminary runs were without any MEG present, and the gas is saturated with water, water was neglected in the calculations.

Figure 4.2.4 shows that the required L/G ratio for reaching the H_2S specification decreases as the MDEA concentration increases. Analysis was performed for 15 wt% to 55 wt% aqueous MDEA because of convergence problems outside this concentration range, and because concentrations above 50-55 wt% MDEA is not recommended [2]. L/G ratios for Case 2 are only marginally higher than for Case 1, and average difference over the concentration range was calculated to be 0.51%. One would expect a small increase in L/G ratios for Case 2, compared to Case 1, but the H_2S concentrations are small for both cases. Comparing rich loading of CO_2 did not show any differences.

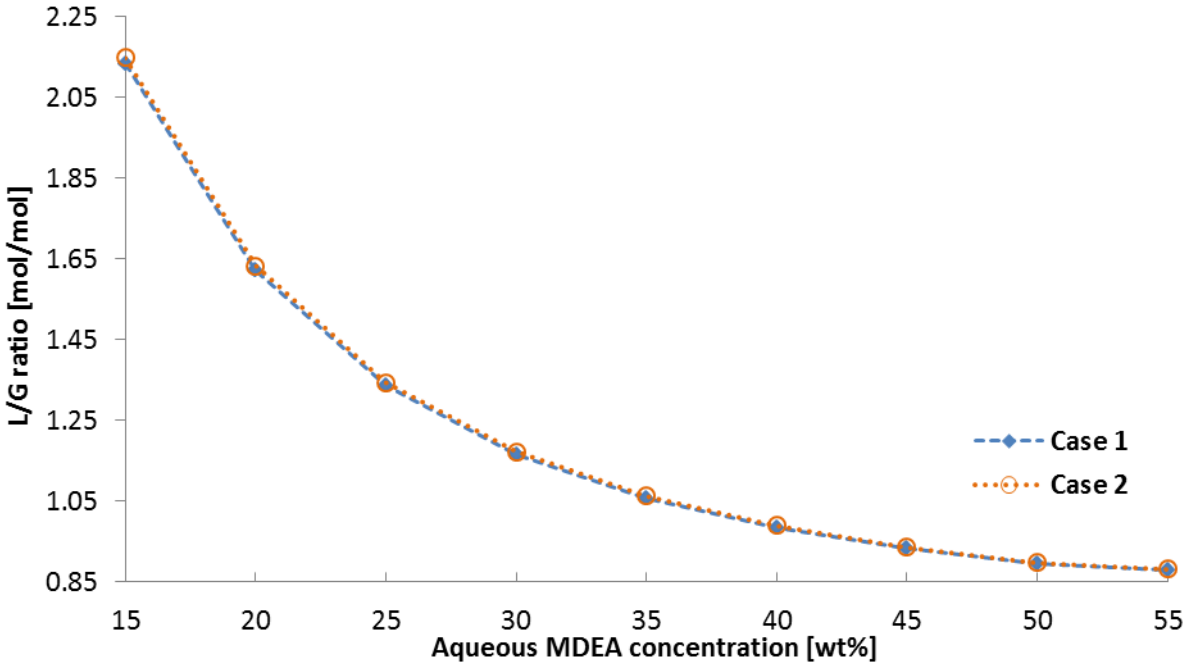

Figure 4.2.4: L/G ratios required for obtaining 4 ppm of H_2S in the sweet gas on a dry basis (water neglected) for different aqueous MDEA concentrations for Case 1 and 2.

Chapter 5 Simultaneous removal of H_2S and H_2O in MDEA-MEG solvents

5.1 Absorption in mixed MDEA-MEG solvents

A mixed MDEA-MEG solvent for combined H_2S and H_2O removal was examined. In this analysis the amount of MEG was increased in the lean solvent, using the same L/G ratios found in Chapter 4.2 (see Figure 4.2.4). The setup in Aspen Plus is given in Figure 5.1.1. The concentration ranges were 15 wt% to 55 wt% MDEA and 0 wt% to 50 wt% MEG. The amount of H_2S in the sweet gas was examined, and the results for Case 1 and 2 are given in Tables 5.1.1 and 5.1.2 respectively. If the H_2S content increased significantly when more MEG was added to the solvent, the analysis was not taken further, indicated by blank cells in the tables.

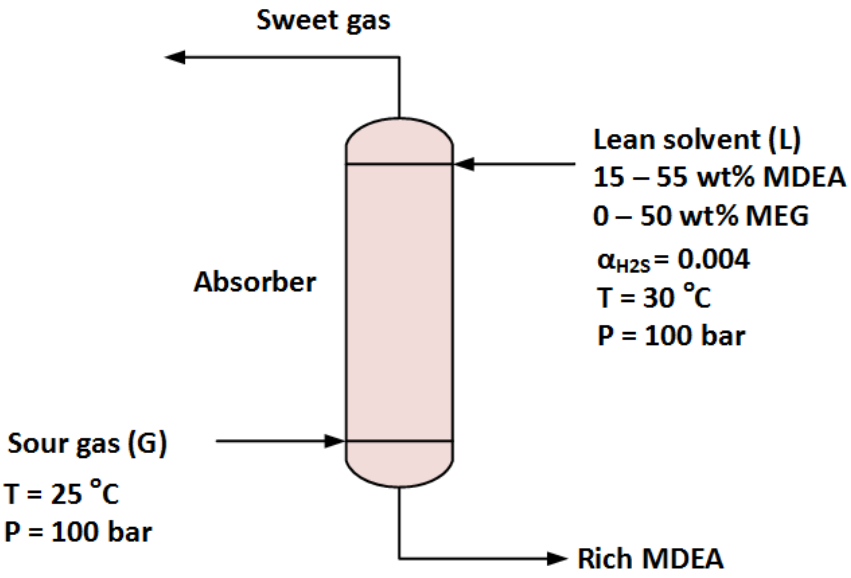

Figure 5.1.1: Setup for analysing absorption of H_2S and H_2O in a mixed MDEA-MEG solvent. An aqueous MDEA solvent was used as the starting point for the analysis, increasing the MEG concentration from 0 wt% to 50 wt%.

The results show that the H_2S content decreases below 4 ppm if the solvent concentration is 15 wt% to 25 wt% MDEA and 10 to 40 wt% MEG. This may be an indication of improved selectivity of H_2S when some water is replaced by MEG. This has also been discussed by Xu et al. [26], and they argued that H_2S is more soluble in MEG than CO_2, and using a mixed MDEA-MEG solvent may increase the selectivity of H_2S against CO_2. VLE validations in this work have also shown that H_2S is more soluble in MEG than CO_2, as it can be seen from Figure 3.3.13. VLE validations for H_2S and CO_2 mixtures in a 30 wt% MDEA + 65 wt% MEG + 5 wt% H_2O solvent gave poor results compared to Xu et al. [26], as discussed in Chapter 3.3.9. From Tables 5.1.1 and 5.1.2 it can be seen that MEG concentrations above 20 wt%, in 30 wt% MDEA are not included, because of insufficient H_2S removal.

Using low MDEA concentrations and high MEG concentrations, increase the L/G ratio required. This can affect the size of the equipment and may result in higher operating and investment costs. Because of small H_2S concentrations it can only be seen marginal differences in L/G for Case 1 and 2. Another observation is that using 55 wt% instead of 50 wt% MDEA in the solvent solution gives marginal differences with respect to the L/G ratio.

Table 5.1.1: Results for H_2S content in the sweet gas [ppm] using an aqueous MDEA solvent and increasing concentration of MEG for Case 1.

Aqueous solvent concentration	MEG [wt%]	0	10	20	30	40	50
MDEA [wt%]	(L/G) [mol/mol]	H_2S content in sweet gas [ppm]					
55	0.88	4.00	38.27	397.51	-	-	-
50	0.89	4.00	37.90	207.19	-	-	-
45	0.93	4.00	24.89	109.12	-	-	-
40	0.98	4.01	16.19	60.74	-	-	-
35	1.06	4.01	9.90	32.87	-	-	-
30	1.17	4.00	4.63	13.45	-	-	-
25	1.34	4.00	0.60	0.85	8.80	-	-
20	1.62	4.00	0.17	0.27	0.50	1.13	46.78
15	2.13	4.00	0.10	0.15	0.25	-	-

Table 5.1.2: Results for H_2S content in the sweet gas [ppm] using an aqueous MDEA solvent and increasing concentration of MEG for Case 2.

Aqueous solvent concentration	MEG [wt%]	0	10	20	30	40	50
MDEA [wt%]	(L/G) [mol/mol]	H_2S content in sweet gas [ppm]					
55	0.88	4.01	38.35	400.66	-	-	-
50	0.90	4.00	37.89	204.87	-	-	-
45	0.94	4.00	24.67	107.04	-	-	-
40	0.99	4.00	15.97	59.37	-	-	-
35	1.06	4.01	9.72	32.00	-	-	-
30	1.17	4.01	4.46	13.05	-	-	-
25	1.34	4.00	0.56	0.75	7.84	52.29	-
20	1.63	4.00	0.17	0.26	0.48	-	-
15	2.15	4.01	0.10	0.15	0.49	-	-

Before continuing the simulations, the amount of water absorbed for the same cases discussed above were examined. Even if the results given in Tables 5.1.1 and 5.1.2 give promising results for mixed MDEA-MEG solvents, simultaneous H_2S and H_2O removal using a single mixed solvent stream into one absorber may not be applicable in Aspen Plus. The amount of water in the gas stream increases for all cases, except for the case with 20 wt% MDEA + 40 wt% MEG + 40wt% H_2O and 15 wt% MDEA + 30 wt% MEG + 55wt% H_2O. The H_2S specification in these cases are fulfilled, but the water content in the sweet gas were 873.7

ppm and 964.2 ppm, respectively, which do not comply with the specifications. The percentage increase in moles H_2O in the gas stream through the absorber for Case 1, is given in Appendix C.2 for the different solvent concentrations. The fact that the water content in the vapor phase increases through the column is because aqueous amine solvents are utilized, and is one of the reasons for why gas dehydration is performed after acid gas removal, as stated by Campbell [13]. Increasing the number of stages in the column did not improve the results. The configuration was not considered further in this work because of this.

5.2 MDEA and MEG as separate feed streams

The patented processing units from 1948, 1950 and 1951 discussed in Chapter 2.4.3 were suggested as two-step absorption processes using one contactor column. The idea was to mainly have acid gas removal in the bottom part of the column, and introducing a water absorbent into the top of the column. One absorber was simulated in Aspen Plus with two solvent feed streams entering the column, one with MEG and one with aqueous MDEA. The configuration was examined for Case 1 and the set up in Aspen Plus is shown in Figure 5.2.1. The basis for the analysis was as follows:

- The analysis was started with both feed streams into the top of the column (n = 1)
- 35 wt% and 45 wt% MDEA solvents at 30 ^oC were examined
- The L_1 /G ratio was adjusted to reach a specification of 4 ppm H_2S in the sweet gas on a dry basis
- 95 wt% - 99.9 wt% MEG at 30 ^oC was examined with varying L_2/G ratios.
- Inlet stage of L_1 was changed moving downward the column.
- Increasing the number of stages in the column beyond the initial eight stages

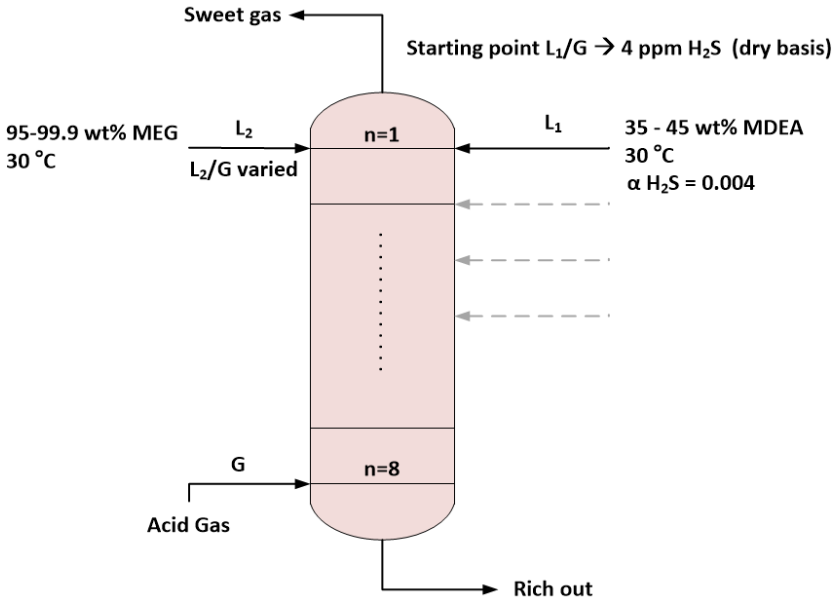

Figure 5.2.1: Set up in Aspen Plus for examining absorption of H_2S and H_2O with two separate solvent feed streams.

The water specification of 42 ppm was not obtained using this approach. Examination of the concentration profile in the column, showed that the water content in the gas phase was increasing up to the stage where aqueous MDEA was fed in, and decreasing in the MEG region. A better approach could be to use a high concentrated MDEA solution, fed into the middle section of the column, and providing lean MEG into the top. However, as discussed in Chapter 4.2, Aspen Plus struggles to handle high concentrations of MDEA, above 55 wt% and is not recommended because of increased viscosity. Because of this, the configuration was not considered further.

Chapter 6 Absorption and regeneration simulations

Mixing MDEA and MEG into one absorbent stream or as two separate feed streams, into one column, did not give satisfying results with respect to water removal. Because of this, acid gas removal and gas dehydration were simulated as two separate absorption processes, including regeneration systems for MDEA and MEG. Absorption of H_2S and CO_2, in MDEA was examined first, and then absorption of water in a MEG solvent was analysed.

6.1 Two step absorption – preliminary analysis

A two-step absorption process was analysed in Aspen Plus for Case 1 and 2, excluding regeneration of solvents. A PFD of the setup in Aspen Plus is shown in Figure 6.1.1. Absorption of H_2S and CO_2 in MDEA was simulated in the first column, while water removal utilizing MEG was simulated in the second column. The L/G ratios into the columns were adjusted so that the H_2S content out of the first absorber was 4 ppm on a dry basis (G_2) and the water content out of the second absorber was 42 ppm (dry gas). The MDEA concentration was varied from 15 wt% to 55 wt%, and examined at 15 ^oC and 30 ^oC. A MEG concentration of 98 wt% at 15 ^oC was held constant in the first run.

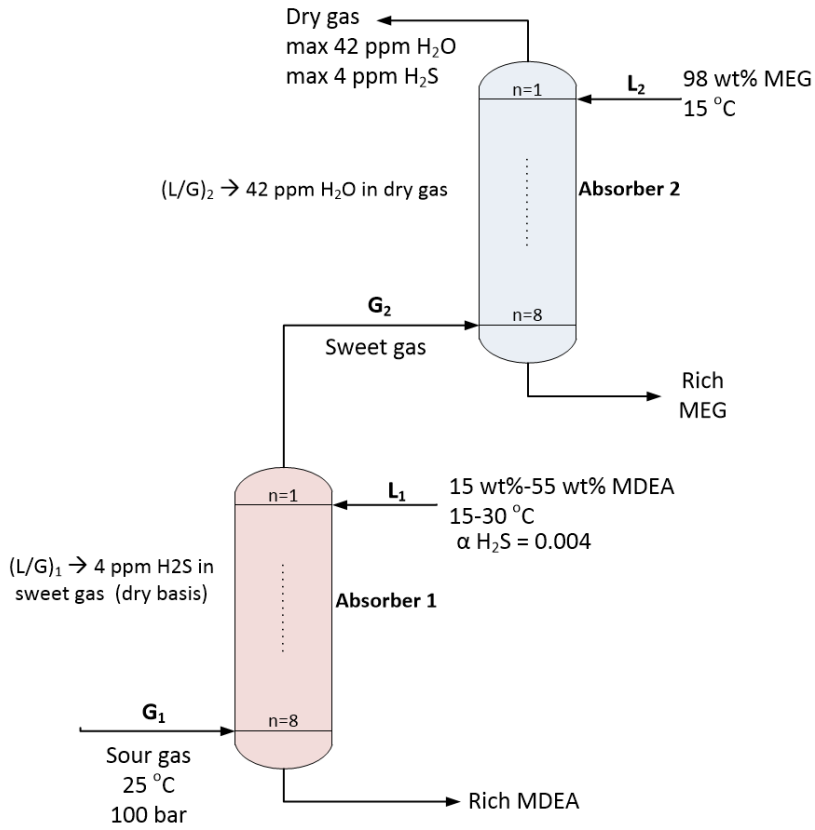

Figure 6.1.1: Set up in Aspen Plus for simulating acid gas absorption and water removal in two separate absorber columns.

Figure 6.1.2 gives the L/G-ratio into the different absorbers as a function of MDEA concentration (in L_1). The L_1/G_1 ratio decreases for increasing MDEA concentrations, as seen in Chapter 4.2 as well. The L_2/G_2 ratio, which gives 42 ppm H_2O in the dry gas, is 0.37 and

does not change due to small water composition changes in the sweet gas. For all cases, the H_2S content in the dry gas was calculated to be 3.3 ppm, which is according to the specification. When the temperature in L_1 is lowered to 15 ^oC, the L_1/G_1 ratio required to meet the H_2S specification decreases because the solubility of H_2S increases at lower temperatures. The average percentage decrease in the L_1/G_1 ratio is 11.3%, and the average percentage decrease in the L_2/G_2 ratio is 11.9%. When the temperature of MDEA is lowered to 15 ^oC, the H_2O content in the sweet gas (G_2) decreases, and the L_2/G_2 ratio needed to reach the water specification is therefore lower. Lowering the MDEA temperature was mainly done to examine if this could lower the L_2/G_2 ratio considerably, which it does not. L/G ratios into the columns for the cases analysed are not dependent on the H_2S content into the columns, for Case 1 and 2, and give the same results due to small initial H_2S concentrations and because the lean loading of MDEA is constant. There are some missing data points in Figure 6.1.2 because the simulation would not converge for these runs.

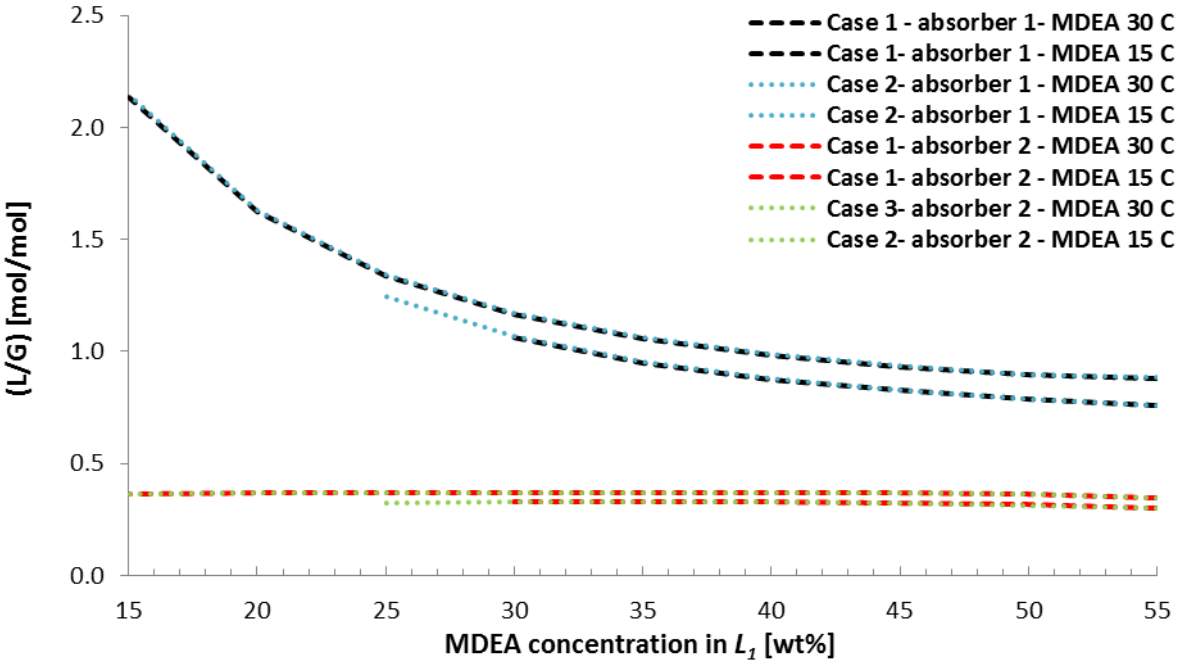

Figure 6.1.2: L/G ratio into the absorbers as a function of MDEA concentration in the acid gas removal column (absorber 1). MEG concentration of 98 wt% at 15 ^oC was held constant in the second absorber. MDEA at 15 ^oC and 30 ^oC were examined.

The MEG concentration and temperature were then varied to examine the absorption performance for various L/G ratios, to get a picture of what MEG concentrations that should be used for fine removal of water. A 45 wt% aqueous MDEA solution, at 30 ^oC, was held constant in the first absorber. For Case 1, this gave a H_2O content of 1537 ppm in the gas entering the second absorber with a temperature of 39.3 ^oC. MDEA at 15 ^oC is not preferable to use because of high viscosity and possibilities of co-absorption of hydrocarbons.

Figure 6.1.3 gives the H_2O content in the dry gas as a function of L_2/G_2 for Case 1, for different MEG concentrations at different temperatures. A 98 wt% MEG solution, at 15 ^oC gives the desirable water specification with L/G = 0.37. However, examining the rich MEG solution revealed small concentration changes through the column, which indicates an

unnecessary high circulation rate. A 99.3 wt% MEG solution at 35 ^oC decreases the L/G ratio to 0.07, which is substantially lower.

In MEG injection systems, MEG is normally regenerated to 90%, but using MEG as a dehydration solvent may require higher concentrations. The results in Figure 6.1.3 are indicating that concentrations above 99 wt% MEG should be used for fine removal of water. In this case, the water content into the second absorber was 1537 ppm, but this can differ for different gas compositions. The gas temperature out of the first column will vary, and is dependent on the lean MDEA circulation rate and temperature, required to remove acid gas components. Analysis should therefore be done to find the optimal concentration and temperature for different gas compositions.

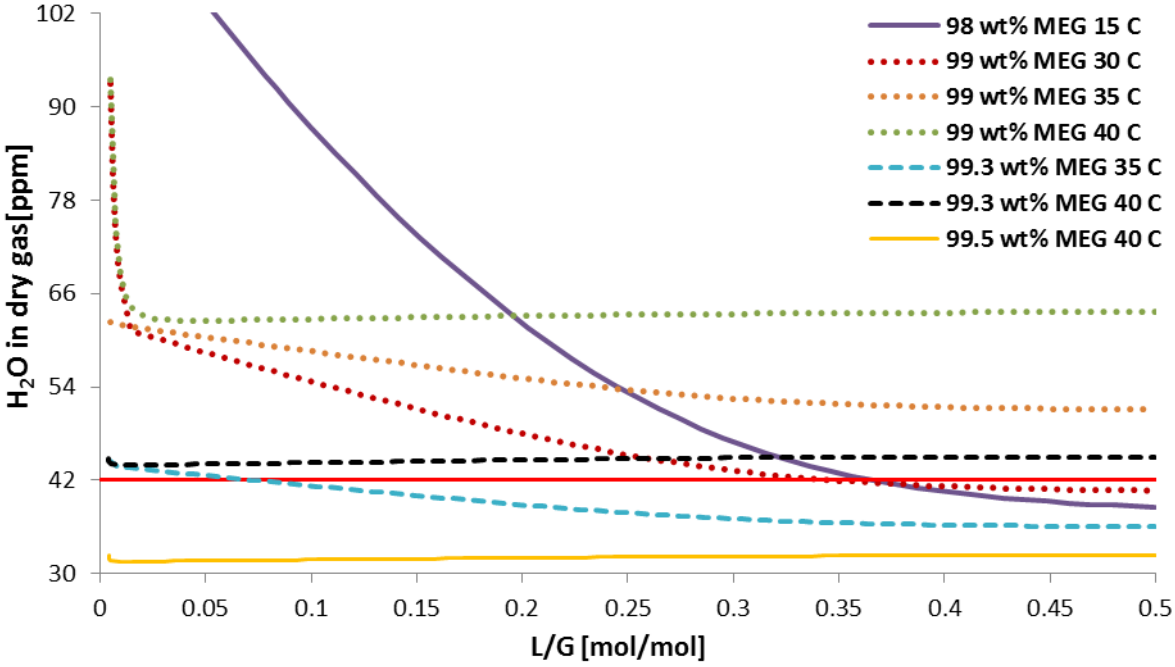

Figure 6.1.3: H_2O in the dry gas, in ppm, as a function of L/G in the second absorber for different MEG concentrations at different temperatures. The water specification of 42 ppm is indicated on the figure (red line).

Because a high concentration of MEG is necessary for dehydrating the gas to the desired specification, it may cause problems in the regeneration system. MEG degrades around 165 ^oC [13, 18], and regeneration of MEG to 90 wt% often requires temperatures up to 140 ^oC to 150 ^oC [19, 45]. By comparison, TEG degrades at 206 ^oC, and is normally used for dehydration because it is more robust with respect to degradation [13].

6.2 Acid gas removal including regeneration of MDEA

The process setup in Aspen Plus for H_2S and CO_2 absorption, including regeneration of MDEA is illustrated in Figure 6.2.1. A screenshot of the PFD from Aspen Plus is given in Appendix C.3. The operating conditions used as simulation input are given in Table 6.2.1. Conditions for the lean MDEA concentration, high pressure (HP) flash and low pressure (LP) equipment were based on plant data from an acid gas removal unit located in Qatar [17]. Simulations were performed for Case 1, 2 and 3, as described in Table 4.1.1. The number of

stages in the absorber was set to eight for all cases, based on the preliminary analysis, holding inlet conditions constant.

Table 6.2.1: Conditions that were used as input for simulating acid gas absorption and the MDEA regeneration system. MDEA concentration, HP pressure and LP pressure were based on Alfadala et al. [17].

Simulation input	Unit	Value
Lean aqueous MDEA concentration	[wt%]	45
Lean MDEA temperature	[^{o}C]	30
Sour gas temperature	[^{o}C]	25
Absorber pressure	[bar]	100
HP flash pressure	[barg]	10
LP valve/LP flash/Stripper pressure	[barg]	2.35
Condenser temperature	[^{o}C]	25

Rich MDEA is taken out of the bottom of the absorber, and depressurized to 10 barg before it flows into the HP-flash. The pressure is then taken down to 2.35 barg, and rich MDEA is heated in the lean-rich heat exchanger. A hot outlet- cold inlet temperature difference approach of 10 ^{o}C was defined, because of convergence problems using other specifications. This can be optimized for the given process, but was not considered in this work. Lowering pinch temperatures in the heat exchanger can affect investment costs, and energy requirements versus costs need to be analysed to find the optimal operating conditions. Lean MDEA exiting the reboiler has a high temperature which strips some of the gaseous components entrained in the rich MDEA solvent in the heat exchanger. Therefore a LP flash was defined to examine the stripping rate.

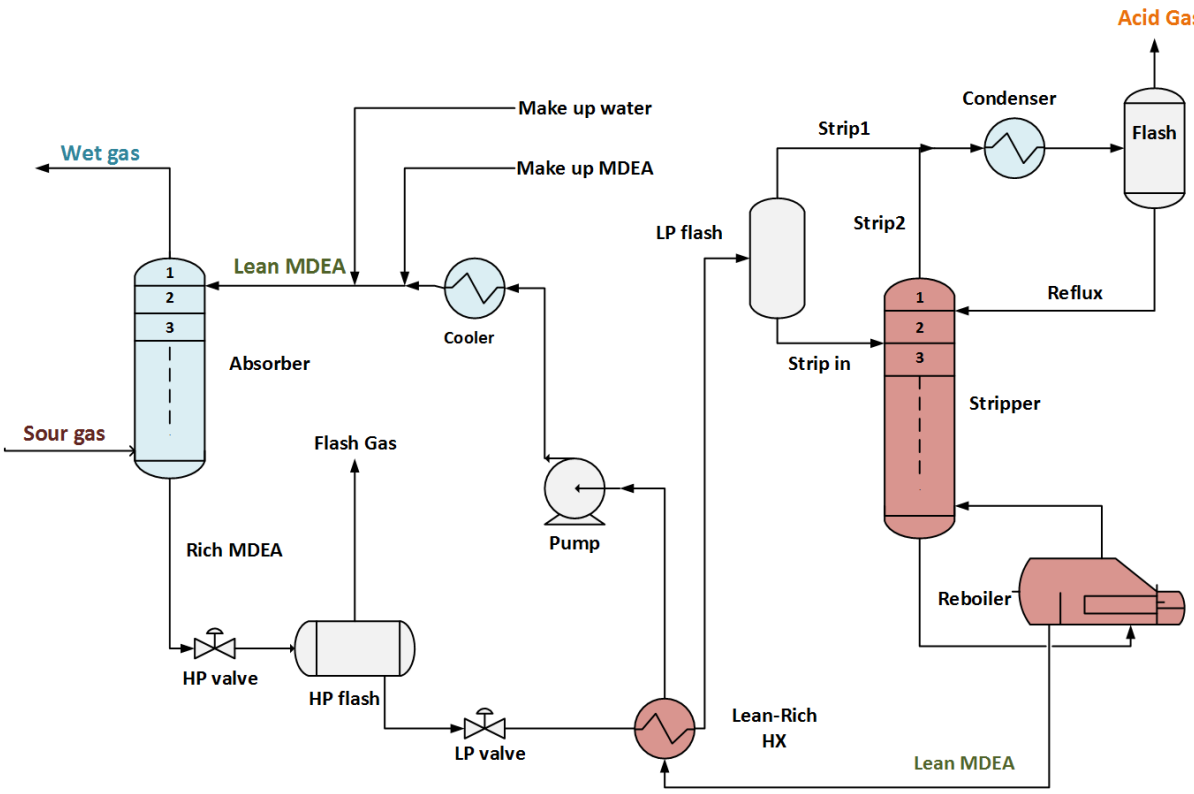

Figure 6.2.1: Process setup in Aspen Plus for simulating acid gas absorption, including regeneration of MDEA. Makeup streams for water and MDEA defined to make sure concentration and flow of lean MDEA, entering the absorber, were constant.

Pressure, reboiler duty and the number of stages were defined in the stripper. The number of stages was, also here, set to eight for all cases, based on preliminary analysis for Case 1. It was desirable to keep the column conditions constant for all cases. Analysing on-stage feed versus above-stage feed gave the same results with respect to acid gas recovery. As seen from the figure, reflux was defined to enter the stripper one stage above the rich MDEA solution.

Lean MDEA is then cooled down and pumped up to 100 bar, which is the absorber pressure. Make up water and MDEA are mixed with lean MDEA before entering the absorber, to account for losses in the outlet streams, and the concentration of MDEA was checked for each run. To make the system converge, some of the specifications in the convergence block were changed. Design specification nesting was changed to 'with tears' because tear streams ('Lean MDEA' and 'Reflux') and a design specification ('Make up water') were defined in the system. Pressure drops in all units were neglected.

6.2.1 System performance

The gas composition cases were examined by performing an energy requirement analysis with respect to specific reboiler duty, Q_s, in MJ/kg acid gas. Case 2 was also examined with inlet temperatures of 35 ^{o}C and 40 ^{o}C, for sour gas and lean MDEA, respectively, based on the operating conditions of the plant, reported by Alfadala et al. [17]. The different conditions are referred to as Case 2.1 and 2.2 in this chapter, where the former case uses a gas temperature of 25 ^{o}C, and the latter lets natural gas and MDEA enter the absorber at 35 ^{o}C and 40 ^{o}C, respectively.

The analysis was performed to examine the desired area of operation with respect to energy requirements in the reboiler, because this is the part of the process that is most energy demanding in terms of heat requirements [46]. L/G ratios into the absorber were varied and the reboiler duty in the stripper was adjusted so that the H_2S content in the sweet gas (wet gas) was 4 ppm $\pm$ 0.05 ppm.

In addition to operate with the lowest energy requirement possible in the reboiler, it is also desirable to use the lowest circulation rate of MDEA possible for reaching specifications, which in turn gives a lower energy demand in the reboiler. The reason for this is that the reboiler provides heat to; heat up the MDEA solvent (sensible heat), reverse the absorption reactions (heat for desorption) and vaporize water to produce stripping steam. Q_s was based the amount of H_2S and CO_2 absorbed in the rich MDEA solvent entering the stripper (strip in). The assumptions for the calculations are given in Appendix C.4. The results from the analysis, giving Q_s for different L/G ratios in the absorber for all cases, are given in Figure 6.2.2.

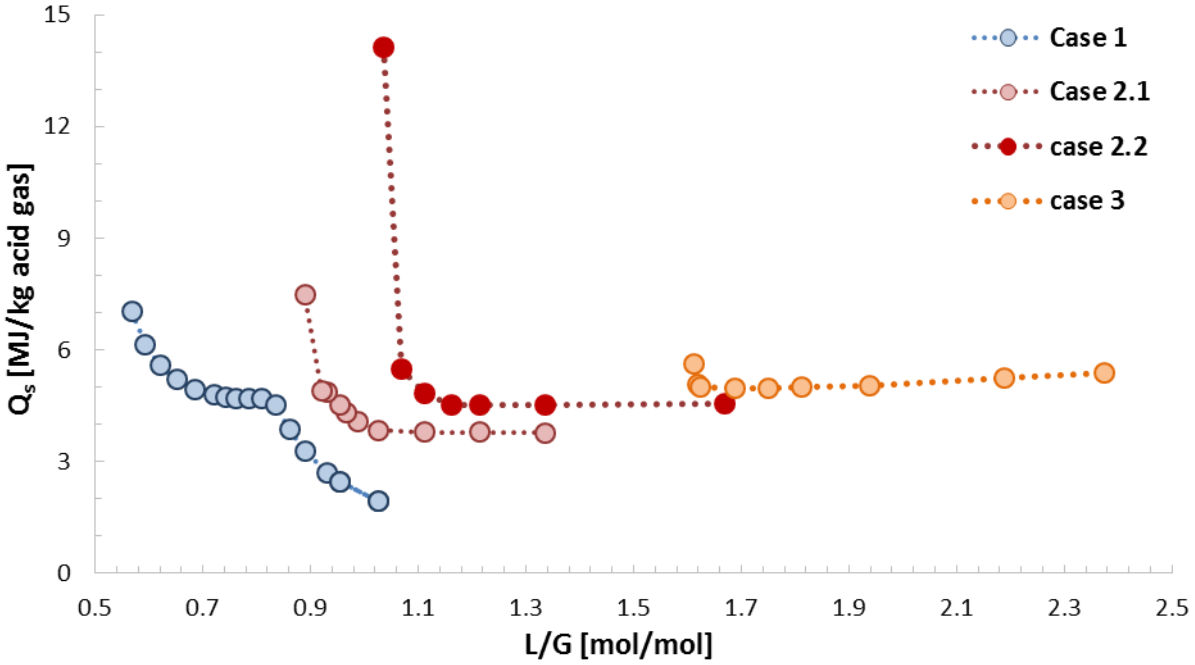

Figure 6.2.2: Specific reboiler duty, Q_s, in MJ/kg acid gas, as a function of molar liquid-gas ratio, L/G, for different gas compositions. The H_2S content in the gas leaving the absorber was held constant at 4 $\pm$ 0.05 ppm. Case 2.1 and 2.2 have the same compositions, but differ in temperature conditions.

Other variables that were examined, included

- Overall percentage recovery of H_2S and CO_2
- Reboiler temperature in the stripper
- Percentage H_2S and CO_2 stripped in the lean-rich heat exchanger of the overall percentage recovery
- H_2S and CO_2 loading in the liquid stream into and out of the absorber, $\alpha_{i,rich}$ and $\alpha_{i,lean}$ [mol *i*/mol MDEA]

These results are given in Chapters 6.2.1.1, 6.2.1.2 and 6.2.1.3 for Case 1, 2 and 3, respectively. From Figure 6.2.2 it can be seen that the required L/G ratio increases as the amount of acid gas increases in the sour gas. The only difference between Case 1 and 2 is the amount of H_2S in the sour gas. Case 1 has an unexpected behaviour, and the specific reboiler duty decreases substantially for L/G ratios above 0.8. This area is commented in Chapter 6.2.1.1, and will not be considered as a desired area of operation. Chapter 6.2.2 gives a summary and an overview of the operational areas that were considered as energy efficient.

6.2.1.1 Case 1 - Low H_2S concentration

Figure 6.2.3 gives the overall percentage recovery of H_2S and CO_2 in the system, and the amount stripped in the lean rich exchanger, as percentage of the total recovery for different L/G ratios. The reboiler temperature is also shown for the different runs. Rich and lean loading of the MDEA solvent, in the absorber, are given in Figure 6.2.4 for H_2S and CO_2.

As seen from Figure 6.2.2 the specific reboiler duty decreases again for L/G ratios above 0.8, as well does the temperature, because of high liquid flows. This also results in a lower stripping rate in the lean-rich heat exchanger, which can be seen from Figure 6.2.3. Since the

L/G ratio in this area is higher, which means that the gas rate entering the system is smaller compared to the liquid MDEA flowrate, moles acid gas compared to moles MDEA decreases. This enables the absorber to give satisfying results even if the lean H_2S and CO_2 loading in MDEA are increasing. This is however not considered as a desired area of operation, because high acid gas loading in the lean amine solvent may result in higher corrosion rates in the whole system. As the reboiler duty decreases, the lean MDEA loading with respect to CO_2 increases above 0.01, causing circulation of acid gas entrained in MDEA. Maximum recommended lean loadings of MDEA have been reported to be 0.004-0.01 [2]. Because of this, it was decided to examine a L/G ratio of 0.75, which gives a Q_s of 4.7 MJ/kg acid gas, for further dehydration analyses. The wet gas conditions are given in Chapter 6.2.2.

Sakwattanpong et al. [47] reported values for specific reboiler duty up to approximately 6 MJ/kg CO_2, depending on the desired lean solvent purity. Fiaschi and Lombardi [48] reported a heat duty of 3269 kW/kg H_2S, which corresponds to 3.269 MJ/kg H_2S. Values for specific reboiler duties between the reported values were therefore accepted.

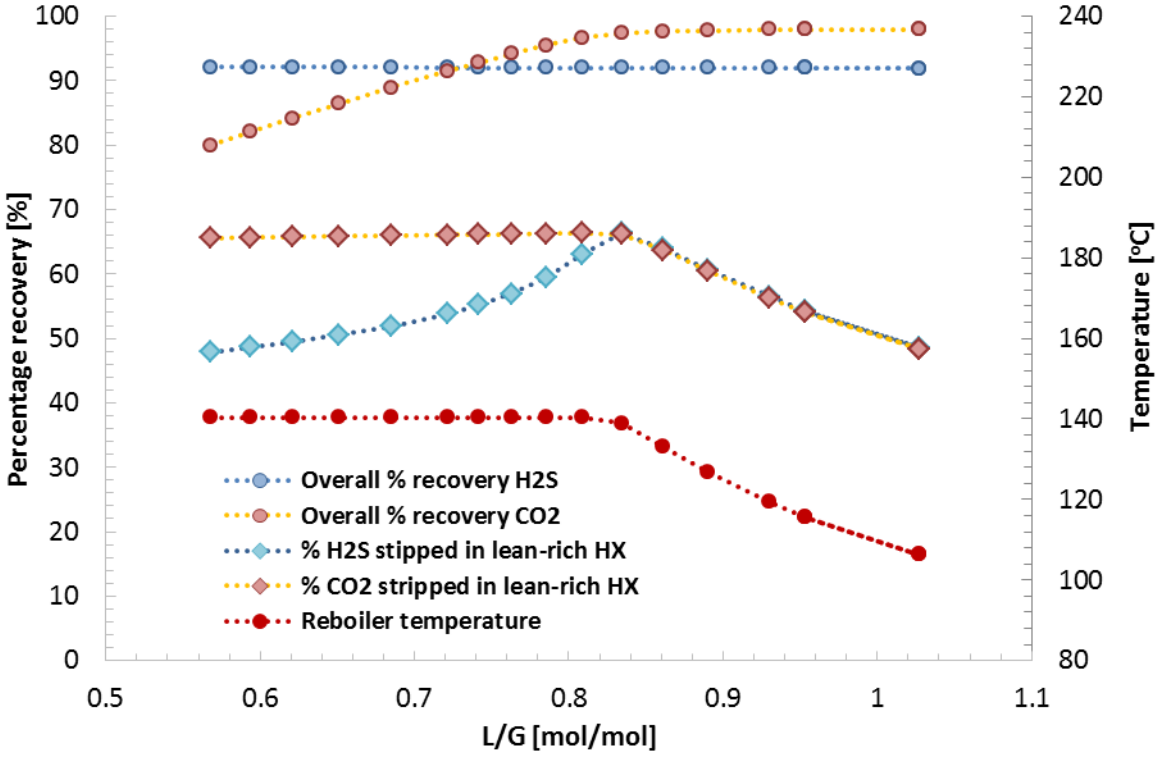

Figure 6.2.3: Gives overall percentage recovery of H_2S and CO_2, and percentage of H_2S and CO_2 stripped in the lean-rich heat exchanger of the total recovery for increasing L/G ratios in the absorber. Temperature in the reboiler is also given.

Up to L/G = 0.8, the overall recovery of H_2S is constant and the overall recovery of CO_2 is increasing. The percentage of this, stripped in the lean rich heat exchanger, gives the opposite trend as seen from Figure 6.2.3. Rich MDEA loadings are decreasing in this area, because the liquid ratio is increasing. It should be noticed that Aspen Plus gives high temperatures in the reboiler, and is around 140 ^oC for L/G ratios below 0.8. There may be a possibility of MDEA degradation at temperatures above 130 ^oC [16]. Reaching H_2S specifications, and simultaneously controlling the temperature in the reboiler would have required higher L/G

ratios in the absorber. Alfadala et al. [17] simulated an acid gas removal unit using MDEA and reported temperatures in the reboiler of 144 ^oC.

Rich loading of H_2S have an expected decreasing trend up L/G = 0.8, since the amount of MDEA in the system is increasing. Lean loading of H_2S is increasing, and the lean MDEA solvent has the capacity of removing acid gas to desired specifications despite this. What should be noticed, is that the lean CO_2 loading, is approximately zero up to L/G = 0.8. It shows that all of the CO_2 is stripped from the MDEA solvent.

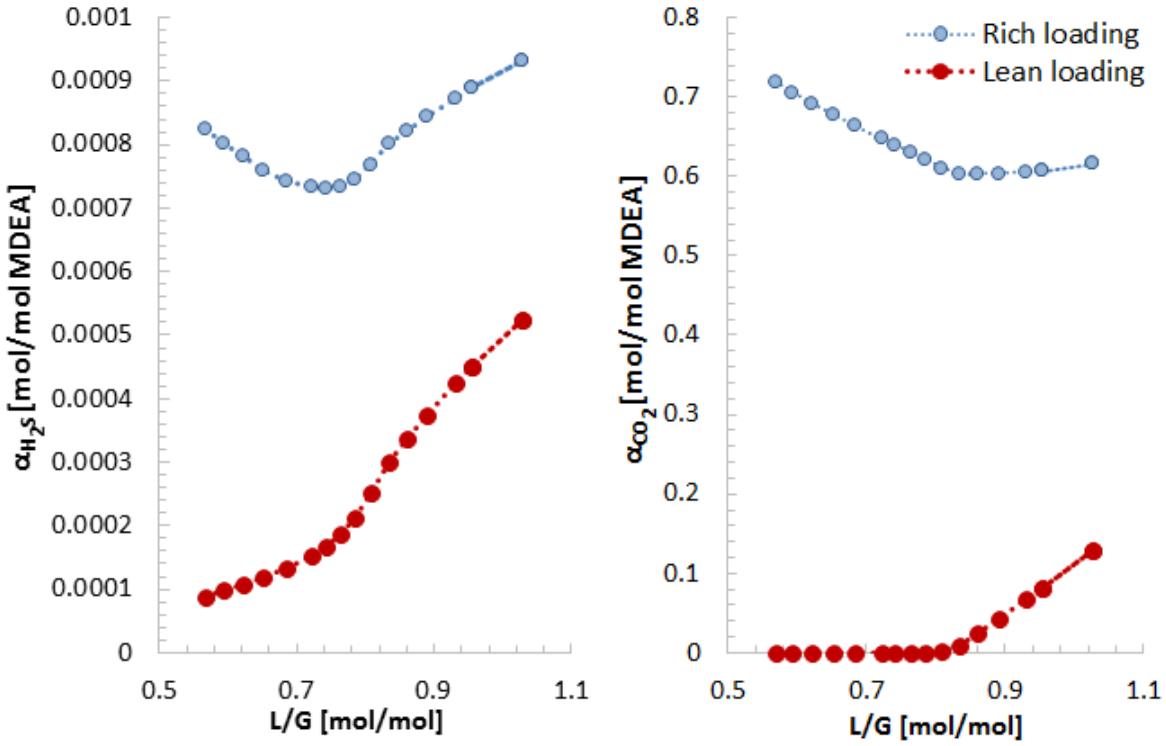

Figure 6.2.4: Loading of H_2S and CO_2 in the liquid phase, α_i, against liquid-gas ratio, L/G, into the absorber. Rich loading is rich MDEA taken out of the bottom and lean loading is lean MDEA flowing into the top.

6.2.1.2 Case 2 – Medium H_2S concentration

Figure 6.2.5 shows the overall percentage recovery of H_2S and CO_2 in the system, and amount stripped in the lean rich exchanger as percentage of the total recovery, for different L/G ratios. The reboiler temperature profile is also shown for increasing L/G ratios. Rich and lean loading of the MDEA solvent are given in Figures 6.2.6 and 6.2.7 for H_2S and CO_2, respectively.

From Figure 6.2.2 it can be seen that when the gas and MDEA temperatures are lowered, the absorption process requires lower L/G ratios, and the energy requirement is also decreased. The fact that Case 2.1 requires a lower L/G ratio was expected, because the solubility of H_2S and CO_2 are higher in MDEA at lower temperatures. Operational areas for further analyses were decided to be L/G ratios of 1.1 and 1.2, for Case 2.1 and 2.2 respectively. Q_s at these points are 3.7 and 4.5 MJ/kg acid gas. At the given L/G ratios the reboiler temperatures are 131 ^oC and 135 ^oC for Case 2.1 and 2.2 respectively. These are more acceptable values based

on reported operational reboiler temperatures [17]. All trends for Case 2.1 and 2.2. are observed to be consistent with each other.

MDEA is known for higher selectivity of H_2S when the CO_2/H_2S ratio increases [13]. In theory this means that Case 1 should have given indications of this compared to Case 2. It can be seen from Figure 6.2.5 that the overall recovery of CO_2 is slightly higher than for H_2S for all L/G ratios for Case 2. For Case 1, the overall recovery of CO_2 is smaller than for H_2S for L/G ratios below 0.72 (see Figure 6.2.3). In this work, the absorption process is based on equilibrium calculations and gives higher absorption rates of CO_2 than it would be realistic to assume. Additionally, as shown in Chapter 3.3.11, presence of CO_2 decreases the H_2S solubility when the CO_2 amount increases.

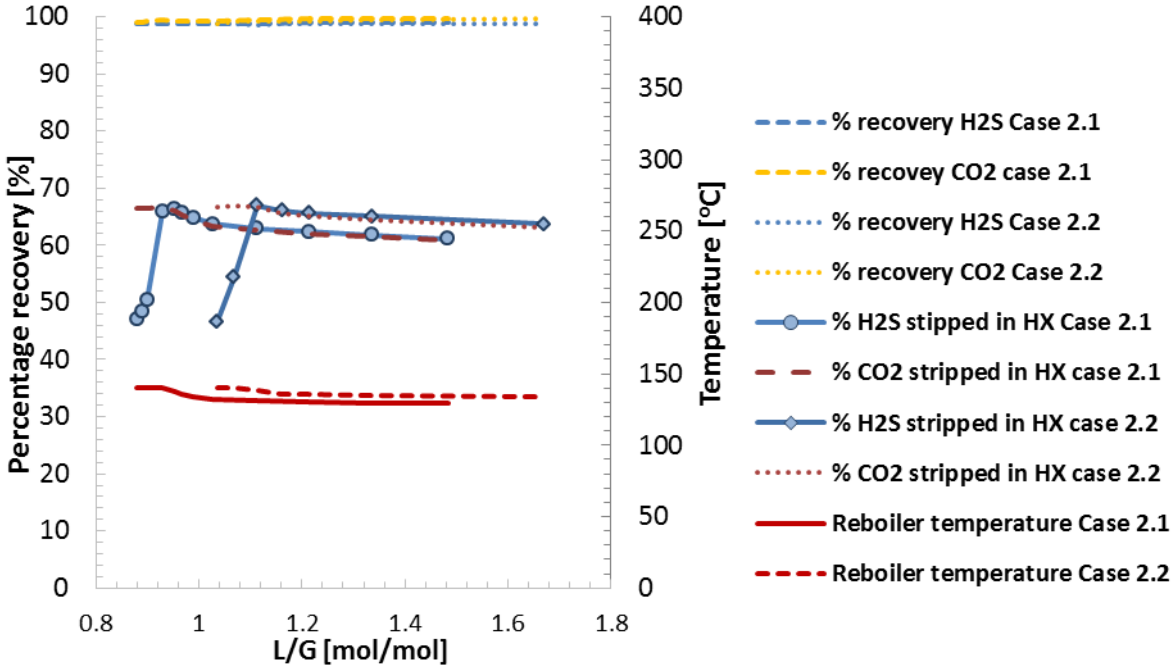

Figure 6.2.5: Overall percentage recovery of H_2S and CO_2, and percentage of H_2S and CO_2 stripped in the lean-rich heat exchanger of the total recovery for increasing L/G ratios in the absorber. Temperature in the reboiler is also given. Analysis done for Case 2 with gas flowing into the absorber at different temperatures. Case 2.1 is gas at 25 ^oC and Case 2.2 is for gas at 35 ^oC.

Rich loading of CO_2 is decreasing for all L/G ratios, which is expected since the amount of MDEA in the system is increasing. However, rich loading of H_2S has a steep increasing trend for L/G ratios below 0.96 and 1.13 for Case 2.1 and 2.2, respectively, before it starts to decrease. From Figure 6.2.5 it can be seen that less H_2S is stripped in the lean-rich heat exchanger in this area, which may indicate that Aspen Plus strips more CO_2 from MDEA than one could expect.

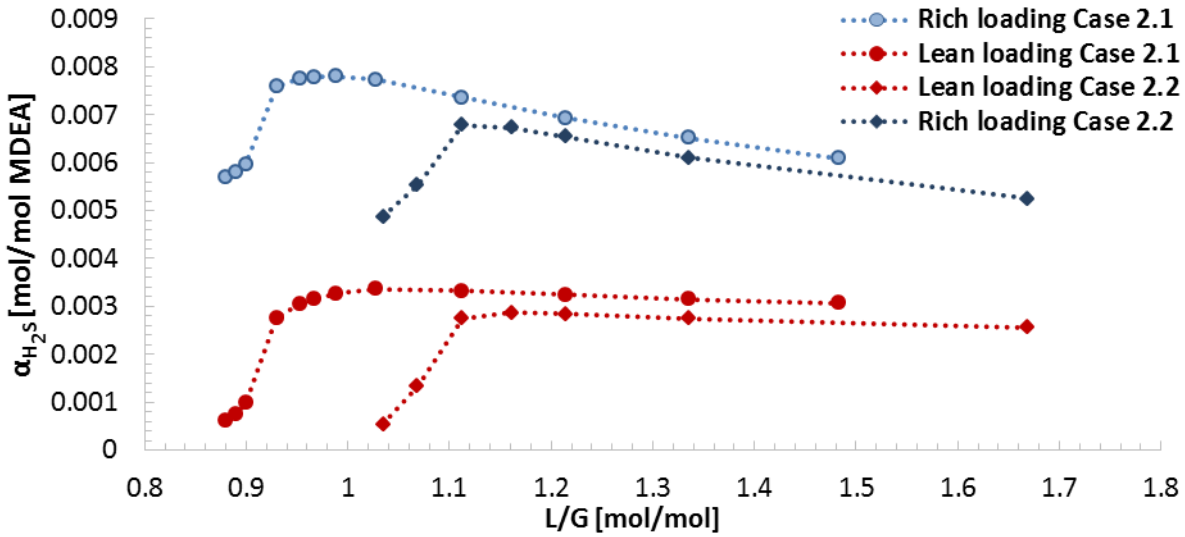

Figure 6.2.6: Loading of H_2S in the liquid phase, α_{H_2S}, against liquid-gas ratio, L/G, into the absorber. Rich loading is in rich MDEA taken out of the bottom and lean loading is in lean MDEA flowing into the top. Analysis done for Case 2 with gas flowing into the absorber at different temperatures. Case 2.1 is gas at 25 ^oC and Case 2.2 is for gas at 35 ^oC.

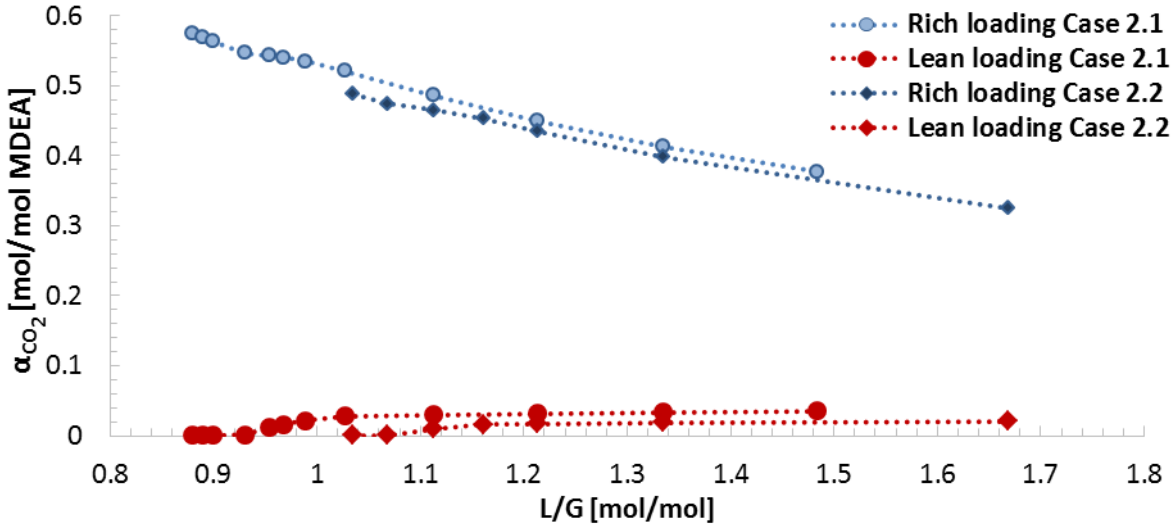

Figure 6.2.7: Loading of CO_2 in the liquid phase, α_{CO_2}, against liquid-gas ratio, L/G, into the absorber. Rich loading is in rich MDEA taken out of the bottom and lean loading is in lean MDEA flowing into the top. Analysis done for Case 2 with gas flowing into the absorber at different temperatures. Case 2.1 is gas at 25 ^oC and Case 2.2 is for gas at 35 ^oC.

6.2.1.3 Case 3 – High H_2S concentration

Figure 6.2.8 shows the overall percentage recovery of H_2S and CO_2 in the system, and the amount stripped in the lean rich exchanger as percentage of the total recovery for different L/G ratios. The reboiler temperature profile is not shown in this case, because it was constant at 140 ^oC for all runs, which is above the recommended limit. Rich and lean loading of the MDEA solvent are given in Figures 6.2.9 and 6.2.10, for H_2S and CO_2 respectively.

In Case 3, the total amount of acid gas entering the absorber is 12.5%, which is much higher than for Case 1 and 2. This is also reflected in the required L/G ratio for obtaining 4 ppm H_2S in the dry gas as seen from Figure 6.2.2. With respect to specific reboiler duty and L/G, the operational area to analyse further, was found to be 1.7, and the wet gas conditions and other

parameters for this case are given in Chapter 6.2.2. At this point Q_s is 4.96 MJ/kg acid gas, which is higher than for the other cases. Increasing the number of stages in the stripper to 12, gave an average decrease of Q_s by 3.1% for L/G ratios higher than 1.69.

The total recovery of H_2S and CO_2 are approximately constant, as seen from Figure 6.2.8. This case differs from Case 1 and 2, in how much CO_2 that is stripped in the heat exchanger, which is higher for than for H_2S over the whole L/G range.

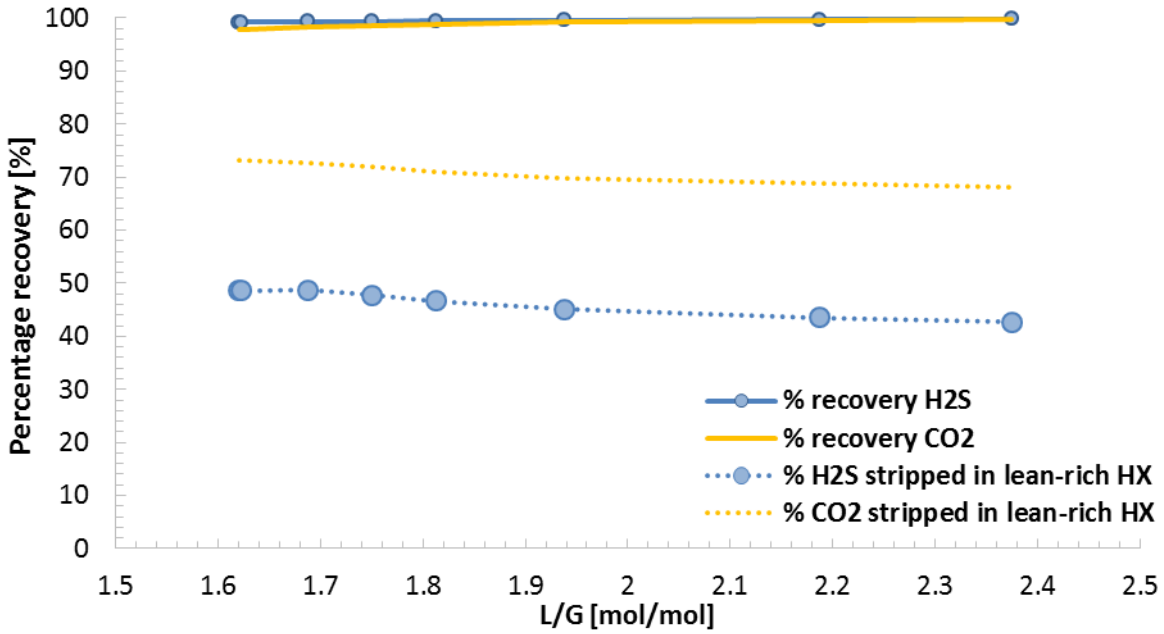

Figure 6.2.8: Gives overall percentage recovery of H_2S and CO_2, and percentage of H_2S and CO_2 stripped in the lean-rich heat exchanger of the total recovery for increasing L/G ratios in the absorber.

Figure 6.2.9 shows that the rich loading of H_2S is considerably higher than for Case 1 and 2, because the H_2S content is much higher in the sour gas. The rich loading of H_2S increases for increasing H_2S content in the sour gas, and the rich loading of CO_2 decreases, and is shown in Table 6.2.2 in Chapter 6.2.2.

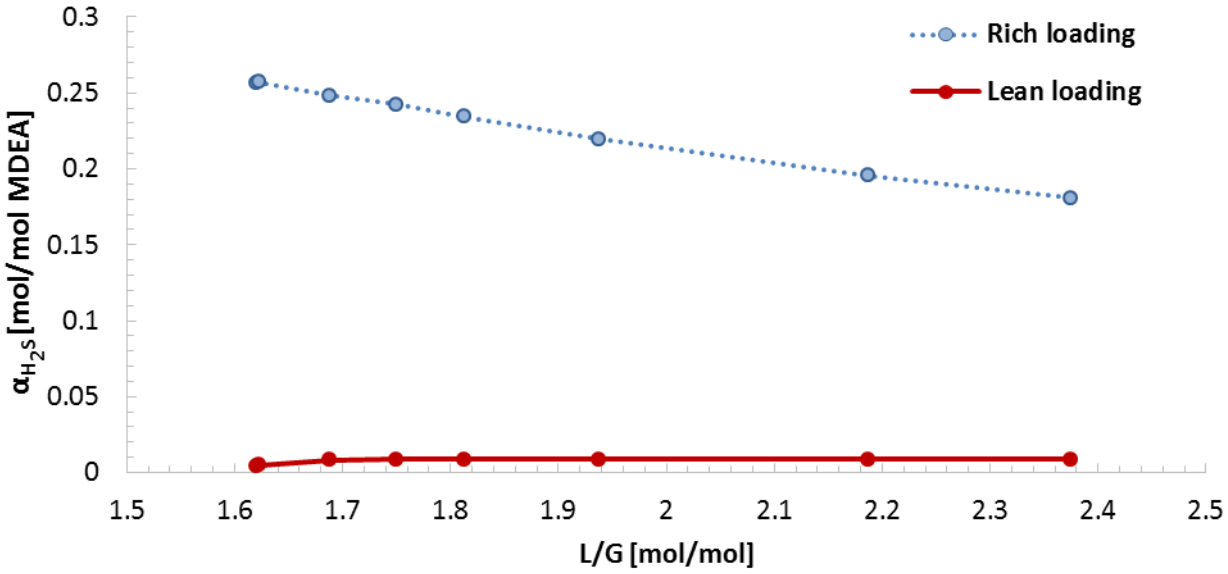

Figure 6.2.9: : Loading of H_2S in the liquid phase, α_{H_2S}, against liquid-gas ratio, L/G, into the absorber. Rich loading is in rich MDEA taken out of the bottom and lean loading is in lean MDEA flowing into the top.

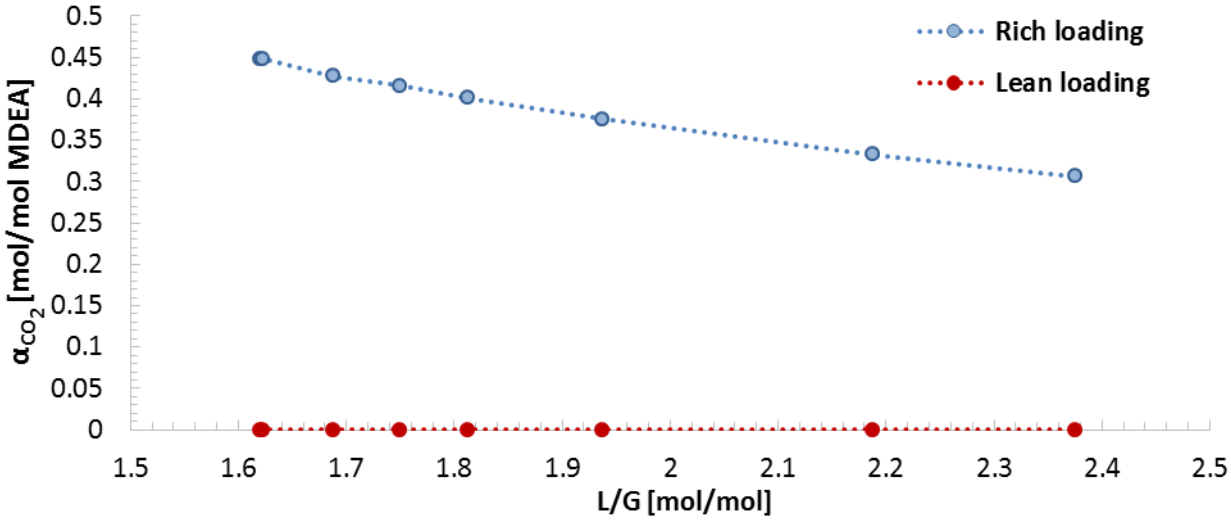

Figure 6.2.10: Loading of CO_2 in the liquid phase, α_{CO_2}, against liquid-gas ratio, L/G, into the absorber. Rich loading is in rich MDEA taken out of the bottom and lean loading is in lean MDEA flowing into the top.

6.2.2 Inspection of operational areas

The operational areas that were considered as energy efficient and chosen for further inspection, for the different gas composition cases, are given in Table 6.2.2. The table also gives the system parameters that were considered relevant. Temperature and composition profiles of the absorber and stripper, for the cases listed in the table, are given in Appendix C.5.

Table 6.2.2 shows that the L/G ratio increases for increasing acid gas contents in the inlet gas, and that lower absorption temperatures lowers the L/G ratio, comparing Case 2.1 and 2.2. Required L/G ratio and specific reboiler, to reach 4 ppm H_2S in the wet gas, are both higher for Case 3 compared to Case 2.1. The H_2S loading in rich MDEA is also increased for Case 3,

and the CO_2 loading in rich MDEA is less than for Case 2.1. Since the initial H_2S concentration in Case 2.1 is 4.45% lower than for Case 3, this indicates that the H_2S content affects the absorption of CO_2 to some degree. The initial CO_2 concentration differs by 2.4% between these cases, but the total recovery of CO_2 is only 1.2% lower for Case 3.

Specific reboiler duty for Case 2.1 is lower than for Case 1, which is not expected since the H_2S content is higher. Comparing these cases, revealed large differences in the wet gas temperature. For Case 1, a higher L/G ratio should be used to reduce vaporization of water in the top of the column. The wet gas of Case 1 holds 3067 ppm H_2O, compared to 1008 ppm for Case 2.1. Examining the temperature profile in the absorber for Case 1, showed that the temperatures in the top and the bottom of the column are approximately the same, which yields more water in the outlet gas stream (see Appendix C.5). Amount of MDEA in the wet gas was also higher for Case 1 compared to the other, and is important to consider in operation because amine losses can be expensive [13]. MDEA is known for having low vapor pressures, and high concentrated solvents can be used without having any significant losses. Amount of MDEA exiting the absorber was considered to be insignificant (less than 0.0002%). The temperature profiles of Case 2.1, 2.2 and 3 have the highest temperatures in the bottom of the column (peak at stage 7), which are associated with the acid gas compositions in the vapor phase throughout the column. It can be seen that all of the CO_2 is absorbed from stage 8 to stage 5 for these cases (see Figure C.5.2).

Table 6.2.2: Operating conditions for Case 1, Case 2.1, Case 2.2 and Case 3 based on using a 45 wt% MDEA solvent. All compositions are on a molar basis if not specified otherwise.

Parameter	**Case 1**	**Case 2.1**	**Case 2.2**	**Case 3**
Aqueous MDEA [wt%]	44.99	45.10	45.06	45.01
Sour gas temperature [^{o}C]	25	25	35	25
MDEA solvent temperature [^{o}C]	30	30	40	30
L/G ratio absorber [mol/mol]	0.75	1.1	1.2	1.7
H2S in wet gas [ppm]	3.99	4.00	4.01	4.00
H2O in wet gas [ppm]	3067	1008	1611	1004
CO2 in wet gas [%]	0.36	0.0015	0.0013	$1.6 \cdot 10^{-8}$
Wet gas temperature [^{o}C]	56.1	30.4	40.4	30.2
$\alpha_{H_2S,lean}$ [mol H_2S/mol MDEA]	0.00017	0.0033	0.0028	0.0086
$\alpha_{CO_2,lean}$ [mol CO_2/mol MDEA]	0.00057	0.030	0.017	$8.6 \cdot 10^{-7}$
$\alpha_{H_2S,rich}$ [mol H_2S/mol MDEA]	0.00073	0.0074	0.0066	0.25
$\alpha_{CO_2,rich}$ [mol CO_2/mol MDEA]	0.64	0.49	0.44	0.43
H_2S recovery [%]	92.1	98.8	98.7	99.3
CO_2 recovery [%]	93.4	99.5	99.2	98.3
H_2S in acid gas [%]	0.087	0.87	0.87	35.8
CO_2 in acid gas [%]	98.8	97.9	97.9	63.1
CH_4 in acid gas [%]	0.17	0.26	0.27	0.10
CH_4 loss in system [%]	0.091	0.14	0.15	0.19
Reboiler temperature [^{o}C]	140.4	130.9	135.7	140.3
Specific reboiler duty [MJ/kg acid gas]	4.72	3.79	4.51	4.96

For all cases, there were observed high total recoveries H_2S and CO_2. The reason for unexpected high recoveries of CO_2 is believed to be that the simulations were equilibrium based. As seen from Table 6.2.2 the CO_2 content in the wet gas is less than 1% for all cases. The VLE validations, discussed in Chapter 3, showed that Aspen Plus under-predicts solubility of H_2S and CO_2 at high temperatures, and the gases are therefore easily stripped from the MDEA solvent. The required L/G ratios are also believed to be higher than in reality because of choice of calculation method and based on the VLE validation results for H_2S. However, because of lack of literature data for comparison, this is uncertain.

The reboiler temperatures were commented in the previous chapters, and it can be noticed that it is lowest for Case 2.1. The temperature profiles in the stripper column are mostly affected by the amount of CO_2 desorbed. The temperature profiles are approximately constant where the composition of CO_2 in the vapor phase is constant, which can be seen from Figures C.5.4 and C.5.5 in Appendix C.5. Low pressure equipment was defined at 2.35 barg in this work, and lower pressures can be defined to examine if this keeps the reboiler temperatures at lower values. As mentioned, the simulations performed by Alfadala et al. [17], where the stripper pressure also was defined to 2.35 barg, resulted in a reboiler temperature of 144 ^oC.

Total loss of CH_4 for all cases were less than 0.2%, and increased for increasing L/G ratios in the absorber. Co-absorption of hydrocarbons can be a reason for foaming in amine processing units, which is a common operating problem, and is desirable to be kept at a minimum level. Solubility of hydrocarbons is lower in amine solvents when acid components are present, and therefore CH_4 losses for all cases were considered to be low [2, 13].

6.3 Water removal including regeneration of MEG

The wet gas conditions presented in Table 6.2.2 for Case 1, 2.1 and 3 were analysed, using MEG as the dehydrating solvent. A PFD of the setup in Aspen Plus is given in Figure 6.3.1. A screen shot of the process in Aspen Plus is given in Appendix C.3. The simulations were based on using 99 wt% to 99.5 wt% MEG at 35 ^oC based on the preliminary analysis with respect to L/G ratio discussed in Chapter 6.1. Case 1 was also run with MEG entering at 30 ^oC because of the wet gas inlet temperature. Dehydration will be improved by using lower glycol solvent temperatures and are not recommended to rise above 38 ^oC [10]. The wet gas for Case 1 holds a temperature of 56.1 ^oC, and may cause some glycols losses due to vaporization [18].

The absorber was defined in the same way as before. Lean MEG is entering and contacted counter current with the wet gas coming from the amine processing unit at 100 bar. The flowrate of MEG was adjusted so that the water content in the dry gas was 42 ppm. Rich MEG was then flashed at 3 bar, to remove co-absorbed CH_4. This was based on normal operating conditions for conventional dehydration units, where flash tank pressures typically are 3 bar to 7 bar [13]. In the lean rich heat exchanger, cold outlet flow was defined to have a temperature of 104 ^oC [49] . This was to get more realistic temperatures entering the distillation column, because it was observed high temperatures in the reboiler, which is commented later.

A 'DSTWU distillation column' was used, and the recovery of H_2O (light component) and MEG (heavy component) in the distillate were defined. This is a shortcut distillation method in Aspen plus for single feed and two stream products, using a partial or total condenser. A partial condenser with vapor distillate was defined. The Winn correlation, which is a modification of the Fenske equation, is used to calculate the minimum number of stages. It also calculates optimum feed stage location, reflux ratio and reboiler duty [50]. Recovery of MEG in the distillate was set to 10^{-5}, and the recovery of H_2O was adjusted, so that the concentration of MEG in the recycle streams was equal to the lean MEG entering the absorber. The column pressure was defined to be 1.3 bar [19]. Lean MEG was pumped up and cooled to the desired temperature again and a make up-stream with MEG was introduced, to account for MEG losses in the flash gas.

The modifications of the convergence block that were done for the acid gas removal unit, discussed in Chapter 6.2, were also tried for this system. Simulating the process as a loop resulted in convergence problems. The tolerance for errors in the different units was modified but because of the convergence problems, the simulation was done as shown in Figure 6.3.1. The MEG concentration in the recycle stream was checked to be equal to the lean MEG entering the absorber.

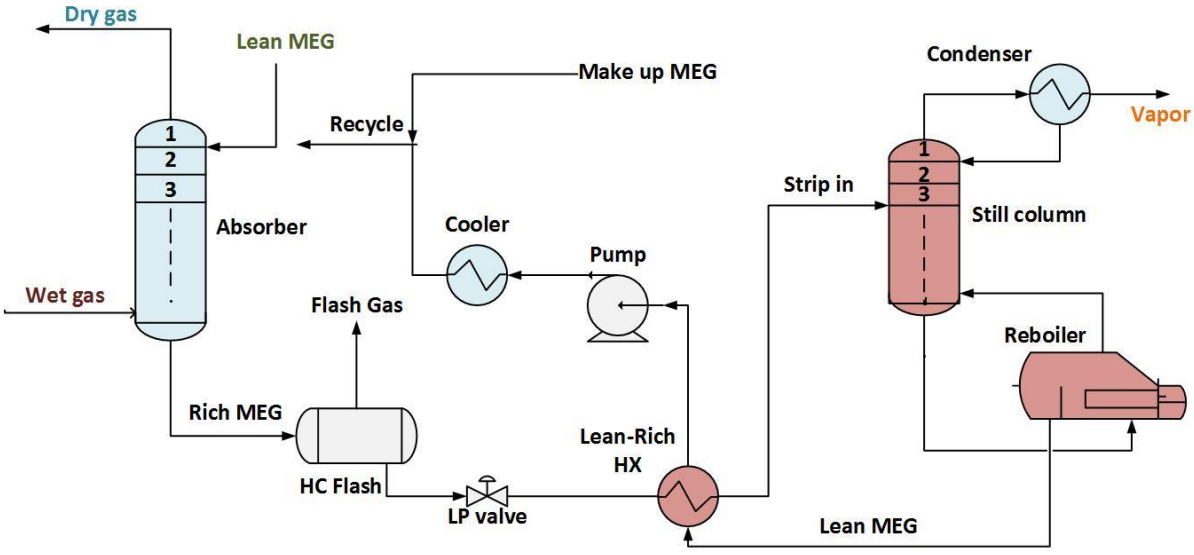

Figure 6.3.1: Process setup in Aspen Plus for gas dehydration using MEG. Makeup stream for MEG used for keeping concentration and flow of the recycle stream equal to the lean MEG entering the absorber.

Because of high temperatures observed in the reboiler, only a selection of results are presented from the dehydration simulations. Table 6.3.1 gives the results that were found for Case 1 and 2.1 using a 99.2 wt% MEG solvent entering at 35 ^{o}C. MEG concentrations above 96% may be difficult to achieve without using stripping gas or lower pressures than ambient [13]. This is because achieving higher concentrations will require high reboiler temperatures, and MEG degrades at temperatures above 165 ^{o}C [18]. Examining this configuration was not within the scope of this thesis.

Table 6.3.1: Simulation results for the dehydration process. The results are based on using a 99.2 wt% MEG solvent with an inlet temperature of 35 ^oC.

Process parameter	Unit	Case 1	Case 2.1
MEG concentration	[wt%]	99.2	99.2
MEG temperature	[^oC]	35	35
H_2O in wet gas	[ppm]	3067	1008
H_2O in dry gas	[ppm]	41.99	41.99
L/G absorber	[mol/mol]	0.45	0.0016
MEG reqiured	[kg MEG/kg H2O absorbed]	497.5	5.4
Rich MEG	[wt%]	99	83.7
$\alpha_{H_2O,rich}$	[mol H_2O/mol MEG]	0.035	0.67
CH_4 in flash gas	[%]	97.7	99.4
CH_4 loss	[%]	0.6	0.002
Reboiler duty	[MJ/kg H_2O stripped]	139.5	10.2
Temperature reboiler	[^oC]	195.4	195.3

Analysis showed that concentrations above 98 wt% MEG were needed to reach the water specification of 42 ppm out of the dehydration column. It was also found that concentrations as high as 99 wt% - 99.5% MEG should be used with respect to L/G ratios. The optimal MEG concentration and inlet temperature should be examined because it is dependent on the water content and temperature of the wet gas entering the absorber. Case 1, with a water content of 3067 ppm at 56.1 ^oC, required a L/G ratio of 0.45 when 99.2% MEG at 35 ^oC was used. The rich MEG solution was then 99wt% out of the absorber, which indicates a unnecessary high L/G ratio. This may be because the wet gas temperature is high, and solubility is lower at higher temperatures. The amount of MDEA used in the acid gas absorber should be increased to assure lower temperatures of the wet gas. Because the gas is carrying some of the reaction heat, and evaporates some of the aqueous MDEA solvent, the water content increases to a high level. Increasing the MEG concentration to 99.5% and lowering the temperature to 30 ^oC resulted in a L/G ratio of 0.13. However, regenerating MEG to this purity may be difficult, and it can be a better approach to increase the L/G ratio and energy requirement in the MDEA system.

Case 2.1 has a wet gas temperature of 30.4 ^oC and consists of 1008 ppm H_2O. Utilizing a 99.2% MEG solvent at 35 ^oC requires a L/G ratio of 0.0016. These results seem more reasonable with respect to the rich MEG concentration, which is 83.7% as seen from Table 6.3.1.

Most of the CH_4 is taken out of the flash before the stripping column, and the CH_4 loss in the system was low when reasonable MEG concentrations were used. For Case 1, the loss is 0.6% because the L/G ratio is high.

What should be noticed is that the reboiler temperatures in the stripping column, increase above 190 ^oC. Because MEG has a decomposition temperature of 165 ^oC, an alternative regeneration unit should be examined as mentioned above.

Chapter 7 Conclusion

7.1 Conclusions of this work

The scope of this thesis was to examine combined H_2S and water removal from natural gas by absorption in MDEA and MEG. The work was performed by simulations in Aspen Plus and a built-in template 'ElecNRTL_Rate_Based_MDEA_model' was used for all simulations without any modifications.

A VLE validation was performed to examine how well the solubility of gas components in MDEA and MEG are predicted in Aspen Plus compared to literature data. This gave AD's ranging from 3.5% to 218.6% calculated over the experimental loading range, for temperatures from 25 ^oC to 130 ^oC. In the process simulations a 45 wt% aqueous MDEA solution was used for H_2S and CO_2 absorption. Of the MDEA solutions examined in the VLE validations, 50.1 wt% was closest to the concentration used in the simulations. For CO_2 the AD's were 20.8%, 30.5%, 46% and 80.9% for 25 ^oC, 40 ^oC, 70 ^oC and 120 ^oC, respectively, in a 50.1 wt% solution compared to Jou et al. [14] for $\alpha_{CO_2} < 0.8$. Aspen plus under-predicted solubility of CO_2 at high temperatures, and deviations were observed to have a decreasing trend at lower temperatures. Aspen Plus under-predicted the solubility for H_2S and the AD's in 50.1 wt% MDEA were above 220% at all temperatures (for $\alpha_{H_2S} < 0.5$). However, the solubility predicted by Aspen Plus in 23.7 wt% MDEA fitted well and had AD's of 15.6% and 12.2% at 40 ^oC and 100 ^oC, respectively. The solubility curves that were simulated for H_2O in MEG, were very close to literature values and the largest AD was 6.8% at 60 ^oC.

The absorption performance using a mixed MDEA-MEG solvent, with 15 wt% to 55 wt% MDEA and 0 wt% to 50 wt% MEG, gave promising results with respect to H_2S removal, but was found to give insufficient absorption of water. A literature review on combined purification and dehydration processes showed three suggestions for two-step absorption processes in one contactor column. A simulation of a similar configuration showed that the water content increased in the lower part of the column, up to the feed stage of aqueous MDEA, and thereafter decreased, but was insufficiently to meet the specification limit of 42 ppm H_2O.

Acid gas removal in MDEA and water absorption in MEG, including regeneration of the solvents, were therefore simulated separately. The simulations were performed for three different natural gas compositions, having H_2S and CO_2 contents ranging from 49.8 ppm and 5.6% to 4.5% and 8%, respectively. The molar L/G ratio required to reach 4 ppm H_2S in the sweet gas increased for increasing acid gas concentrations. No recommendations for optimal operating conditions were made, due to lack of operational data that could be used for comparison. However, some operational areas which were considered energy efficient, where chosen for further analysis. Molar L/G ratio in the absorber and specific reboiler duty, for obtaining 4 ppm H_2S in the sweet gas using a 45 wt% MDEA solvent at 100 bar, ranged from 0.75 to 1.7 and 3.79 MJ/kg acid gas to 4.96 MJ/kg acid gas, respectively. The results for

specific reboiler duty were found to be within acceptable bounds compared to reported values in literature. For these cases H_2S and CO_2 recovery were up to 99.3% and 99.5%. Equilibrium based calculations were defined in the absorber and the amount of absorbed CO_2 were high for all simulations, and concentrations less than 1% were observed in the sweet gas. The VLE validations showed that Aspen Plus under-predicted solubility of H_2S and CO_2 at high temperatures, and there is reason to believe that this gives a higher acid gas recovery than one could expect. The L/G ratios are also believed to be higher than in reality because of the VLE validation results for H_2S, which showed that Aspen Plus under-predicted the solubility. However, because of lack of literature data, this is uncertain.

For water removal, it was found that MEG concentrations above 99% should be used depending on the water content and temperature of the wet gas flowing into the dehydration absorber. Conventional regeneration of MEG to this level of purity resulted in reboiler temperatures above 190 ^oC, and was found to be above the recommended limits with respect to degradation, which are around 165 ^oC.

7.2 Recommendations for further work

During the work of this thesis it was challenging to find literature concerning the combined process that was desired to examine. It was especially hard to find information about MEG as a dehydration solvent because TEG is mostly used in industrial plants. More experimental data regarding this, and VLE data for H_2S and CO_2 in MDEA-MEG solvents could give a better insight of the system behaviour.

An equilibrium calculation approach was used in the simulations, and high recoveries of both H_2S and CO_2 were observed. Using rate-base calculations, non-equilibrium, will take the mass transfer and reaction kinetic limitations into account and may provide more accurate simulation results.

The simulations of MEG regeneration were performed in a simple distillation column in this work. Regeneration of MEG to a purity level above 99% gave high reboiler temperatures. Enhanced stripping at low pressures (below ambient), could be performed to examine if this gives more acceptable temperatures.

References

[1] J. Rolker, T. Lenormant and M. Seiler, "A new Chemical System Solution for Acid Gas Removal," Chemie Ingenieur Technik, vol. 84, no. 6, pp. 849-858, 2012.

[2] A. L. Kohl, Gas Purification, 5th ed., Housten Texas: Gulf Publ. Co., 1997, pp. 40-186, 187-277.

[3] E. Solbraa, "Gas Processing (lecture in TEP08, NTNU)," Department of Energy and Process Engineering, NTNU, Trondheim, 2015.

[4] O. Økland, S. Davies, R. M. Ramberg and H. Rognø, "Steps to the Subsea Factory," in Offshore Technology Conference, Rio de Janeiro, 2013.

[5] SUBPRO, "Subsea production and processing (SUBPRO)," 2015. Available: https://www.ntnu.edu/web/subpro/subpro. [Accessed 02 June 2016].

[6] J. G. Speight, Natural Gas - A Basic Handbook, London: Gulf Publishing Company, 2007, pp. 3-33, 133-160.

[7] International Energy Agency, "Key World Energy Statistics," IEA, 2015.Avaiable: www.iea.org [Accessed 02 June 2016]

[8] U.S. Energy Information Administration , "International Energy Outlook 2016 - Ch. 3. Natural Gas," 2016. Available: http://www.eia.gov/forecasts/ieo/nat_gas.cfm. [Accessed 02 June 2016].

[9] J. Kittel, E. Fleury, B. Vuillemin, S. Gonzalez and F. Ropital, "Corrosion in alkanolamine used for acid gas removal: From natural gas processing to CO2 capture," Materials and Corrosion, vol. 63, no. 3, pp. 223-230, 2012.

[10] A. J. Kidanay and W. R. Parrish, Fundamentals of natural gas processing, Boca Raton: CRC Press/Taylor & Francis Group, 2006, pp. 2-23, 91-132, 133-163, 380-381, 388-389.

[11] C. A. Koh, R. E. Westacott, W. Zhang, K. Hirachand, J. L. Creek and A. K. Soper, "Mechanisms of gas hydrate formation and inhibition," Fluid phase Equilibria, Vols. 194-197, pp. 143-151, 2002.

[12] J. Carroll, "Natural Gas Hydrates - A guide for Engineers," 3rd ed., Elsevier, 2014, pp. 135-172.

[13] J. M. Campbell, Gas conditioning and processing 2, Norman: Campbell Petroleum Seires, 1992, pp. 51-112, 333-394.

[14] F.-y. Jou, A. E. Mather and F. D. Otto, "Solubility of hydrogen sulfide and and carbon dioxide in Aqueous Methyldiethanolamine solutions," Industrial & Engineering Chemistry Process Design and Development, vol. 21, no. 4, pp. 539-544, 1982.

[15] J. Reza and A. Trejo, "Degradation of Aqueous solutions of alkanolamine blends at high temperature, under the presence of carbon dioxide and hydrogen sulfide," Chemical Engineering Communications, vol. 193, no. 1, pp. 129-238, 2006.

[16] M. Pandey, "Process optimization in Gas sweetening Unit - A case study," in International Petroleum Technology Conference, Doha, 2005.

[17] H. E. Alfadala and E. Al-Musleh, "Simulation of an Acid Gas Removal Process Using Methyldiethanolamine; an equilibrium approach," in Proceedings of the 1st annual Gas Processing Symposium, Qatar, Elsevier, 2009, pp. 256-265.

[18] GPSA, "Section 20 - Dehydration," in Engineering Data Book, Tulsa Oklahoma, Gas Processors Suppliers Association, 2014.

[19] K. Sandengen, "Hydrates ans Glycols - MEG injection and processing," 2010. Available: http://www.ipt.ntnu.no/~jsg/undervisning/naturgass/lysark/LysarkSandengen2010.pdf. [Accessed 27 May 2016].

[20] A. J. L. Hutchinson, "Process for treating gases". United States of America Patent 2,177,068, 24 October 1939.

[21] E. R. McCartney , "Gas Purification and Dehydration Process". United States of America Patent 2,435,089, 27 January 1948.

[22] W. F. Chapin, "Purification and dehydration of gases". United States of America Patent 2,518,752, 15 August 1950.

[23] E. R. McCartney, "Extraction of Acidic impurities and moisture from gases". United States of America Patent 2,547,278, 3 April 1951.

[24] D. Eimer, "Simultaneous removal of water and hydrogen sulfide from natural gas (Phd. thesis)," The Norwegian Institute of Technology (NTNU), Trondheim, 1994.

[25] R. J. MacGregor and A. E. Mather, "Equilibrium solubility of H2S and CO2 and their mixtures in a mixed solvent," The Canadian journal of Chemical Engineering, vol. 69, no. 6, pp. 1357-1366, 1991.

[26] H.-J. Xu, C.-F. Zhang and Z.-S. Zheng, "Solubility of Hydrogen Sulfide and Carbon Dioxide in a Solution of Methyldiethanolamine mixed with Ethylene Glycol," Industial & Engineering Chemistry Research, vol. 41, no. 24, pp. 6175-6180, 2002.

[27] F. Y. Jou, J. J. Carroll, A. E. Mather and F. E. Otto, "The solubility of Carcon Dioxide and Hydrogen Sulfide in a 35 wt% Aqueous solution of methyldiethanolamine," The Canadian Journal of Chemical Engineering, vol. 71, pp. 264-268, 1993.

[28] F.-Y. Jou, J. J. Carroll, A. E. Mather and F. D. Otto, "Solubility of methane and ethane in aqueous solutions of methyldiethanolamine," Journal of Chemical and Engineering Data, vol. 43, no. 5, pp. 781-784, 1998.

[29] F.-Y. Jou, R. Deshmukh, F. D. Otto and A. E. Mather, "Vapor-liquid equilibria of hydrogen sulfide and carbon dioxide and ethylene glycol at elevated pressures," Chemical Engineering Communications, vol. 87, no. 1, pp. 223-231, 1990.

[30] A. C. Galvão and A. Z. Francesconi, "Solubility of methane and carbon dioxide in ethylene glycol at pressures up to 14 MPa and temperatures ranging form (303 to 423) K," The Journal of Chemical Thermodynamics, vol. 42, no. 5, pp. 684-688, 2010.

[31] D.-Q. Zheng, W.-D. Ma, R. Wei and T.-M. Guo, "Solubility study of methane, carbon dioxide and nitrogen in ethylene glycol at elevated temperatures and pressures," Fluid Phase Equilibria, vol. 155, no. 2, pp. 277-286, 1999.

[32] S. Horstmann, H. Gardeler, M. Wilken, K. Fisher and J. Gmehling, "Isothermal Vapor−Liquid Equilibrium and Excess Enthalpy Data for the Binary Systems Water + 1,2-Ethanediol and Propene + Acetophenone," Journal of Chemical & Engineering Data, vol. 49, no. 6, pp. 1508-1511, 2004.

[33] C. Gonzales and H. C. Van Ness, "Excess Thermodynamic Functions for ternary systems. 9. Total-Pressure data and G for water/ethylene glycol/ethanol at 50 degrees," Journal of Chemical&Engineering data, vol. 28, pp. 410-412, 1983.

[34] M. A. Villamañãn, C. Gonzales and H. C. Van Ness, "Excess thermodynamic properties for water/ethylene glycol," Journal of Chemical&Engineering data, vol. 29, pp. 427-429, 1984.

[35] C. J. Geankoplis, Transport Processes and Separation Process Principles, Massachusetts: Prentice Hall, 2009, pp. 696-697.

[36] Aspentech, "Aspen Physical Property System- Physical Property Methods V7.3," Aspen Technology, Burlington, 2011.

[37] D. M. Austgen, G. T. Rochelle and C.-C. Chen, "Model of vapor-liquid equilibria for aqueous acid gas-alkanolamine systems. 2. Representation of H 2 S and CO 2 solubility in aqueous MDEA and CO2 solubility in aqueous mixtures of MDEA with MEA or DEA," Industrial & Engineering Chemistry Research, vol. 30, no. 3, pp. 543-555, 1991.

[38] G. Kuranov, B. Rumpf, N. A. Smirnova and G. Maurer, "Solubility of Single Gases Carbon Dioxide and Hydrogen Sulfide in Aqueous Solutions of N-Methyldiethanolamine in the Temperature Range 313−413 K at Pressures up to 5 MPa," Industrial & Engineering Chemistry Research, vol. 35, no. 6, pp. 1959-1966, 1996.

[39] A. Vrachnos, G. Kontogeorgis and E. Voutsas, "Thermodynamic modeling of acidic gas solubility in aqueous solutions of MEA, MDEA and MEA-MDEA blends," Industrial and Engineering Chemistry Research, vol. 45, no. 14, pp. 5148-5154, 2006.

[40] L. Chunxi and W. Fürst, "Representation of CO2 and H2S solubility in aqueous MDEA solutions using an electrolyte equation of state," Chemical Engineering Science, vol. 55, no. 15, pp. 2975-2988, 2000.

[41] A. Vrachnos, . E. Voutsas, K. Magoulas and A. Lygeros, "Thermodynamics of acid gas-MDEA-water systems," Industrial and Engineering Chemistry Research, vol. 43, no. 11, pp. 2798-2804, 2004.

[42] E. Skylogianni, Phd Candidate in Subsea Production and Processing, NTNU, Internal discussion, Vapor-liquid equilirbrium data,Trondheim, 2016.

[43] H. Knuutila, Internal discussion, Trondheim: NTNU, 2016.

[44] M. I. Lilleng, Specialization project "Simulation of selective hydrogen sulfide removal at high pressures using Aspen Plus," NTNU - Department of Chemical Engineering, Trondheim, 2015.

[45] M. N. Psarrou, L. O. Jøsang, K. Sandengen and T. Østvold, "Carbon dioxide solubility and monoethylene glycol degradation at MEG reclaiming/regeneration conditions," Journal of chemical & engineering data, no. 56, pp. 4720-4724, 2011.

[46] H. Knuutila, Chemical absorption - Energy considerations (Lecture notes in TKP7 Gas Purification), Department of Chemical Engineering, Trondheim: NTNU, 2015.

[47] R. Sakwattanapong, A. Aroonwilas and A. Veawab, "Behavior of Reboiler Heat Duty for CO2 Capture Plants Using Regenerable Single and Blended Alkanolamines," Industrial and Engineering Chemistry Research, vol. 44, no. 12, pp. 4465-4473, 2005.

[48] D. Fiaschi and L. Lombardi, "Integrated gasifier combined cycle plant with integrated CO2-H2S removal: Performance analysis, life cycle assessment and exergetic life cycle assessment," International Journal of Applied Thermodynamics, vol. 5, no. 1, pp. 13-24, March 2002.

[49] M. D. Rincon, C. Jimenez-Junca and C. R. Duarte, "A novel absorption process for small-scale natural gas dew point control and dehydration," Journal of Natural Gas Science and Engineering, vol. 29, pp. 264-274, 2016.

[50] AspenTech, "Aspen Plus User Guide version 10.2," Aspen Technology, Cambridge, 2002.

Appendix A: VLE validation

This appendix gives supplementary data and VLE curves retrieved from Aspen Plus for the model validation that was performed in this thesis.

A.1 - Deviations between Aspen Plus VLE and literature VLE data

Table A.1.1 gives average absolute deviation (AD) and absolute average deviation (AAD) between experimental solubility data and values retrieved from Aspen Plus. Deviations in partial pressure were calculated for a given loading. This was calculated over the loading range given, and AD and AAD is given for all the concentrations, c_s, and temperatures analysed. Number of data points validated for each temperature is denoted as *n*.

Table A.1.1: Overview of VLE validations done for different gas-solvent (*g*-*s*) systems. Average deviation (AD) and absolute average deviation (AAD) was calculated between experimental partial pressure data and the VLE model available in Aspen Plus. The partial pressure from Aspen was found at a given loading from the experimental source and deviation from experimental partial pressure was calculated. Number of experimental data point that was taken for the respective source is denominated as '*n*'.

System *g-s*	Data source	Solvent concentration c_s	Temperature	Partial pressure range P_g	Loading range α_g	*n*	AD	AAD
			[°C]	[kPa]	[mol g/mol s]			
CO_2-MDEA	[14]	4.28 kmol/m^3	25	0.00385-6370	0.00621-1.381	13	32.1	29.8
		(50.1 wt%)	40	0,00231-6570	0.00202-1.29	15	33.1	21.4
			70	0,00161-6280	0.00037-1.232	13	100.1	68.0
			120	0,143-5290	0.00105-0.743	9	80.9	42.9
	[14]	2.0 kmol/m^3	25	0.001-6380	0.005-1.833	14	23.2	19.5
		(23.7 wt%)	40	0.000217-6330	0.003-1.682	15	28.4	26.7
			70	0.00208-6020	0.0009-1.397	12	32.5	32.4
			120	0.0725-5490	0.00124-1.152	9	57.9	48.7
	[25]	2.0 mol/L	40	1.17-3770	0.124-1.203	5	47.0	6.4
		(23.7 wt%)						
H_2S-MDEA	[14]	4.28 kmol/m^3	25	0.00593-1960	0.0096-1.699	16	115.0	122.0
		(50.1 wt%)	40	0.00314-2800	0.00508-1.723	16	174.8	174.6
			70	0.0013-4990	0.00129-1.727	15	169.9	159.7
			120	0.342-5840	0.0095-1.328	9	96.5	89.3
	[14]	2.0 kmol/m^3	40	0.0026-2260	0.00725-1.906	13	15.6	13.1
		(23.7 wt%)	100	0.745-1550	0.029-1.256	9	12.2	62.8
	[25]	2.0 mol/L	40	0.52-1600	0.13-1.725	27	21.7	18.7
	[14]	1.0 kmol/m^3	40	0.0023-2730	0.0111-2.902	13	21.9	11.1
		(11.9 wt%)						
CH_4-MDEA	[28][a]	34.7 wt%	25	95-13210	0.000042-0.00302	9	50.5	10.8
			40	253-12780	0.000075-0.00264	8	49.5	9.1
			70	244-11210	0.000062-0.00244	7	67.0	10.2
			130	470-10990	0.000088-0.00326	6	112.5	47.6

Table A.1.1 continued

System *g-s*	Data source	Solvent concentration c_s	Temperature	Partial pressure range P_g	Loading range α_g	n	AD	AAD
CO_2-MEG	[29][a]	99.5%	25	29.3-20290	0.000693-0.1388	8	22.1	22.5
			50	44-19510	0.000794-0.1327	8	53.0	51.1
			100	76-18310	0.000723-0.1206	8	31.3	18.2
			125	130-18310	0.001162-0.1098	7	100.5	52.6
	[30][a]	99.8%	50	425.5-2833.5	0.0045-0.0464	4	15.5	15.5
			100	620.5-4558.5	0.0047-0.0485	4	34.53	22.3
			125	718-5421	0.005-0.0508	4	72.9	32.5
	[31][a]	99.9%	50	895-38000	0.0117-0.148	11	39.7	33.7
			100	967-38200	0.0083-0.1724	10	137.6	85.8
			125	960-38400	0.0049-0.1723	9	218.6	111.4
H_2S-MEG	[29][a]	99.5%	25	3.24-2030	0.000511-0.4055	8	42.4	28.9
			50	3.2-3520	0.000335-0.4494	8	43.6	38.9
			75	4.9-5660	0.000337-0.482	8	38.3	38.9
			100	3.64-6750	0.000152-0.3174	8	14.6	17.2
			125	6.46-2780	0.00011-0.09681	6[b]	16.9	17.3
CH_4-MEG	[30][a]	99.8%	30	1367.4-7702.4	0.0015-0.0119	5	16.5	15.6
			50	1489.4-8706.4	0.0018-0.013	5	11.9	11.3
			100	1794.4-11216.4	0.0031-0.0192	5	14.5	6.7
			125	1946.9-12471.4	0.0038-0.0237	5	29.4	7.0
			150	2099.4-13726.4	0.0047-0.0291	5	47.4	7.4
	[31][a]	99.9%	50	2390-39500	0.003-0.0268	11	26.9	2.2
			100	200-39617	0.0003-0.0322	10	21.8	3.5
			125	330-39600	0.0005-0.0421	10	7.9	2.6
H_2O-MEG	[32][a]	99.99%	60	0.28-19.92	0.00327-0.99968[c]	37	6.8	9.8
	[34][a]	99%	60	0.543-19.428	0.0188-0.9797[c]	22	3.5	3.6
	[33][a]	99.5%	50	0.316-12.082	0.0185-0.9803	21	4.2	3.6

[a]Solubility data for component *g* in solvent *s* given in mole fraction, x_i, not loading, α_i.

[b]Highest data point excluded. Aspen failed to validate data point.

[c]Highest and lowest data pints excluded. Aspen failed to validate some data points.

A.2 - Solubility of H_2S and CO_2 in 23.7 wt% MDEA and 50.1 wt% MDEA

Figure A.2.1 gives solubility of CO_2 in a 50.1 wt% aqueous MDEA solution compared to a 23.7 wt% aqueous MDEA solution at 25 ^oC, 40 ^oC, 70 ^oC and 120 ^oC. Figure A.2.2 compares H_2S and CO_2 solubility in a 50.1 wt% MDEA solution at 25 ^oC, 40 ^oC, 70 ^oC and 120 ^oC.

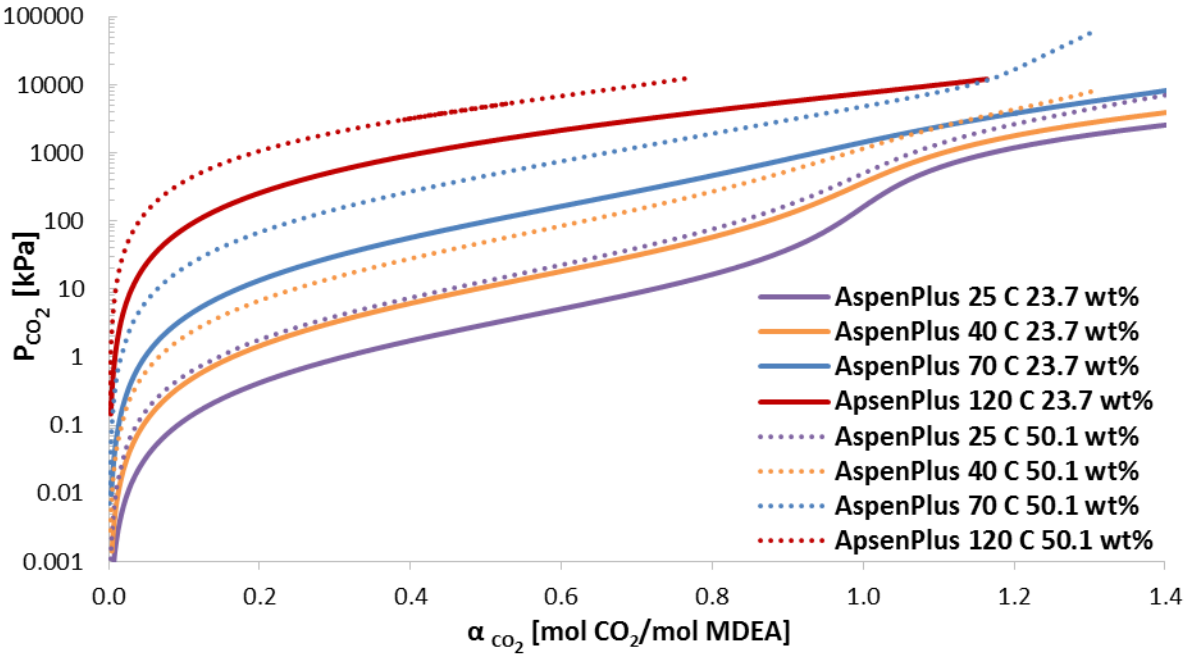

Figure A.2.1: Partial pressure of carbon dioxide, P_{CO_2}, on a log scale as a function of loading, α_{CO_2}, in the liquid phase. The figure shows the VLE models retrieved from Aspen Plus for CO_2 in a 50.1 wt% aqueous MDEA solution compared to a 23.7 wt% MDEA solution at 25 ^oC, 40 ^oC, 70 ^oC and 120 ^oC.

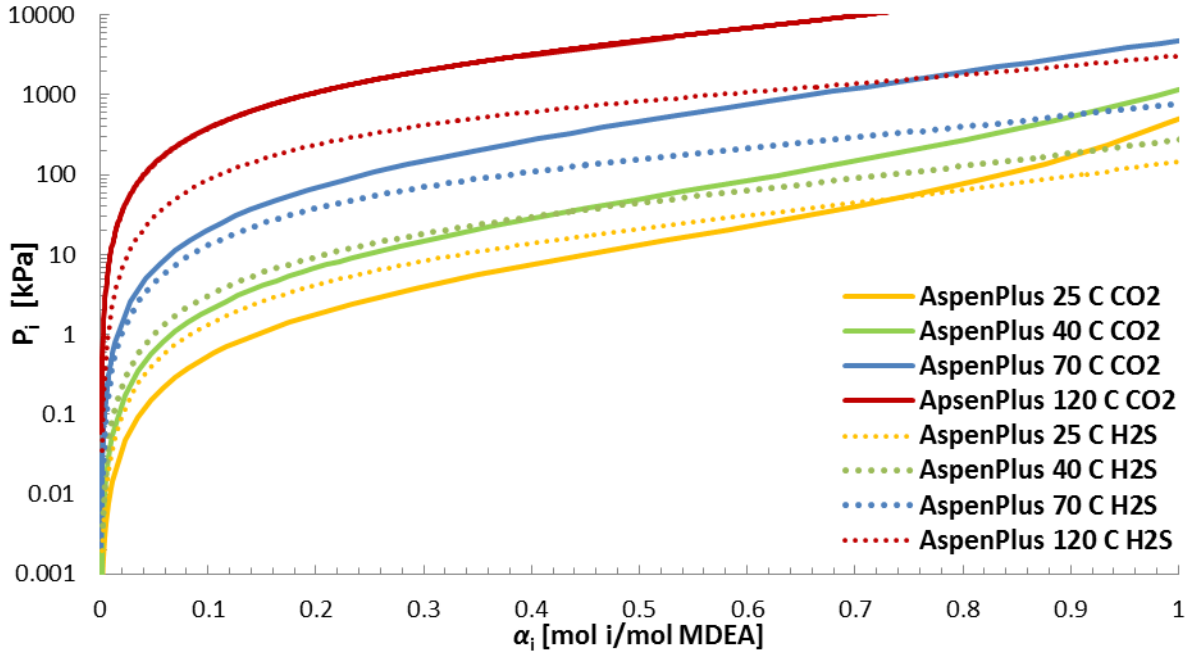

Figure A.2.2: Partial pressure of H_2S and CO_2, P_i, on a log scale as a function of loading, α_i, in the liquid phase. The figure shows the VLE models retrieved from Aspen Plus for H_2S and CO_2 in a 50.1 wt% aqueous MDEA solution at 25 ^oC, 40 ^oC, 70 ^oC and 120 ^oC.

A.3 - Solubility of H_2S in MEG

Figure A.3.1 gives VLE models for H_2S in pure MEG (purity > 99.5%) at 25 ^oC to 125 ^oC compared to reported data by Jou et al. [29].

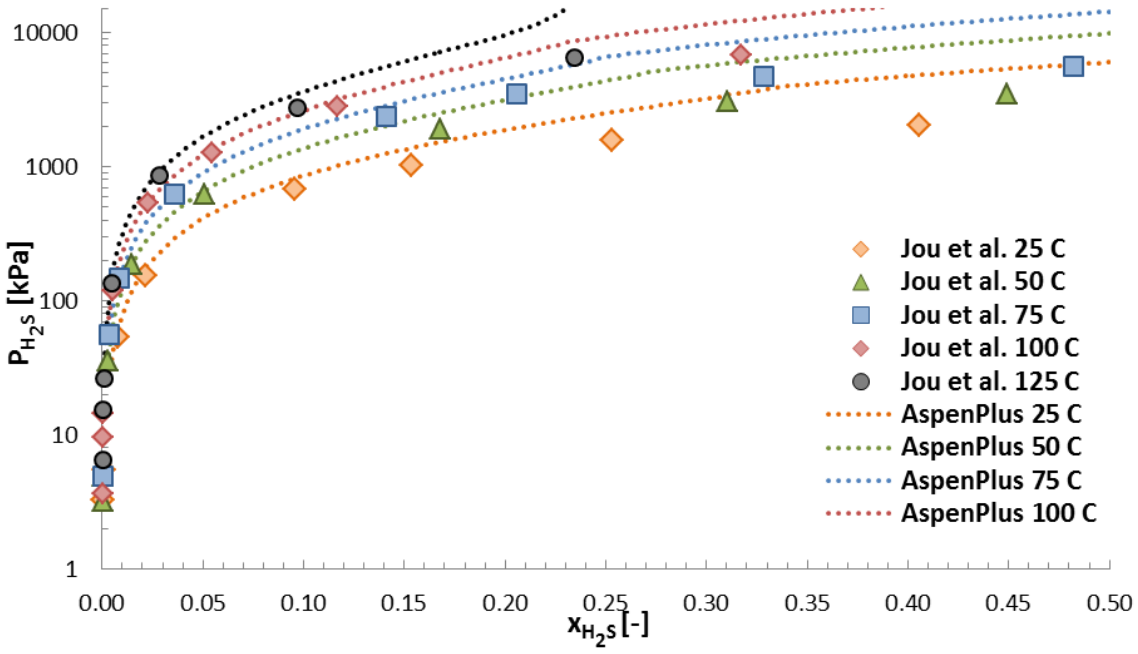

Figure A.3.1: Partial pressure of hydrogen sulfide, P_{H_2S}, on a log scale as a function of mole fraction, x_{H_2S}, in the liquid phase. The figure shows the VLE models in Aspen Plus for H_2S in pure MEG (purity > 99.5%) at 25 °C to 125 °C compared to experimental data reported by Jou et al. [29].

A.4 - Solubility of H_2O in MEG and TEG at 50 °C to 150 °C

Figure A.4.1 gives the solubility of H_2O in MEG and TEG at 50 °C to 150 °C predicted by Aspen Plus. It can be seen that Aspen Plus gives the same partial pressures for H_2O in MEG and TEG in the loading range given.

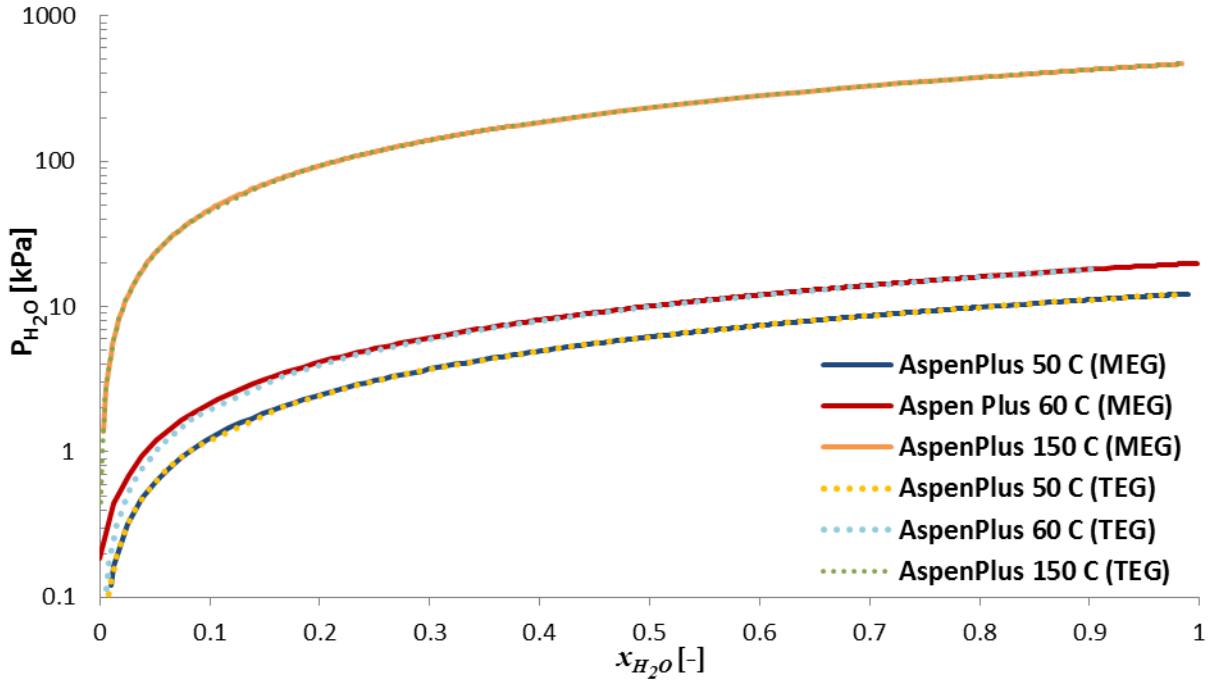

Figure A.4.1: Partial pressure of water, P_{H_2O}, on a log scale as a function of mole fraction, x_{H_2O}, in the liquid phase. The figure shows the VLE models in Aspen Plus for H_2O in pure MEG and TEG (purity > 99.5%) at 50 °C, 60 °C and 150 °C.

A.5 - Solubility of H_2S in a mixed MDEA-MEG-H_2O solvent

Figure A.5.1 compares solubility of H_2S in different MDEA-MEG-H_2O solvents at 40 ^oC. Solubility curves from Aspen Plus are compared to literature data [26, 42].

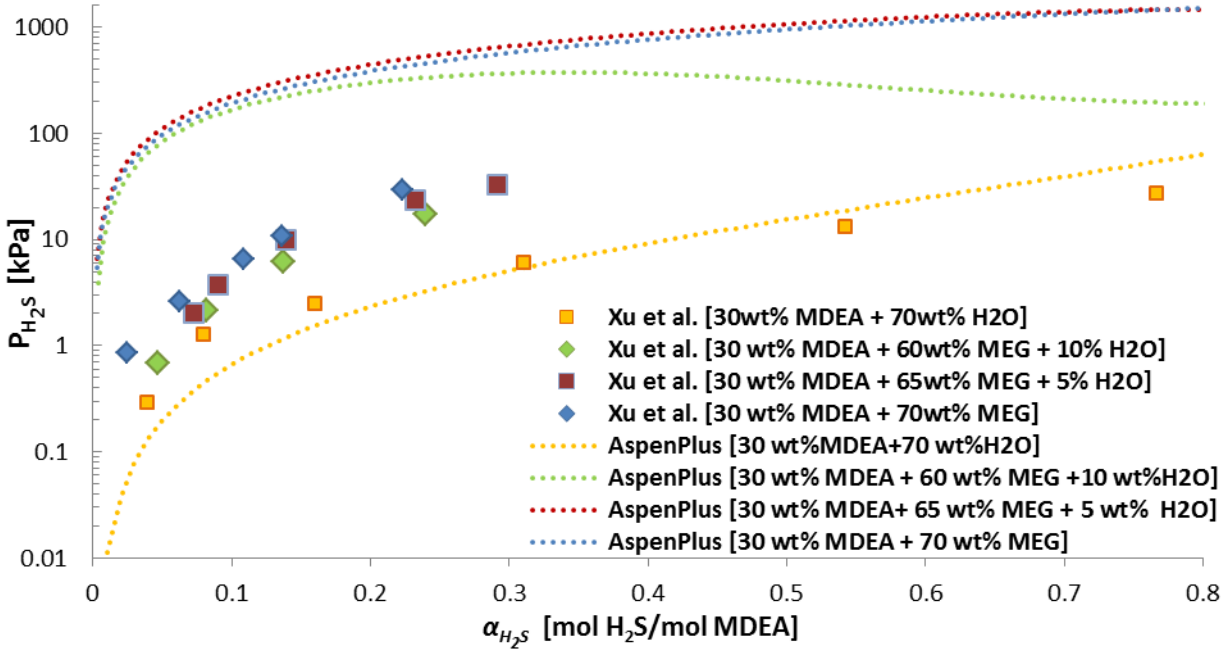

Figure A.5.1: Comparison of solubility of H_2S in different MDEA-MEG-H_2O solvents at 40 ^oC. VLE models obtained from Aspen Plus compared to Xu et al. (2002) [26, 42].

Appendix B: Water specification calculations

B.1 - Water specification for dry gas

The water specification for Norwegian transport pipelines is -18 ^oC at 70 bara [3].This corresponds to a maximum water content of 32 kg/10^6 std m^3 at standard conditions. The conversion table that was used is given in Figure B.1.1 [13].

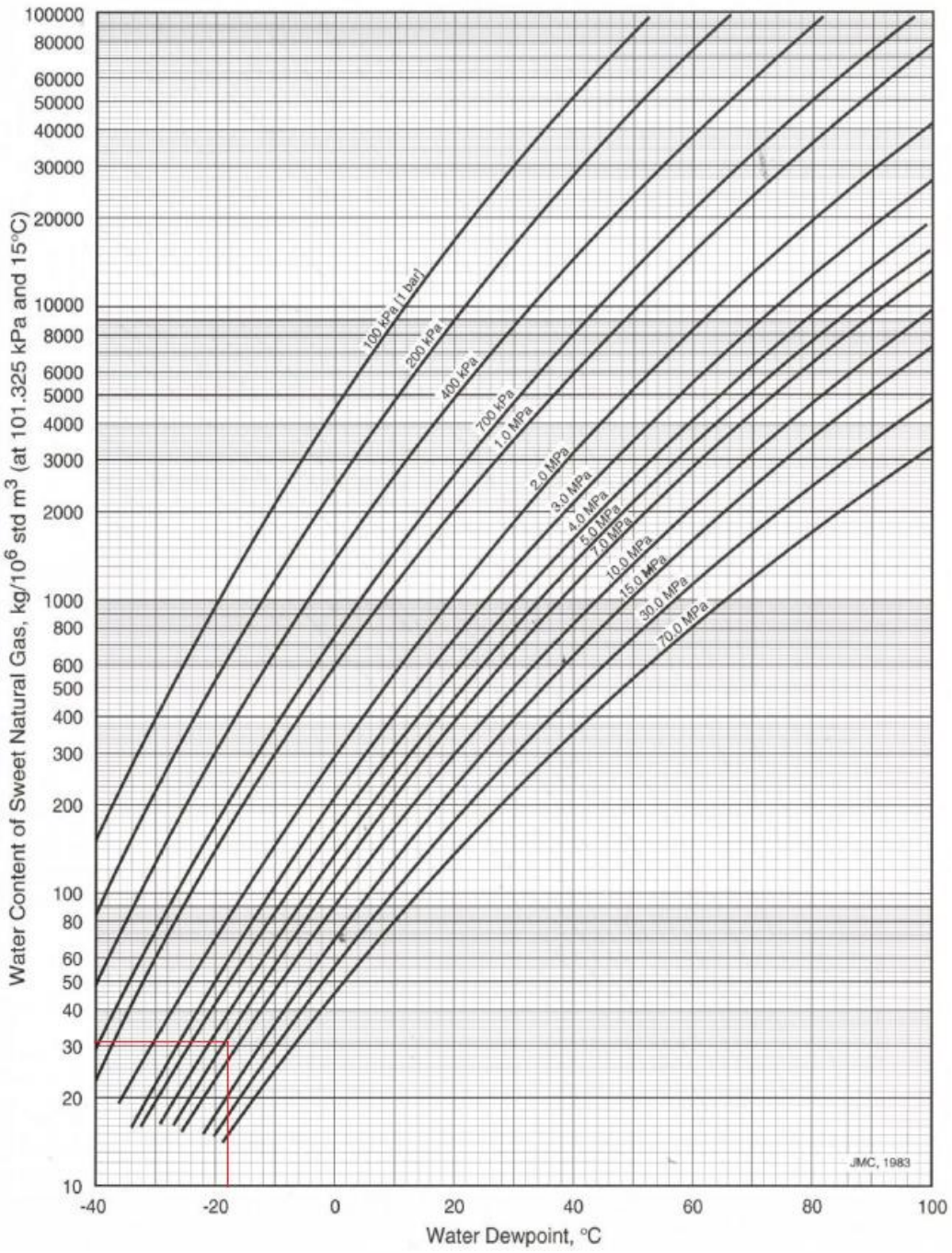

Figure B.1.1: Water content of sweet natural gas at standard conditions at different pressures and water dewpoints. Red lines indicate values used in calculations [13].

The molar volume at standard conditions (101.325 kPa and 15 ^oC) in m^3/mol, $V_{m,std}$, is given by Equation B.1. *R* is the ideal gas constant in m^3Pa/kmol, *T* is the temperature in K and *P* is the pressure in Pa.

$$V_{m,std} = \left(\frac{V}{n}\right)_{std} = \left(\frac{RT}{P}\right)_{std} \quad \text{(B.1)}$$

Number of moles, n_{gas}, in 10^6 m^3 natural gas was found from Equation B.2

$$n_{gas} = \frac{10^6 m^3}{V_{m,std}} \quad \text{(B.2)}$$

The molar mass of water, Mm_{H_2O}, is 18.02 kg/kmol. The molar water specification was calculated from Equation B.3.

$$n_{H_2O,spec} = \frac{32\ kg\ /10^6\ std\ m^3}{Mm_{H_2O}} \quad \text{(B.3)}$$

The water content allowable in the transport gas was found to be maximum 42 ppm on a molar basis.

Appendix C: Process simulations

C.1 - Preliminary absorber analysis

The loading of H_2S and CO_2 in the rich MDEA leaving the bottom of the column as a function of number of stages for different L/G ratios are given in Figure C.1.1. Analysis was done for gas composition Case 1 using 50 wt% MDEA entering at 30 ^oC.

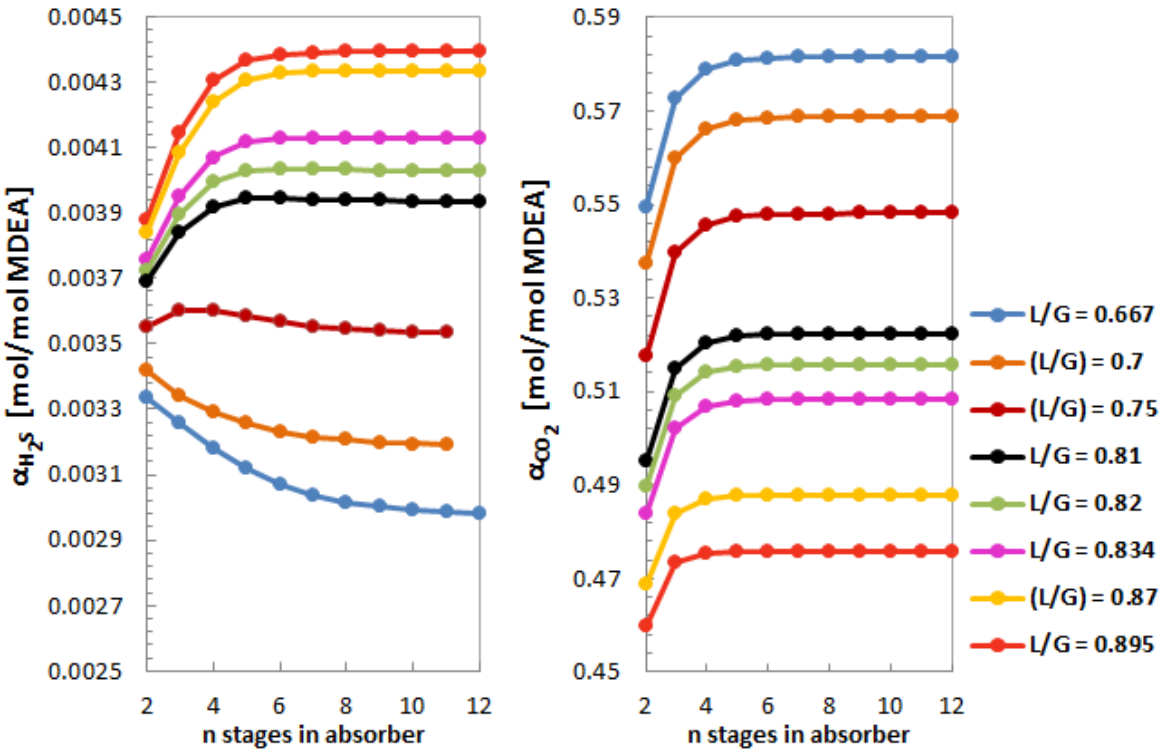

Figure C.1.1: Loading of H_2S and CO_2 in rich MDEA, α_i, out of the absorber as a function of number of stages, *n*, for different L/G ratios [mol/mol]. Analysis done for gas composition Case 1 using a 50 wt% MDEA solution entering at 30 ^oC.

C.2 - Absorption in mixed MDEA-MEG solvents

The percentage increase in moles H_2O in the gas stream through the absorber for Case 1 is given in Figure C.2.1 for different MDEA-MEG concentrations.

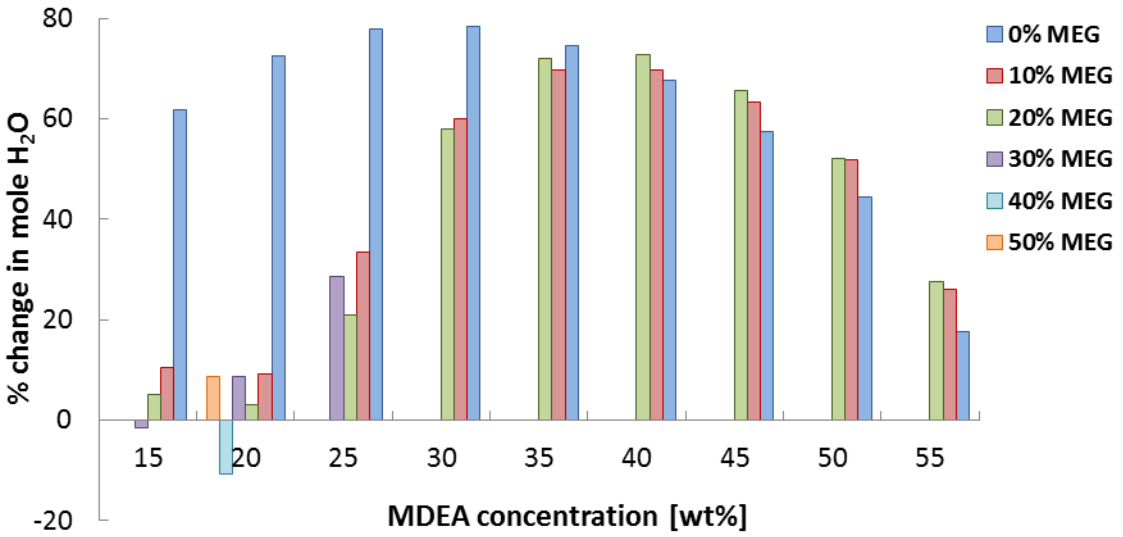

Figure C.2.1: Percentage change of H_2O in the gas stream through the absorber for different MDEA-MEG concentrations for Case 1.

C.3 - Aspen Plus process flow diagrams

Figure C.3.1 shows a screen shot of the H_2S and CO_2 absorption process using MDEA that was simulated in Aspen Plus. The regeneration unit for MDEA is also included. Figure C.3.2 shows a screen shot of the gas dehydration process using MEG that was simulated in Aspen Plus.

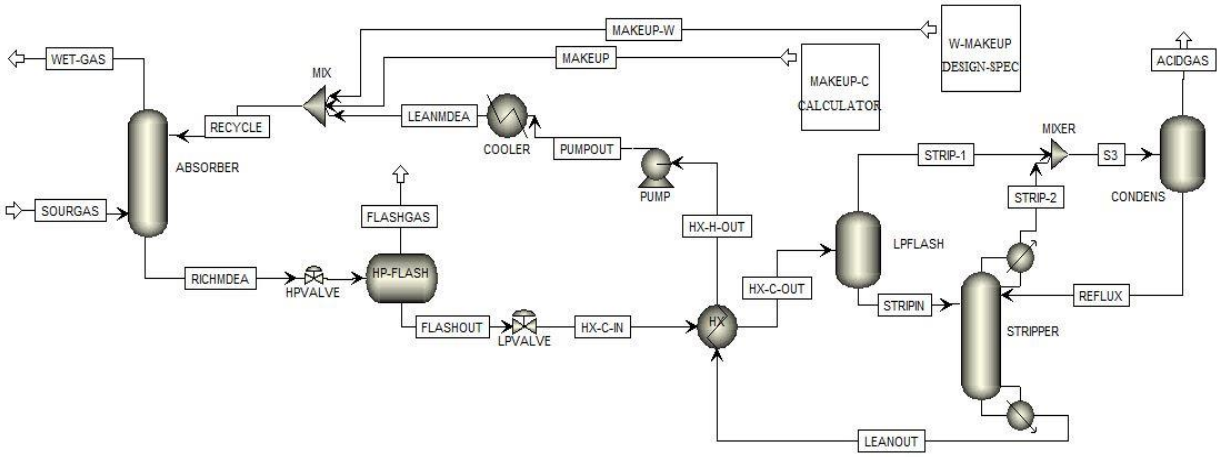

Figure C.3.1: Screen shot of the H_2S and CO_2 absorption process using MDEA simulated in Aspen Plus.

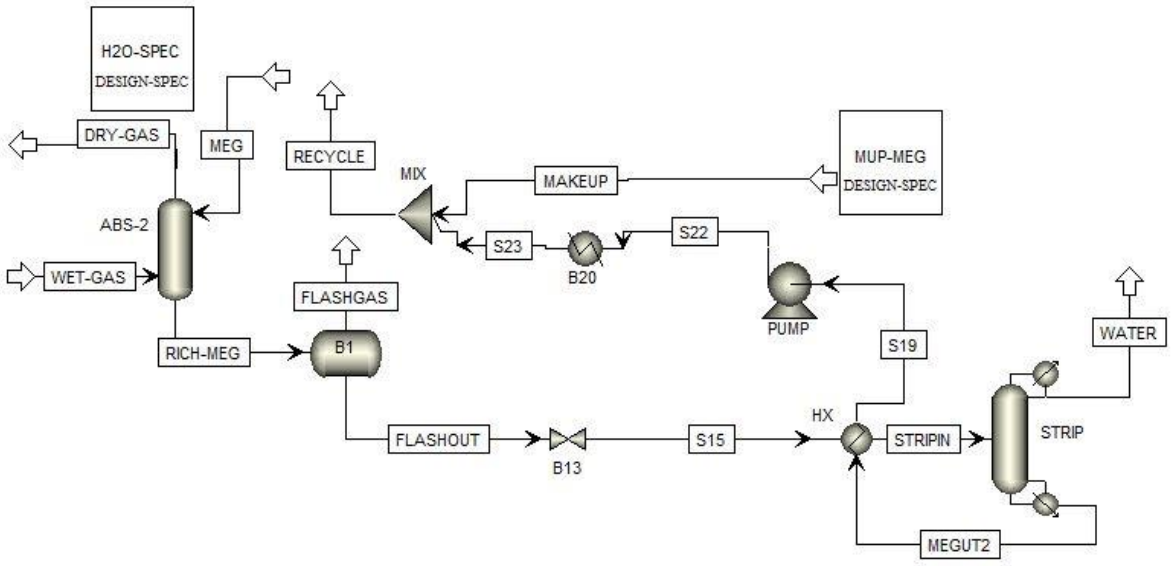

Figure C.3.2: Screen shot of the gas dehydration process using MEG simulated in Aspen Plus.

C.4 - Specific reboiler duty and acid gas loading

Loading of H_2S and CO_2, α_i, in rich and lean streams were calculated from Equation C.1. The loading is in given by mol *i*/mol MDEA. For calculating the H_2S loading, the acid components H_2S, HS^- and S^{-2} were taken into account. For CO_2, acid gas components were CO_2, HCO_3^- and CO_3^{-2}.

$$\alpha_i = \frac{\dot{n}_{acid\ components}}{\dot{n}_{MDEA} + \dot{n}_{MDEAH+}} \tag{C.1}$$

In Equation C.1, $\dot{n}_i$, is the mole flow of component *i*, in kmol/h.

The assumptions for calculating the specific reboiler duty used for analysing the energy requirement for different gas compositions, is given below. The amount of absorbed H_2S and CO_2 in the liquid stream entering the stripper ('strip-in'), $\dot{m}_{acid\ gas}$, was calculated by Equation C.2,

$$\dot{m}_{acid\ gas} = \sum_{i=1}^{n} m_i \tag{C.2}$$

where m_i is the mass flow in kg/h of component i, into the stipper. The components that were assumed as acid gas components were CO_2, H_2S, HCO_3^-, CO_3^{-2}, HS^- and S^{-2}. The specific reboiler duty in MJ/kg acid gas, Q_s, required to hold the H_2S content in the wet gas at 4 ppm $\pm$ 0.05 ppm was calculated by Equation C.3,

$$Q_s = \frac{Q_{reboiler} \times 1000\ MJ/GJ}{\dot{m}_{acid\ gas}} \tag{C.3}$$

where $Q_{reboiler}$ is the reboiler duty in GJ/h.

C.5 - Concentration and temperature profiles

Temperature and composition profiles of the absorber and stripper, for the cases 1, 2.1, 2.2 and 3 obtained by using a 45 wt% MDEA solvent are given in Figures C.5.1 to C.5.6.

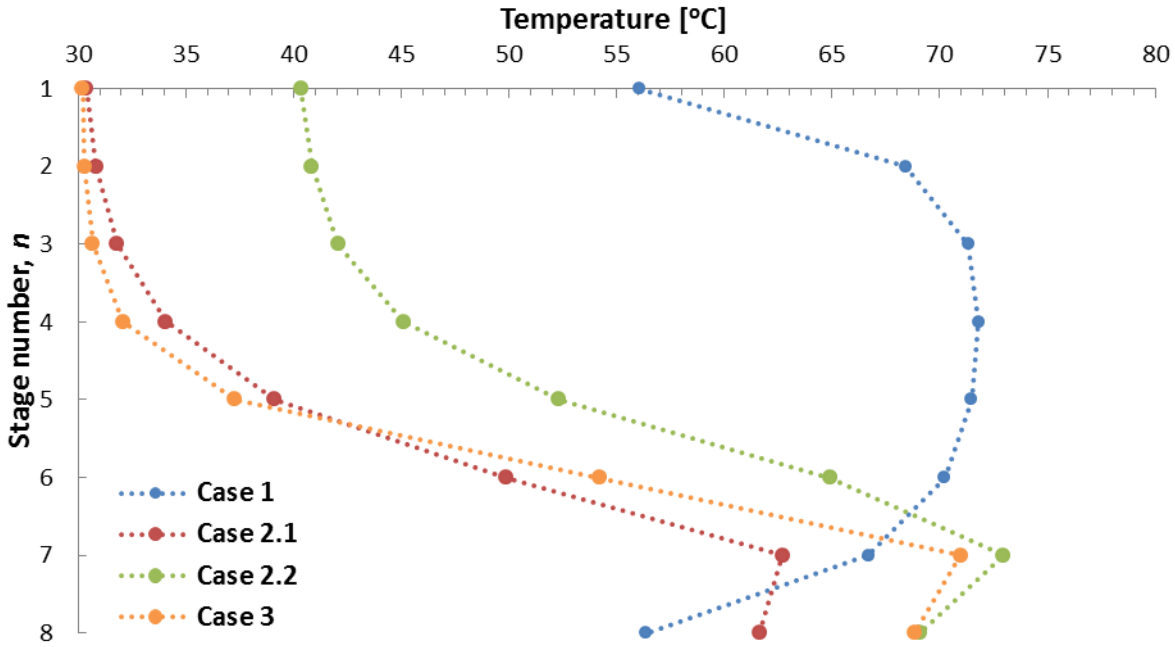

Figure C.5.1: Temperature profile of the absorber for Case 1, 2.1, 2.2 and 3. Stage 1 is the top of the column.

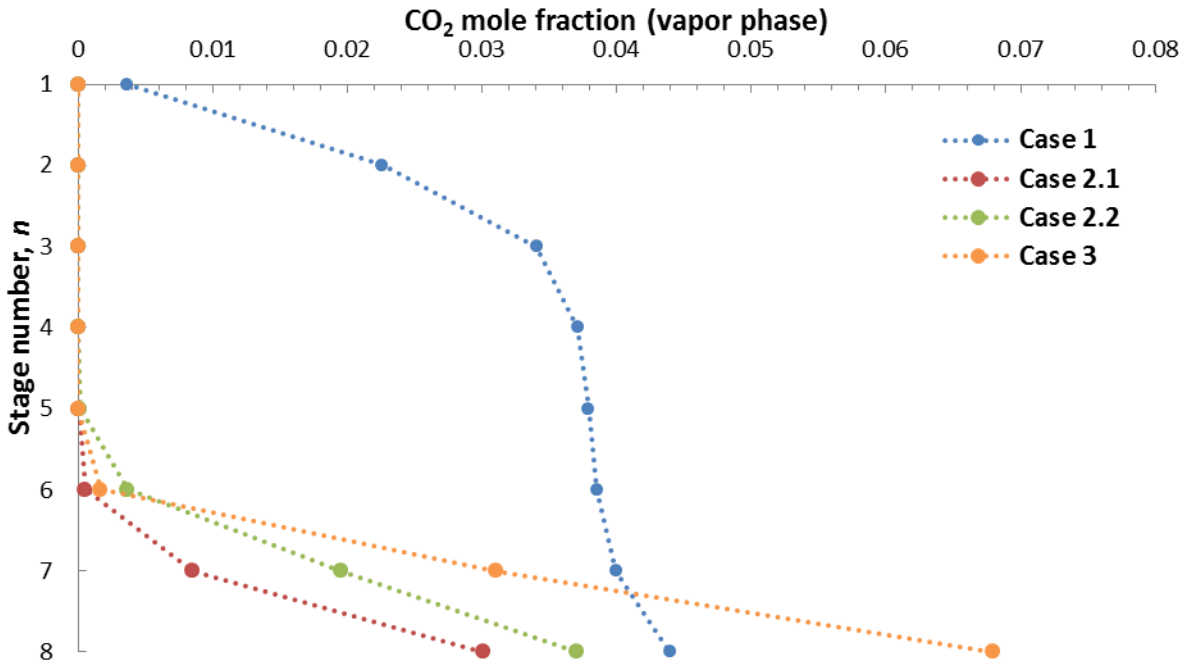

Figure C.5.2: Concentration profile of CO_2 in the absorber for Case 1, 2.1, 2.2 and 3. The concentration is given as mole fraction in tha vapor phase, y_{CO_2}. Stage 1 is the top pf the column.

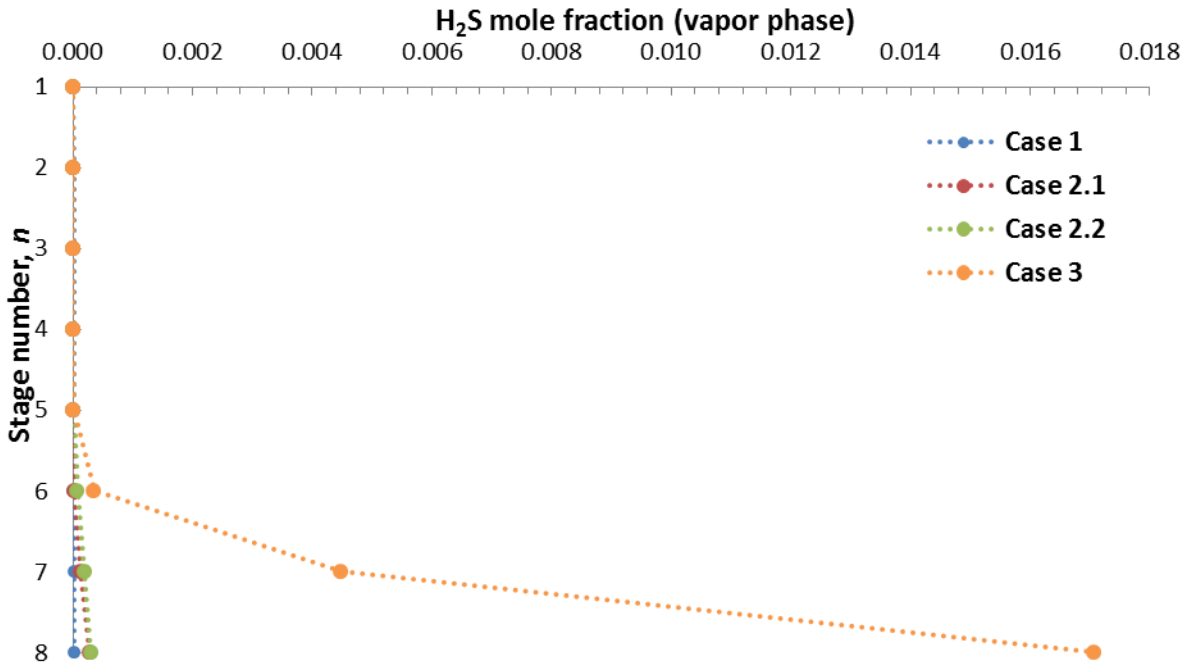

Figure C.5.3: Concentration profile of H_2S in the absorber for Case 1, 2.1, 2.2 and 3. The concentration is given as mole fraction in tha vapor phase, y_{H_2S}. Stage 1 is the top pf the column.

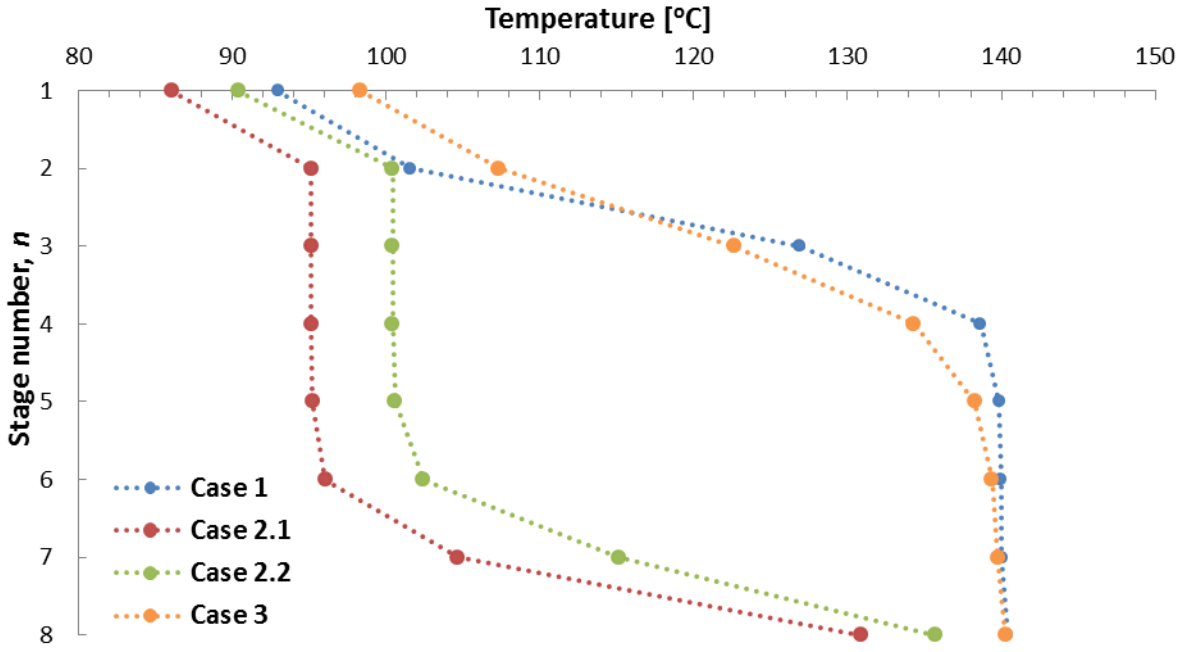

Figure C.5.4: Temperature profile of the stripper for Case 1, 2.1, 2.2 and 3. Stage 1 is the top of the column.

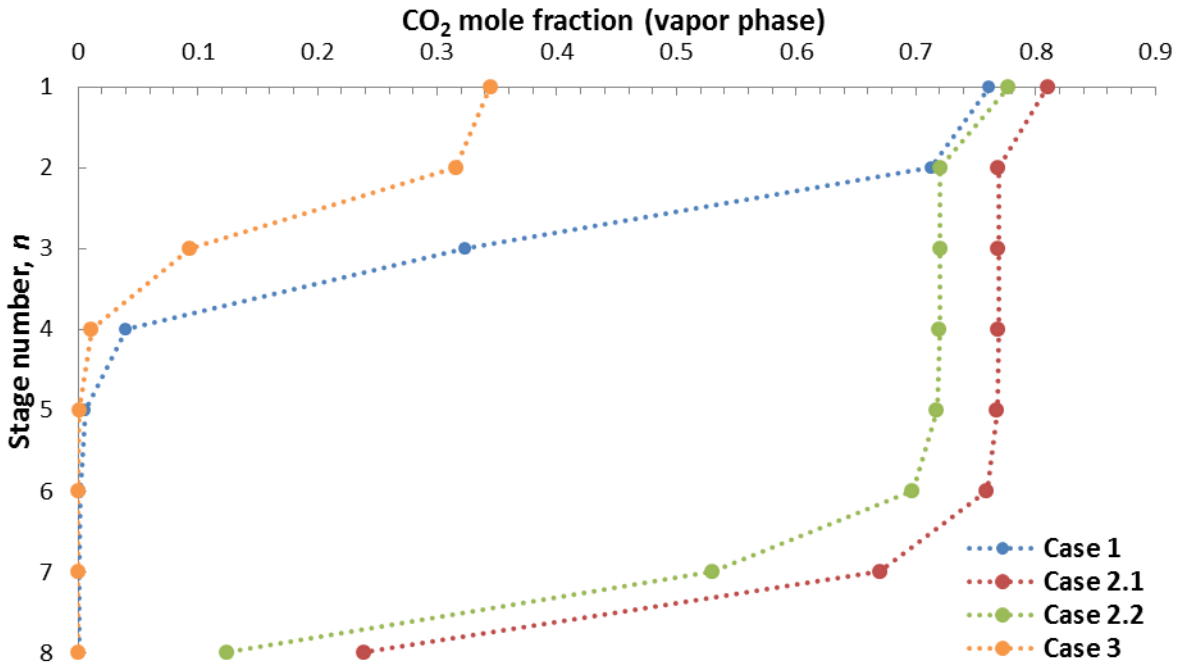

Figure C.5.5: Concentration profile of CO_2 in the stripper for Case 1, 2.1, 2.2 and 3. The concentration is given as mole fraction in tha vapor phase, y_{CO_2}. Stage 1 is the top pf the column.

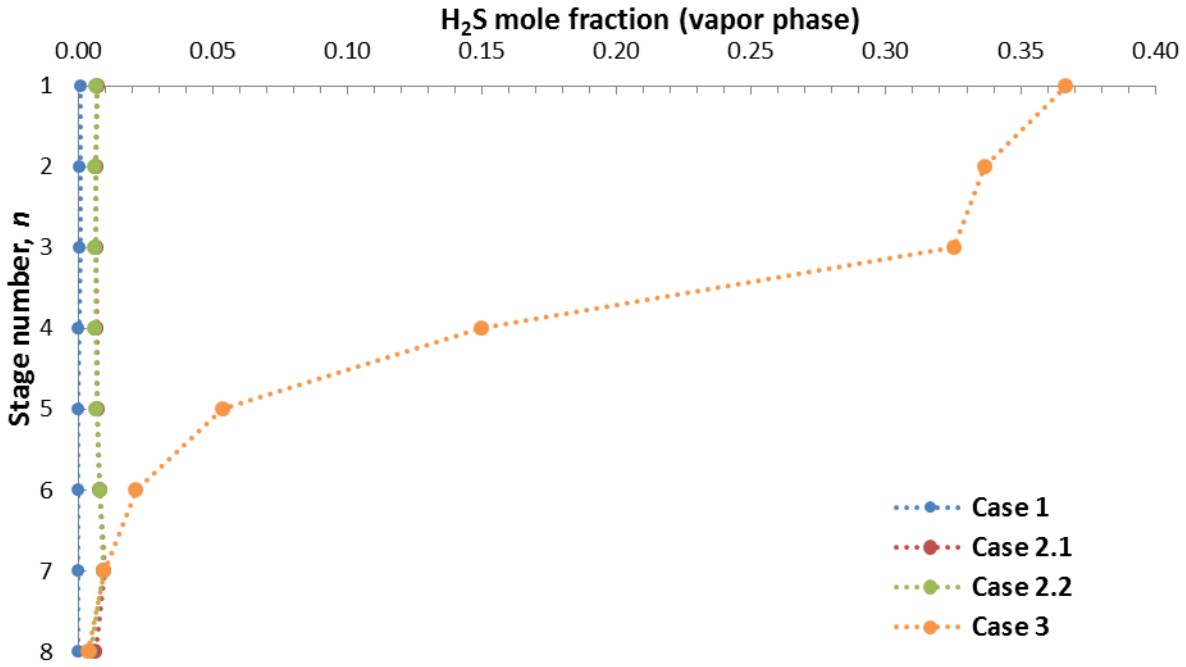

Figure C.5.6: Concentration profile of H_2S in the stripper for Case 1, 2.1, 2.2 and 3. The concentration is given as mole fraction in tha vapor phase, y_{H_2S}. Stage 1 is the top pf the column.